2011

CHARACTERIZATION OF ATG8 GENE HOMOLOGS IN VERTICILLIUM DAHLIAE AND VERTICILLIUM ALBO-ATRUM

Sylvie M. van Twest

CHARACTERIZATION OF *ATG8* GENE HOMOLOGS IN *VERTICILLIUM DAHLIAE* AND *VERTICILLIUM ALBO-ATRUM*

(Spine title: STUDY OF *ATG8* GENE HOMOLOGS IN *V. DAHLIAE* AND *V. ALBO-ATRUM*)

(Thesis format: Monograph)

By

Sylvie M. van Twest

Graduate Program
In Biology

A thesis submitted in partial fulfilment
of the requirements for the degree of
Master of Science

The School of Graduate and Postdoctoral Studies
The University of Western Ontario
London, Ontario, Canada

THE UNIVERSITY OF WESTERN ONTARIO
SCHOOL OF GRADUATE AND POSTDOCTORAL STUDIES

CERTIFICATE OF EXAMINATION

Supervisor

Dr. Katherine Dobinson

Co-Supervisor

Dr. Richard Gardiner

Supervisory Committee

Dr. Percival-Smith

Dr. Denis Maxwell

Examiners

Dr. Percival-Smith

Dr. Thorn

Dr. Karagiannis

The thesis by

Sylvie M. van Twest

entitled:

Characterization of *ATG8* gene homologs in *Verticillium dahliae* and *Verticillium albo-atrum*

is accepted in partial fulfilment of the
requirements for the degree of
Master of Science

Date_____

_____
Chair of the Thesis Examination Board

ABSTRACT

The vascular wilt fungi *Verticillium dahliae* and the closely related *Verticillium albo-atrum* are devastating plant pathogens. Both pathogens produce resting structures that accumulate in soil, and are difficult to eradicate. *V. dahliae* produces microsclerotia (MCS), while *V. albo-atrum* produces dark resting mycelia (DRM). The role of *ATG8,* an autophagy marker was studied by generating *ATG8* knockouts in *V. dahliae (vdatg8),* and *V. albo-atrum (vaatg8).* Although dispensable for pathogenicity in both species, in *V. dahliae ATG8* was involved in dimorphic growth, conidiation, and MCS formation, but not glycogen accumulation. Increased temperatures restored conidiation and MCS formation in *vdatg8,* indicating that autophagy is involved in, but not essential for MCS formation in *V. dahliae*. In *V. albo-atrum ATG8* was involved in glycogen accumulation, but not DRM formation. Considerable functional redundancy exists in *V. dahliae* MCS formation, and although *VdATG8* and *VaATG8* amino acid sequences are almost identical, *ATG8* function is species specific.

Keywords: *Verticillium dahliae*, *Verticillium albo-atrum*, autophagy, *ATG8*, microsclerotia, dark resting mycelia, temperature

ACKNOWLEDGEMENTS

First of all I am deeply grateful to my supervisor, Dr. Katherine Dobinson for the opportunity to work in her lab. Her endless guidance, support, kindness, and wisdom were invaluable and deeply appreciated.

I would like to thank my co-supervisor Richard Gardiner, and my committee members Dr. Percival-Smith and Dr. Maxwell for their assistance and support.

I am immensely grateful to everyone in the Dobinson lab for all their support and knowledge. Special thanks go to Sandy Grant for her endless encouragement, and technical acumen, Nadia Morales for her friendship, generosity of spirit and assistance, and Stefan Amyotte for his mentorship and guidance. I would also like to thank Kuflom Kuflu for his vast expertise, patience and assistance.

Thanks are also due to Ida Van Grinsven for sequencing, and Alex Molnar for his assistance with graphics.

Finally, I would like to thank my family and friends for their continual support and encouragement.

TABLE OF CONTENTS

LIST OF TABLES

LIST OF FIGURES

LIST OF APPENDICES

LIST OF ABBREVIATIONS

ATG8	Autophagy-related gene 8
ATMT	*Agrobacterium tumefaciens*-mediated transformation
BIVGB	Broad Institute Verticillium Group Database
BLAST	Basic Local Alignment Search Tool
BM-C	Basal medium lacking glucose
BM-N	Basal medium lacking nitrate
cDNA	Complementary DNA
CM	Complete media
CSPD	Disodium 3-(4-methoxyspiro{1,2-dioxetane-3,2'-(5'-chloro)tricyclo[3.3.1.13,7]decan}-4-yl)phenyl phosphate
DMS	Developing microsclerotia
DHN	Dihydroxynaphthalene
DIG	Digoxigenin
dpi	Days post inoculation
DRM	Dark resting mycelia
*e*CFP	Enhanced cyan florescent protein
EST	Expressed sequence tag
EtOH	Ethanol
eYFP	Enhanced yellow florescent protein
hpi	Hours post inoculation
LB	Lysogeny broth
MCS	Microsclerotia
MDC	Monodansylcadaverine
PE	Phosphatidylethanolamine
NO_3	Nitrate
ORF	ORF
NCBI	National Centre for Biotechnology Information
PCR	Polymerase chain reaction
PMSF	Phenylmethylsulfonyl fluoride
qRT-PCR	Quantitative Reverse transcriptase polymerase chain reaction
RT-PCR	Reverse transcriptase polymerase chain reaction
SDS	Sodium dodecyl sulfate
SGD	Saccharomyces Genome database
SPT	Soil pectate tergitol
SSPE	Sodium Chloride-Sodium Phosphate-EDTA
SXM	Simulated xylem fluid medium
TOR	Target of rapamycin kinase
VDH1	*Verticllium dahliae* hydrophobin 1
VMK1	*Verticillium* MAP kinase 1

CHAPTER 1: INTRODUCTION

1.1 Verticillium

Founded in 1816 by Nees von Esenbeck, the genus *Verticllium* includes many globally significant pathogens (Isaac 1967). The genus is characterized by distinctive conidiophores that bear clusters of conidia at the apices of whorled phialides (Isaac 1967; Schnathorst 1981) (Figure 1.1). Although originally heterogeneously diverse, the genus is now comprised of only four soil-borne species: *V. dahliae* Kleb., *V. albo-atrum*, *V. nubilum*, and *V. tricorpus* that all cause vascular wilt disease (Klosterman et al. 2009). Additionally, another wilt causing pathogen called *V. dahliae* var. *longisporum* (Stark 1961) which has longer conidia than *V. dahliae* and produces elongate, irregular microsclerotia has recently been raised from a variety to a species called *Verticillium longisporum* (Karapapa et al. 1997). Of these species, *V. dahliae* and *V. albo-atrum* have been the most widely studied given their wide host range and disease severity (Pegg & Brady 2002).

V. dahliae and *V. albo-atrum* cause vascular wilt in more than 200 dicotyledonous genera ranging from crops to trees (Fradin & Thomma 2006). However, *V. albo-atrum* is considered to have a narrower host range, with infections primarily restricted to alfalfa, hop, soybean, tomato and potato (Fradin & Thomma 2006). Both species cause disease in temperate and subtropical regions, but not in tropical areas. While *V. dahliae* grows best in warmer climes ranging from 25-28˚C, the optimal growth temperatures for *V. albo-atrum* range from 20-25˚C (Fradin & Thomma 2006).

Besides differences in optimal growth temperatures, *V. dahliae* and *V. albo-atrum* are distinguished by the resting structures they produce. While *V. dahliae* produces swollen hyphae that differentiate to form clusters of spherical, melanized cells called microsclerotia (MCS), *V. albo-atrum* hyphae do not differentiate, but simply melanize to form dark resting mycelia (DRM).

1.2 Life cycles of *V. dahliae* and *V. albo-atrum*

Both *V. dahliae* and *V. albo-atrum* have similar life cycles that can be divided into parasitic, saprophytic and dormant phases (reviewed by Fradin & Thomma, 2006, see Figure 1.1). While *V. dahliae* is a monocyclic pathogen in that infection and inoculum production only occurs once during the growing season, *V. albo-atrum* may produce conidia on infected tissues (Jimenez-Diaz & Millar 1988). Since airborne conidia may cause secondary infections, disease caused by *V. albo-atrum* can be polycyclic (Jimenez-Diaz & Millar 1988).

The parasitic stage for both pathogens starts with hyphal penetration from germinated resting structures or conidia through root tips or wounds, and progresses with colonization of the root cortex and xylem by mycelia and conidia, and ultimately symptom development (Pegg & Brady 2002). Colonization of the vasculature occurs once the pathogen has crossed the endodermis (Fradin & Thomma 2006). At this stage, the fungus produces conidia that move in the transpiration stream until they are trapped by vessel end walls (Pegg & Brady 2002). To continue colonization, these conidia must germinate and grow as mycelia to cross the end wall plates and move laterally between adjacent vessel elements (Pegg & Brady 2002). Further systemic colonization is aided by

the dimorphic nature of *Verticillium*, where mycelia can produce conidia that can either germinate to grow as mycelia or bud to produce yeast-like cells (Fradin & Thomma 2006). Given that strain aggression has been observed to be high for rapidly colonizing strains that produce abundant conidia (Schnathorst 1963), dimorphism is assumed to be critical to infectivity.

Despite the presence of vessel end walls, which slow the upward stream of conidia and yeast-like cells, and force the spores to stop and grow as mycelia to penetrate these barriers, colonization is rapid and the fungus can be detected in the xylem elements by four days post-infection (Chen et al. 2004; Gold & Robb 1995; Heinz et al. 1998). The colonization stage is typified by cycles of fungal proliferation and elimination that are inversely proportional to expression levels of the plant defense gene phenylalanine ammonia lyase (PAL) (Heinz et al. 1998). While the cyclical colonization pattern has been attributed to inadequate host defenses (Heinz et al. 1998), another possibility is that the fungus itself undergoes autolysis (Vessey & Pegg 1973), and actively reduces its biomass to escape detection.

As colonization of the vascular system occurs, symptoms develop acropetally. Cotyledons and lower, then upper leaves first develop chlorotic blotches that later become necrotic, and affected leaves may abscise. Other symptoms associated with Verticillium wilt include vascular discolouration, stunting, reduced leaf size, and epinasty (Fradin & Thomma 2006; Pegg & Brady 2002) (Figure 1.2).

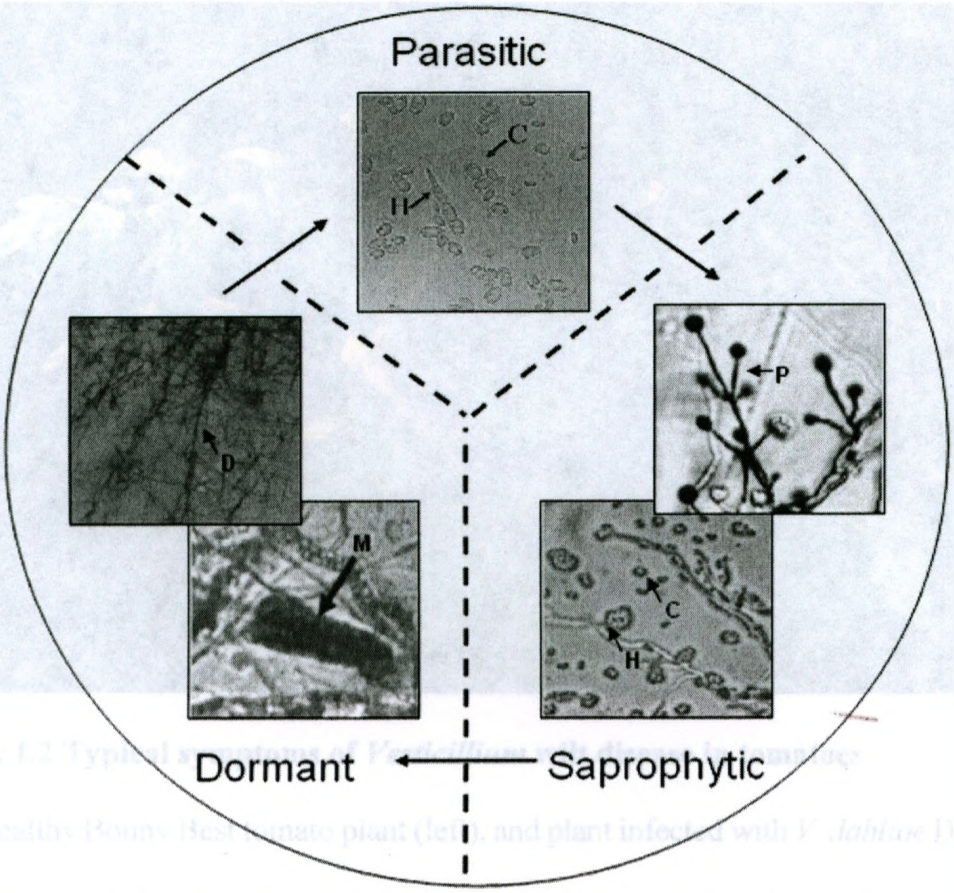

Figure 1.1. Lifecycle of *V. dahliae* and V. *albo-atrum* The lifecycles of *V. dahliae* and *V. albo-atrum* have three stages: parasitic, saprophytic and dormant. During the parasitic stage, the dimorphic fungus produces conidia (C), yeast-like cells and hyphae (H). In the saprophytic stage, plant tissues start to die and the fungus produces characteristic conidiophores (P); image from A. Klimes, hyphae (H) and resting structures. *V. dahliae* produces microsclerotia (M) while *V. albo-atrum* produces dark resting mycelia (D) that persist in soils until germination is stimulated by plant root exudates. Diagram adapted from that made by S. Amyotte (2010). The parasitic phase image and one saprophytic (P) image are from A. Klimes, and S. Amyotte took the photo of dark resting mycelia.

Fig. 1.2 Typical symptoms of *Verticillium* wilt disease in tomatoes

A healthy Bonny Best tomato plant (left), and plant infected with *V. dahliae* Dvd-T5 (right). The infected plant is stunted and has leaves and branches that show chlorosis, necrosis, and dieback. (Image was taken by A. Klimes).

Some plant species infected with *Verticillium* spp. may initially exhibit wilting when exposed to direct sunlight or heat, but recover overnight. As the disease progresses the wilt becomes permanent and plant tissues start to senesce. Once plant tissues start to die, the fungus enters a brief saprophytic stage. With *V. dahliae* this stage terminates with microsclerotia (MCS) formation (Wilhelm 1955), while *V. albo-atrum* may produce conidia on infected plant tissue that can disperse in air currents to cause new infections (Jimenez-Diaz & Millar 1988) or produce melanized dark resting mycelia (DRM). Both species can also over-winter as mycelia contained within perennial hosts, or in tubers, bulbs or seeds (Fradin & Thomma 2006).

1.3 Disease Control

V. dahliae and *V. albo-atrum* are responsible for billions of dollars in crop damages annually (Pegg & Brady 2002). Effective disease control is complicated by the persistence of resting structures, and broad host range of the fungi, limited sources of disease resistance, and lack of systemic fungicides that can target the fungus once it has colonized the vasculature (Fradin & Thomma 2006). Resting structures retain viability in the absence of susceptible hosts, and are the primary disease inoculum. Accumulation of these resting structures is a concern given that microsclerotia can survive 10-15 years in soil (Wilhelm 1955) while the dark resting mycelia survive for up to 5 years (Sewell & Wilson 1964), and that only one microsclerotium per gram of soil is enough to cause significant wilt in crops such as strawberry and tomato (Grogan et al. 1979; Nicot & Rouse 1987). Since *Verticillium* has such a broad host range, it also can survive on economically important species and weeds alike, creating a reservoir for the pathogen

(Pegg & Brady 2002). In addition, the host range of Verticillium is continually expanding, with former non–host plants such as lettuce becoming susceptible (Subbarao et al. 1995).

For *V. dahliae* typical disease management practices such as crop rotation and pathogen avoidance are complicated by the genetic plasticity of the fungus, which facilitates its wide host range, leaving few areas inoculum-free. Other methods to reduce inoculum include soil solarization and chemical fumigation (Fradin & Thomma 2006). Soil fumigation, though effective in some regions, requires a suitable environment, and many chemical fumigants have been banned due to environmental concerns. Since resting structures readily build up in soil and are difficult to eradicate, targeting their development presents a good option for disease control.

1.4 Resting Structure Development

Research in our laboratory focuses on the molecular mechanisms governing resting structure formation in *V. dahliae* and *V. albo-atrum*. Early microscopic studies of the two fungi showed that early stages of differentiation that lead to resting structure formation are similar, despite their divergent outcomes (Griffiths 1970). Both MCS and DRM originate from highly septate, swollen hyphae. In *V. dahliae* the swollen hyphae continue to differentiate by budding laterally to produce clusters of spherical cells that then become melanized to form MCS. To form DRM, the hyphal cell walls of *V. albo-atrum* thicken and are filled with heavy deposits of melanin.

Melanins are dark pigments produced by oxidative polymerization of phenolic or indolic compounds (Fradin & Thomma 2006). Studies with *V. dahliae* melanin deficient

mutants showed that melanins in Verticillium are derived from precursor 1,8-dihydroxynaphthalene (DHN) (Wheeler et al. 1978). Melanins confer environmental protection and durability and are essential to the persistence of MCS and DRM, since un-pigmented MCS have reduced persistence (Hawke & Lazarovits 1994).

Far from being simply melanized clusters, the cells that comprise MCS originate as identical, thin walled, vacuolate hyaline cells. As these cells develop, two morphologically and functionally distinct types emerge. Thick walled, melanized cells contain food reserves while thin walled, hyaline cells germinate more readily than the thick walled cells (Gordee & Porter 1961). As the MCS continue to mature, some cells die. Autolysis coincides with the accumulation of autophagic vesicles in the cytoplasm of declining cells, while auto-parasitic hyphae infect adjacent cells to extract nutrients and nourish some cells, while compromising others (Griffiths 1970; Griffiths & Campbell 1971).

Before becoming melanized, fibrillar material is secreted between individual cells (Griffiths 1970). Melanized particles are extruded by living cells into this fibrillar matrix between individual cells, and continue to build up in the interhyphal spaces (Griffiths 1970). Mature MCS have both live and dead cells; the majority of dead cells are heavily melanized and located on the outside of the MCS.

Although microscopic studies have revealed the morphological changes that result in resting structures, the molecular mechanisms that govern resting structure development are still poorly understood. To identify candidate genes responsible for resting structure development, cDNA libraries were constructed in our laboratory from *V. dahliae* cells

grown in two environments; a simulated xylem fluid medium (SXM) where the fungus exhibits dimorphic growth, and conditions that favour near-synchronous MCS development (Neumann & K. F. Dobinson 2003). Genes that may be involved in resting structure development can be identified from these collections and studied in more detail.

To date, a hydrophobin (*VDH1*) and a Verticillium mitogen-activated protein (MAP) kinase (*VMK1*) have been shown to be involved in MCS formation (Rauyaree et al. 2005; Klimes & Dobinson 2006). While *VDH1* was isolated from the aforementioned cDNA library, *VMK1* was isolated with degenerate primers based on conserved regions of the *M. grisea PMK1* gene (Rauyaree et al. 2005). Both *vdh1* and *vmk1* mutants are defective in MCS production, and studies with the hydrophobin gene showed that conidiophore collapse and fusion of aerial hyphae are important for MCS formation (Klimes & Dobinson 2006). In contrast hydrophobin knockouts in *V. albo-atrum* were not defective in DRM production and showed no aberrant phenotype despite showing patterns of gene expression similar to those of *V. dahliae* (Amyotte 2010). Thus, studying the same genes in *V. dahliae* and *V. albo-atrum* may provide insights into resting structure development and where this pathway diverges to produce different structures.

The *V. dahliae* cDNA libraries from simulated xylem fluid media (SXM) and developing microsclerotia (DMS) have proven to be useful tools for identifying genes potentially involved in resting structure development or dimorphic growth. Accordingly, sequences highly similar to the yeast macroautophagy marker gene *ATG8* were identified in both cDNA collections, indicating a potential role for autophagy in *V. dahliae* development, specifically for resting structure formation and dimorphic growth. Taken

together with the early observations that autophagic vesicles were visible during MCS formation, and that autolysis occurs during parasitic growth *in planta* (Vessey & Pegg 1973), this additional molecular information raised our interest and led to my project studying the role of autophagy and *ATG8* homologs in *V. dahliae* and *V. albo-atrum.*

1.5 Autophagy

Cellular homeostasis is important for normal growth and development and is maintained by a balance between protein biosynthetic and degradative pathways. The main pathways for protein degradation are the ubiquitin-proteosome pathway, and autophagy (Nair & Klionsky 2005). Under vegetative growth conditions, most protein degradation occurs via the ubiquitin-proteosome pathway. Overall, autophagy is a response to nutrient starvation, hypoxia, overcrowding, high temperatures, and accumulation of damaged/superfluous organelles and cytoplasmic components (Levine & Klionsky 2004). Although autophagy is upregulated during stress, it also occurs at a basal rate, and is the only pathway that can degrade large protein aggregates or entire organelles (Nair & Klionsky 2005).

Autophagy is a catabolic membrane trafficking response that is highly conserved in eukaryotes, from yeast to humans (Pollack et al. 2009). During autophagy, cytoplasm and organelles are non-selectively sequestered within double membraned vesicles termed autophagosomes (Abeliovich & Klionsky 2001). These autophagosomes dock to vacuolar membranes, fusing the outer membrane of the autophagosome to the vacuolar membrane (Ichimura et al. 2004) (Figure 1.3). Inside the vacuole, proteases degrade the

resulting autophagic body, enabling breakdown and recycling of cytoplasmic contents and long-lived organelles (Pollack et al. 2009; Yang et al. 2005).

Induction of autophagy occurs when TOR (target of rapamycin) kinase activity is inhibited. TOR is involved in nutrient sensing, regulation of transcription, translation and protein degradation (Pollack et al. 2009; Yang et al. 2005). When active, TOR kinase hyperphosphorylates ATG1 and ATG 13, preventing their interaction, and in so doing inhibits autophagy (Codogno & Meijer 2000) (Figure 1.4). However, upon nutrient deprivation or exposure to autophagy inducers such as rapamycin, TOR kinase is inactivated and an unknown phosphatase dephosphorlyates ATG1 and ATG13, allowing them to interact with ATG17 and other autophagy proteins needed for autophagosome formation (Klionsky & Emr 2000) (Figure 1.4).

Autophagosome formation requires two ubiquitin-like conjugation complexes, ATG12-ATG5 and ATG8-phosphatidylethanolamine (PE) (Yang et al. 2005). Both conjugation complexes are necessary for autophagosome formation and expansion (Yang et al. 2005) (Figure 1.5). If the ATG12-ATG5 complex is defective, ATG8 localization is compromised (Yang et al. 2005).

1.5.1 The *ATG8* gene

ATG8 is a membrane bound protein that is cleaved at the C terminal arginine residue by ATG4 to expose a free glycine residue (Yang et al. 2005). Once cleaved, ATG8 undergoes a lipidation reaction with phosphatidylethanolamine (PE), allowing autophagosomal membrane expansion around cytoplasmic contents (Pinan-Lucarré et al. 2003).

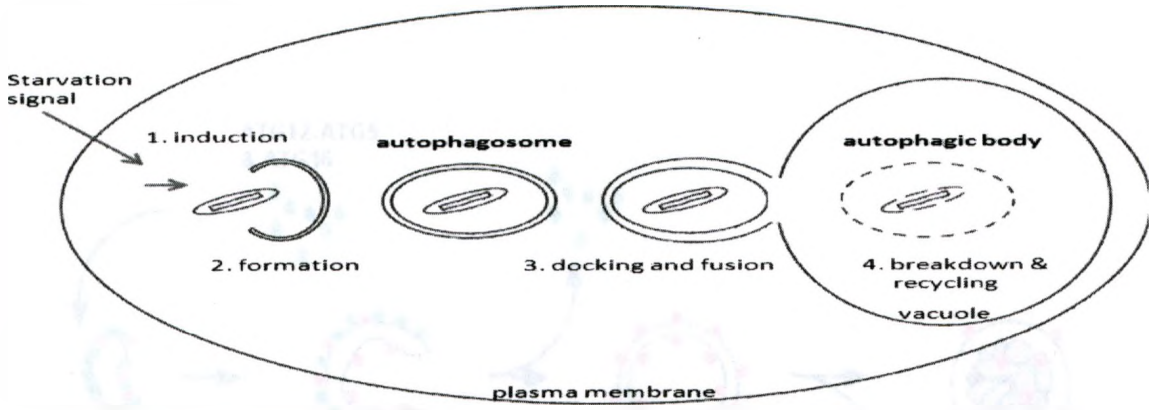

Figure 1.3 Schematic model of autophagy in fungi. Diagram adapted from Klionsky & Emr (2000).

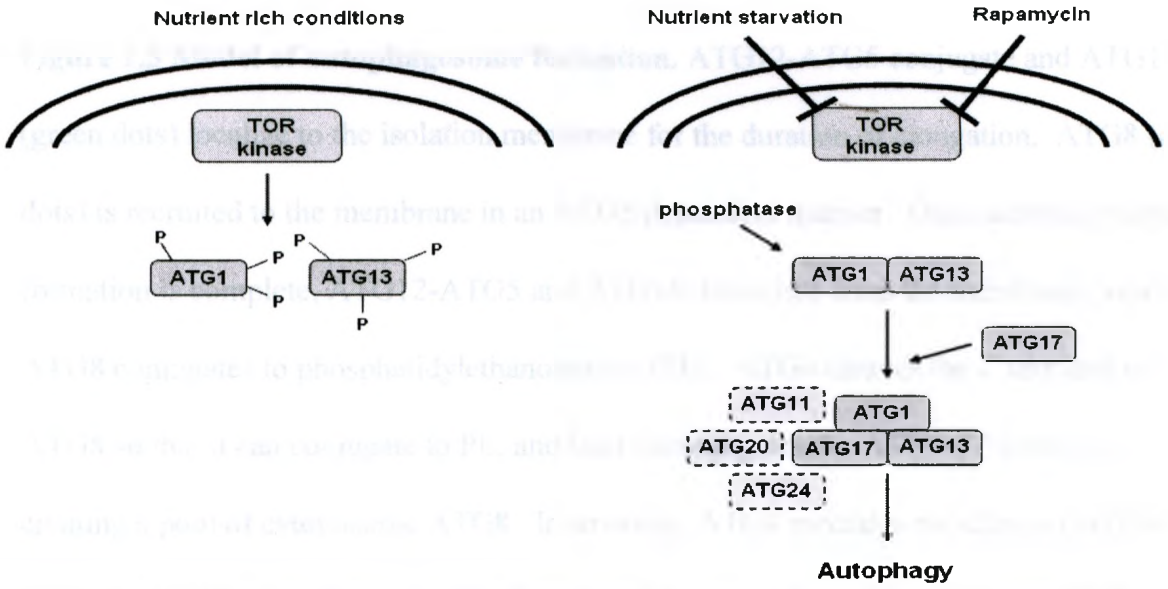

Figure 1.4 Model for autophagy induction. Left panel: Under nutrient rich conditions, TOR kinase is active and hyperphosphorylates ATG1 and ATG13, preventing their interaction. Right panel: Nutrient starvation or rapamycin treatment inactivates TOR kinase, and a phosphatase dephosphorylates ATG1 and ATG13 so they can interact with one another, and form an initiation complex (ATG1-ATG13-ATG17) that is needed for autophagosome formation. Diagram adapted from Pollack (2009).

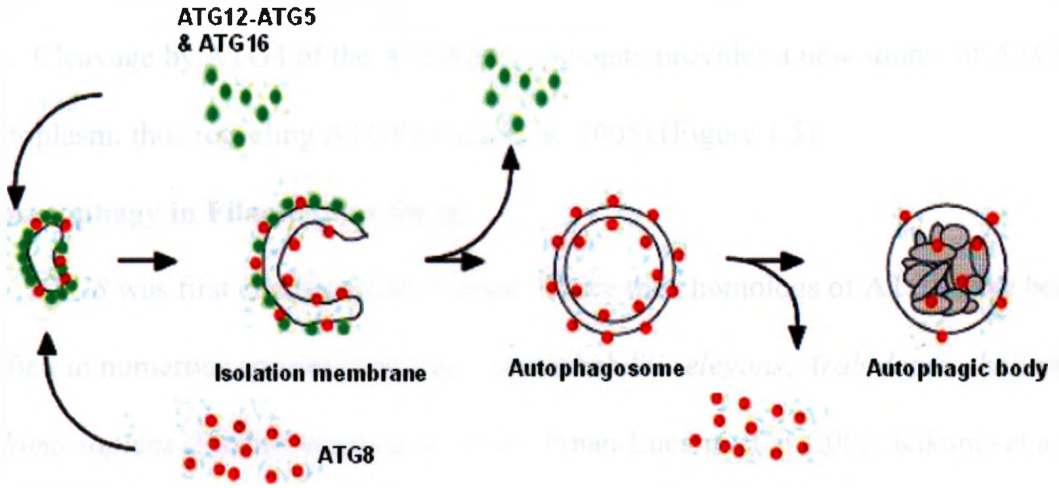

Figure 1.5 Model of autophagosome formation. ATG12-ATG5 conjugate and ATG16 (green dots) localize to the isolation membrane for the duration of elongation. ATG8 (red dots) is recruited to the membrane in an ATG5 dependent manner. Once autophagosome formation is complete, ATG12-ATG5 and ATG16 dissociate from the membrane, while ATG8 conjugates to phosphatidylethanolamine (PE). ATG4 cleaves the C terminal of ATG8 so that it can conjugate to PE, and later deconjugates the ATG8-PE complex, creating a pool of cytoplasmic ATG8. In so doing, ATG4 mediates recycling of ATG8, which can exist in conjugated and unconjugated forms. Adapted from Mizushima & Levin (2010)

ATG8 is considered to be a marker for autophagy since it is present in early autophagic membranes, autophagosomes and autophagic bodies (Abeliovich & Klionsky 2001). Cleavage by ATG4 of the ATG8-PE conjugate provides a new source of ATG8 in the cytoplasm, thus recycling ATG8 (Yang et al. 2005) (Figure 1.5).

1.5.2 Autophagy in Filamentous Fungi

ATG8 was first characterized in yeast. Since then homologs of ATG8 have been identified in numerous species including *Caenorhabditis elegans*, *Arabidopsis thaliana*, and *Homo sapiens* (Pinan-Lucarré et al. 2003; Pinan-Lucarré et al. 2005; Kikuma et al. 2006). In filamentous fungi autophagy is involved in nutrient recycling during starvation and is also involved in cellular differentiation and developmental processes such as sporulation (Pollack 2009). However, the outcome of *ATG8* mutation varies between fungal species. In the filamentous deuteromycete *Aspergillus oryzae*, for example, mutation of *AoATG8* showed that autophagy is involved in the differentiation of aerial hyphae, conidiation, and conidial germination (Kikuma et al. 2006) In contrast, because autophagic cell death of conidial cells is required for appressorium formation and infectivity in the rice blast fungus *Magnaporthe grisea*, impaired autophagy renders the fungus non-pathogenic (Veneault-Fourrey et al. 2006).

1.5.3 Comparison of *ATG8* gene homologs in *V. dahliae* and *V. albo-atrum*

Both *V. dahliae* and *V. albo-atrum* have *ATG8* gene homologs. In *V. dahliae,* the gene (*VdATG8*) encodes a 366 bp open reading frame (ORF) interrupted by a 209 bp intron and a 55 bp intron, and the gene product is 120 amino acids long. In *V. albo-atrum*, the gene (*VaATG8*) encodes a 281 bp ORF interrupted by a 121 bp intron and a 55

bp intron, and the gene product consists of 92 amino acids. The sequence of the longer intron is 87% conserved, while the sequence and location of 55 bp intron is 100% conserved between the two species. According to sequence analysis, *VdATG8* and *VaATG8* share 96% conservation at the amino acid level.

Consistent with the highly conserved nature of *ATG8* in other species (Abeliovich and Klionsky, 2001), I found that the amino acid sequences of *VdATG8* and *VaATG8* are well conserved with those of other filamentous fungi (Figure 1.6). In yeast, cleavage of Arg117 in ATG8 by ATG4 to reveal glycine 116 is essential for conjugation of ATG8 to PE, and subsequent autophagosome formation. Conservation of the glycine at position 116 in *VdATG8, VaATG8* and other fungal ATG8 gene homologs (Figure 1.6) suggests that the autophagic process in filamentous fungi is similar to that of other eukaryotes.

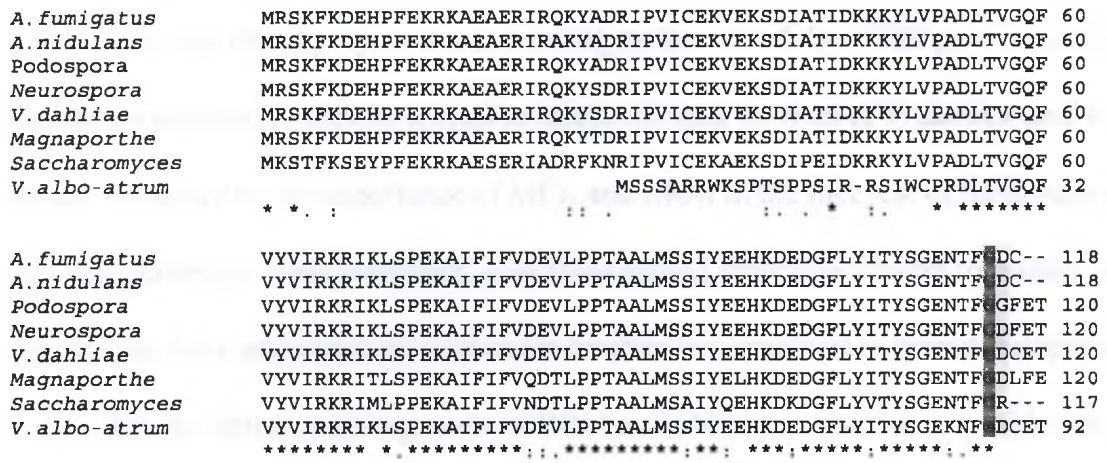

Figure 1.6 Clustal alignment of *ATG8 in V. dahliae, V. albo-atrum, Aspergillus fumigatus, A. nidulans, Podospora anserina, Neurospora crassa, Magnaporthe grisea,* and *Saccharomyces cerevisiae.* The yellow highlighted amino acid at position 117 is cleaved by ATG4 to reveal glycine at position 116 (highlighted in green).

1.6 Research Rationale and Objectives

The aim of my project was to investigate the role of the *ATG8* gene in autophagy and developmental processes critical to infectivity and survival of *V. dahliae and V. albo-atrum*. Relative to the importance of MCS and DRM in the lifecycle of these pathogens, and the challenges these persistent, long lived resting structures present to disease control, few studies have addressed the molecular mechanisms involved in their development. Given that the initial morphogenesis of DRM and MCS is so similar, it would seem that an initial developmental pathway diverges to give rise to different resting structures. Studying the same gene in both species may help further elucidate differences between the developmental pathways that result in MCS and DRM formation.

Since autophagy has been observed to be associated with resting structure development since the earliest microscopic studies (Griffiths 1970; Griffiths & Campbell 1971) and expressed sequence tag (EST) data for *V. dahliae* revealed expression of autophagy genes during microsclerotial development, *ATG8* is a good candidate for study. Furthermore, in various filamentous fungi, *ATG8* is involved in cellular differentiation and affects critical processes including germination, sporulation, and infectivity (reviewed in Pollack 2009). Besides resting structure development, autophagy may play a role in plant colonization during the parasitic stage of the *Verticillium* life cycle. In the nutrient poor environment of the xylem, autophagy may enable fungal survival via nutrient recycling.

Thus, I hypothesized that ATG8 plays a role in development of *V. dahliae* and *V. albo-atrum* and subsequent resting structure formation, and secondly, that autophagy is involved in the observed proliferation and elimination of yeast-like cells during the colonization phase of plant infection.

To investigate this hypothesis, *ATG8*-disrupted strains were created in both *V. dahliae* (*vdatg8*) and *V. albo-atrum* (*vaatg8*). Comparative studies between *ATG8* disrupted and wild-type strains were done to assess the role of *ATG8* in developmental processes such as germination, sporulation, radial growth, microsclertia formation and pathogenicity. *In planta* colonization by disrupted and wild-type strains was studied using stem sectioning and PCR assays. To understand *VdATG8* expression and localization under autophagy-inducing and –inhibiting conditions, quantitative real time PCR (qRT-PCR) was done, and *VdATG8* expression and localization constructs were made.

CHAPTER 2: MATERIALS & METHODS

2.1 Fungal strains and growth conditions

All *Verticillium* strains used in this study are described in Table 2.1, and derived from monoconidial cultures and maintained in Dr. K.F. Dobinson's culture collection (Agriculture and Agri-Food Canada, London ON). Fungal isolates are maintained as silica gel stocks or at -20°C on filter paper. The wild-type *V. dahliae* strain Dvd-T5 used in this study was isolated from tomato in Essex county in 1993 (Dobinson et al. 1996), while wild-type *V. albo-atrum* 383-2 was isolated from potato in Ontario in 1989.

ATG8 knockouts in *V. dahliae* (*vdatg8*) and *V. albo-atrum* (*vaatg8*) were previously created from Dvd-T5 and 383-2, respectively, using a *VdATG8* knockout vector (Table 2.1). Details regarding construction of the *ATG8* KO vector, and revertant strains are located in Appendix II. I made *VdATG8* expression and protein localization constructs. Methods used to make these strains are detailed below (section 2.2.1 and 2.2.2). *E. coli* MRF[1] cells are host cells for plasmids used in the study, while AGL1 *Agrobacterium tumefaciens* cells were used for fungal transformations.

Table 2.1 Strains used in this study

Strain name	Description	Source
Dvd-T5	Wild-type *V. dahliae*	Dobinson 1996
VDAT 38-5 & 38-3	*vdatg8* knockouts in Dvd-T5	Appendix II
VDAT 38-6	ectopic *vdatg8* construct in Dvd-T5	Appendix II
VDAT 44-7 & 44-43	*VdATG8* revertant strains in VDAT38-5	Appendix II
VDAT 50-2 & 50-5	*VdATG8* ectopic in VDAT38-5	Appendix II
VDAT 43-11	GAPD::eYFP in Dvd-T5	Stefan Amyotte (PhD thesis, 2010)
VDAT 74	*VdATG8*(p)::eCFP in Dvd-T5	section 2.2.1
VDAT 75	*VdATG8*(p)::eCFP in VDAT43-11	section 2.2.1
VDAT 77	*VdATG8*::eYFP$_N$ (N-terminal fusion) in Dvd-T5	section 2.2.2
383-2	Wild-type *V. albo-atrum*	G. Lazarovits
VAAT10-9	*vaatg8* knockouts in 383-2	Appendix II
VAAT10-11	*vaatg8* knockouts in 383-2	Appendix II
VAAT10-12	*vaatg8* knockouts in 383-2	Appendix II
VAAT10-10	Ectopic *vdatg8* construct in 383-2	Appendix II

* Wild-type strains used in this study are Dvd-T5, a race 1 strain of *V. dahliae* and 383-2, a *V. albo-atrum* strain. Strains prefaced by Vd and Va are *V. dahliae* and *V. albo-atrum*, transformants respectively.

2.2.1 Construction of *VdATG8* expression vector

The *VdATG8* expression construct contains the *VdATG8* promoter region fused to an enhanced cyan fluorescent protein (*e*CFP) gene (Figure 2.2A). The 1kb *ATG8* promoter-containing fragment was amplified from genomic Dvd-T5 DNA with the atg8EcoF1 and atg8promoterBamR1 *primers* (sequences for these primers, and all others used in this study are listed in Appendix I). These primers introduced *Eco*RI and *Bam*HI sites into the 5' and 3' ends, respectively, of the *ATG8* promoter region amplicon. After double digestion with *Eco*RI and *Bam*HI, the amplicon was ligated into *Eco*R1/*Bam*H1-digested pGEM to form pGEMSVT5C. To confirm correct integration of the promoter-containing fragment into pGEM, pGEMSVT5C was sequenced with vector-specific primers Sp6 and T7, as well as autoF7, autoF10, autoR5 and autoF1 primers. Verification of the correct sequence identity was done by assembling the sequences in SeqMan (Lasergene 6), and aligning the resulting contig to the original *VdATG8* promoter sequence.

To construct the expression vector, pGEMSVT5C was digested with *Eco*RI and *Bam*HI to cut out the *ATG8* promoter-containing fragment. The binary destination vector pSK1518 (Klimes et al. 2008), which contains a hygromycin B resistance gene and the *eCFP* gene, was also digested with *Eco*RI and *Bam*HI. The *ATG8* promoter-containing region was then ligated into pSK1518 to form the *VdATG8*(p)::*e*CFP construct, designated pSV101. To confirm correct integration of the promoter into pSK1518, the construct was sequenced using the vector-specific primers M13F and M13R, as well as auto F1 and atg8promoterBamR1 primers. The pSV101 vector was transformed into

Dvd-T5 (designated VDAT74) and VDAT43 (designated VDAT75) by *Agrobacterium tumefaciens*-mediated transformation (ATMT), as described below.

2.2.2 Construction of *VdATG8* localization vector

Since the C-terminus of ATG8 is cleaved during the autophagic process, a vector containing a fluorescent reporter protein gene fused to the N-terminus of ATG8 was made. The *ATG8* promoter was fused to enhanced yellow fluorescent protein *(e*YFP) (for vector construction flow chart see Figure 2.1) lacking a stop codon to allow in-frame translational read-through to the *ATG8* ORF (for construct schematic see Figure 2.2B). Both pSV101 (containing the A*TG8* promoter fragment) and the destination vector pSK885 (Amyotte 2010) were double digested with *Eco*RI and *Bam*HI. The *ATG8* promoter fragment was gel-purified before ligation into pSK885 (which contains a geneticin resistance marker gene) to produce pSV106. pSV106 was sequenced with M13F and M13R primers to confirm correct integration of the promoter fragment. *eYFP* was then amplified from pSK518 with yfpBamF2 and yfpPstR4 to generate a 1.7 kb amplicon with *Bam*HI and *Pst*I sites at the 5' and 3' ends, respectively, and lacking the stop codon of *eYFP*. Both pSV106 and the 1.7kb *e*YFP amplicon were then double digested with *Bam*HI and *Pst*I so that the *eYFP* fragment could be ligated into pSV106 to form pSV107. This construct was sequenced with M13F, M13R, yfpBamF2 and yfpPstR4 primers to confirm correct ligation and orientation. Finally, the 1.5kb ORF of *VdATG8* was amplified from genomic Dvd-T5 with atgPstF2 and atg8PstR2 to generate an amplicon containing 5' and 3' *Pst*1 sites.

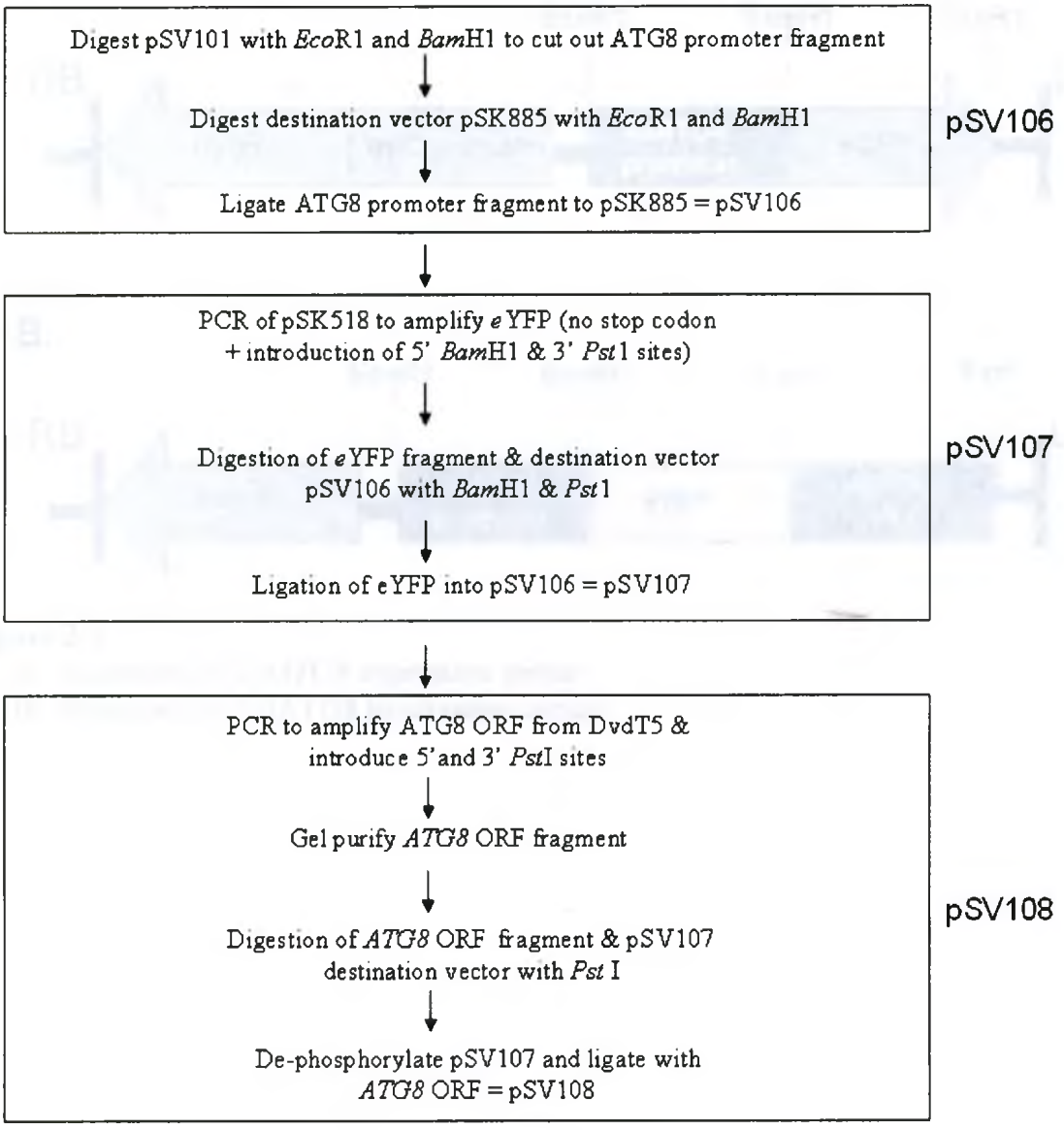

Figure 2.1 Flow chart for ATG8::*e*YFP$_N$ fusion protein construction

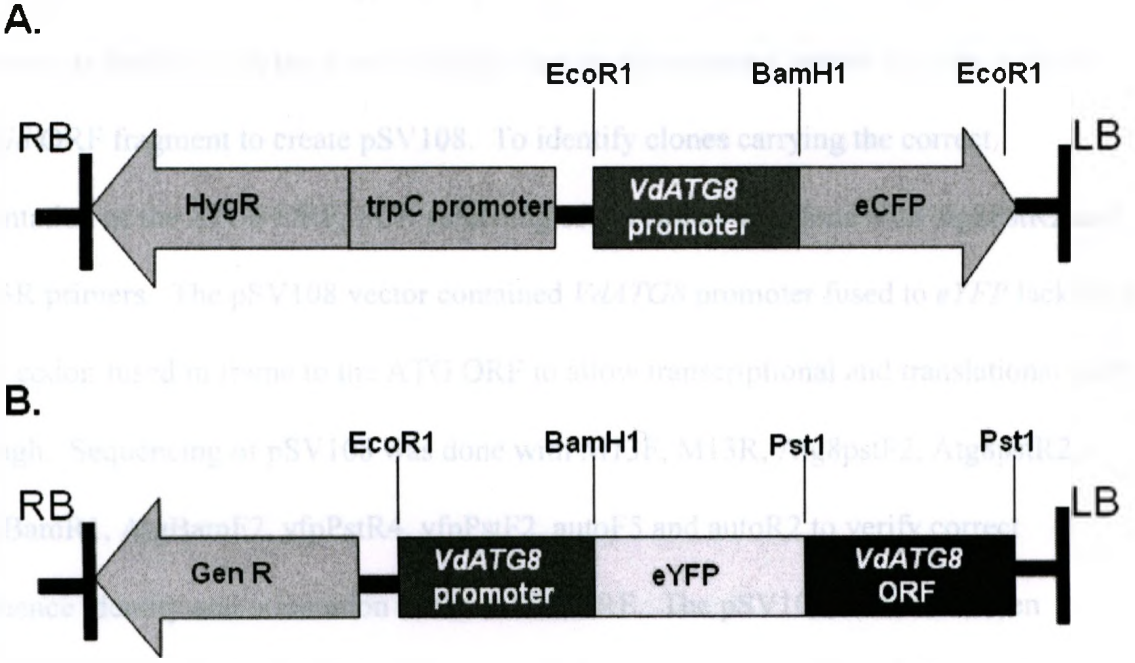

Figure 2.2

A. Schematic of *VdATG8* expression vector
B. Schematic of VdATG8 localization vector

The pSV107 vector and *ATG8* ORF amplicon were both digested with *Pst*I, and the vector was dephosphorylated with shrimp alkaline phosphatase before ligation with the *ATG8* ORF fragment to create pSV108. To identify clones carrying the correct orientation of the *ATG8* ORF, PCR screening of the clones was done with atg8PstR2 and M13R primers. The pSV108 vector contained *VdATG8* promoter fused to *eYFP* lacking a stop codon fused in frame to the ATG ORF to allow transcriptional and translational read though. Sequencing of pSV108 was done with M13F, M13R, Atg8pstF2, Atg8pstR2, AtgBamR1, AtgBamF2, yfpPstR4, yfpPstF2, autoF5 and autoR2 to verify correct sequence identity and orientation of the ATG8 ORF. The pSV108 vector was then introduced into Dvd-T5 via *A. tumefaciens*-mediated transformation and transformants were designated VDAT77.

2.2.3 *Agrobacterium tumefaciens*-mediated transformation (ATMT)

The methods for *A. tumefaciens*-mediated transformation of *V. dahliae* follow those described by Mullins et al. (2001) with modifications by Dobinson et al. (2004). *A. tumefaciens* colonies containing either pSV101 or pSV108 were grown in minimal medium supplemented with kanamycin (50 µg/mL) and chloramphenicol (25 µg/mL) for two days at 28°C. The *A. tumefaciens* cells were then diluted in induction medium to an optical density (OD_{600}) of 0.15, and grown for an additional seven hours at 28°C. An equal volume of cells was then mixed with 100 µL 10^6 Dvd-T5 or VDAT43 spores, and spread over a 0.45 µm pore, 45 mm diameter nitrocellulose filter (Whatman, Hillsboro, OR) overlaid onto co-cultivation agar media amended with 200 µM aceto-syringone. After two days incubation at 24°C, the filters were moved from co-cultivation medium to

selective medium (Complete Medium (CM) amended with cefotaxime (200 μM) and moxalactum (100 μg/mL) to kill *A. tumefaciens*, and hygromycin (25 μg/mL) or geneticin (50 μg/mL) to maintain selection). After a week, fungal transformants had generated clumps of mycelia on the filters. Twenty putative transformants from each transformation experiment were streaked out onto CM amended with hygromycin (25 μg/mL) or geneticin (50 μg/mL). Spores from these cultures were then streaked onto 1% water agar plates with a sterile wire loop. After incubating for 24 hours at 24˚C, single germinating conidia were transferred to CM amended with hygromycin (25 μg/mL) or CM amended with geneticin (50 μg/mL) and left to grow for a week at 24˚C.

2.2.4 Nucleic Acid Isolation

For DNA extraction, 200 mL flasks containing 35 mL liquid CM were inoculated with five mycelial plugs cut with a 0.5 cm cork borer from the growing margins of fungal cultures. The flasks were shaken at 150 rpm at 24°C for four days, and cultures were filtered though sterilized Miracloth (Calbiochem, La Jolla, CA) to remove the mycelia, and centrifuged at 1480 *g* for 10 min at 4 °C to pellet the spores. The spore pellets were then suspended in 1.5 mL microfuge tubes with 200 μL spore breakage buffer and glass beads (approximately 0.5 mm diameter) to just below the surface of the liquid. The suspensions were then alternately vortexed in pulses for 30 s, and placed on ice for 30 s (total of three min). DNA was then extracted with phenol:chloroform (1:1) followed by chloroform:isoamylalchohol (24:1), by vortexing 30 s, centrifuging at 1500 *g*, 5 min, 4°C. DNA was precipitated by addition of 0.5 volumes 7.5 M ammonium acetate and two volumes 100% ethanol (EtOH) in an overnight incubation at -20˚C. A 30 min

centrifugation pelleted the DNA, which was then washed once with 70% EtOH, and dissolved in 35 µL TE + 1 µg RNAseA/mL.

2.2.5 Southern blot hybridization analysis

Southern blot hybridizations were done as described by Dobinson et al. (2003). Approximately 600 ng of *Verticillium* genomic DNA was digested overnight with a restriction endonuclease, and size-fractionated by electrophoresis through 0.8% agarose gels made with 0.5X TBE buffer. The gel was soaked in 0.25 N HCl for 10 min. The DNA was denatured by soaking the gel in Southern denaturing buffer (0.4 N NaOH, 0.8 M NaCl) for 30 min, then in neutralization buffer (1.5 M NaCl, 0.5 M Tris-HCl pH 7.6) for 30 min. The DNA was then transferred to Hybond N+ membranes (Amersham Biosciences, Baie d'Urfe, QC) by capillary blotting with 20X sodium chloride-sodium phosphate-EDTA (SSPE) pH7.4 (3.6 M NaCl, 0.2 M $NaH_2PO_4 \cdot H_2O$, 0.02 M EDTA), and fixed to the membrane by UV cross-linking. Membranes were incubated for at least two hours at 65°C in prehybridization buffer (6X SSPE containing 1% skim milk, 0.5% sodium dodecyl sulfate (SDS) and 50 µg salmon sperm DNA /mL, then transferred to hybridization buffer (6X SSPE, 1% blocking reagent, 0.5% SDS) containing 10 ng digoxigenin (DIG)-labeled DNA hybridization probe, and incubated overnight at 65°C. The membranes were then washed three times for 20 min at 65°C in low stringency buffer (2x SSPE, 0.1% SDS, 0.1% sodium pyrophosphate) then three times (20 min at 65°C) with high stringency buffer (0.2X SSPE, 0.1% SDS, 0.1% sodium pyrophosphate). Chemiluminescent detection of hybridized probes was done using an antibody detection method, and the chemiluminescent alkaline phosphatase substrate CSPD® (Disodium 3-

(4-methoxyspiro{1,2-dioxetane-3,2'-(5'- chloro)tricyclo[3.3.1.13,7]decan}-4-yl)phenyl phosphate) (Roche Diagnostics, Indianapolis, IN) according to the manufacturer's directions, with two modifications: (1) DIG antibody was diluted 1:20000, and (2), CSPD® was diluted 1:2500. Finally, the chemiluminescent reaction was detected by exposing blots overnight to X-ray film (Curix Ultra UV-G-Plus Medical X-Ray film, Belgium).

The DIG-labelled DNA hybridization probes were synthesized for *ATG8* by the incorporation of DIG-labeled dUTP into PCR amplification products. Amplification reactions contained Platinum Taq polymerase (Invitrogen, Inc., Burlington, ON), DIG Labeling Mix (Roche Diagnostics, Indianapolis, IN), Dvd-T5 genomic DNA template (10 ng/μL), and autoF5 and autoR2 primers. Reaction conditions included an initial denaturation at 94°C for 2 min, then 30 amplification cycles of the following: denaturation at 94°C for 45 s, annealing at 65°C for 45 s, elongation at 72°C for 60 s, and a final extension at 72°C for 5 min.

2.3 Comparative Analyses:

2.3.1 Radial Growth, Colony Morphology and Microsclerotia Production

WT and KO strains were plated onto different types of media, and grown under different conditions to assess the effect of the *ATG8* KO on radial growth, colony morphology and microsclerotia development. Additionally, cells were grown on autophagy-inducing and –inhibiting media to determine how these conditions affected growth of WT and KO strains. Mycelial plugs from WT and KO strains were cut with a 0.5 cm cork borer and were plated onto basal medium (BM), BM lacking NO_3 (BM-N),

BM lacking glucose (BM-C), complete medium (CM), CM + 10ng rapamcyin/ml (an autophagy inducer), and CM+1mM 3-methyladenine (an autophagy inhibitor) and incubated at 24˚C. Cultures grown on CM and BM were also incubated at 24˚C and 28˚C. Radial growth was measured, and presence of MCS was noted at 7, 10, 14 and 21 days post inoculation. To examine MCS formation microscopically, cultures were sectioned, and stained with lactophenol acid fuchsin (100 mL distilled water, 100 mLcarbolic acid, 100 mL 85% lactic acid, 200 mL glycerin, 0.1% acid fuchsin). Two replicates were used for each treatment and experiments were done three times.

2.3.2 Conidiation

For comparison of sporulation on agar medium by WT and KO strains, cultures were grown on BM, BM-N, BM-C and CM media (200 µL agar on depression well slides). Ten µL aliquots of conidial suspension (at $1x10^4$ or $5x10^5$ spores/mL) were spread onto the slides, which were placed in a sterile chamber, incubated at 24˚C or 28˚C, and examined microscopically daily over a five day period. Two replicates were used for each treatment and experiments were performed three times.

2.3.3 Spore production in liquid from mycelia-inoculated cultures

In a liquid environment, *V. dahliae* and *V. albo-atrum* produce spores from mycelia, and from the spores themselves (yeast-like growth). To assess spore production in liquid from mycelia-inoculated cultures, CM plates were initiated with WT and KO spores from silica gel stocks and grown at 24°C for two weeks before 0.5 cm plugs were taken from the growing margins and used to inoculate 35 mL liquid CM or CM+1mM 3-methyladenine. Liquid cultures were grown at 24°C in the dark for four days in a shaking

incubator (150 rpm), harvested by filtering through sterilized Miracloth to remove the mycelia, and the filtrate centrifuged at 1480 *g* for 10 min to pellet the spores. Spores were re-suspended in 1 mL sterile distilled water, and counted with a hemacytometer. Statistical analysis was done using the t test where $P<0.01$ was deemed significant with n = 3 cultures/strain/experiment. Experiments were done three times.

2.3.4 Spore production in liquid from spore-inoculated cultures

To assess spore production in liquid-grown cultures inoculated with spores, $1x10^5$spores/mL were added to 5 mL liquid simulated xylem media (SXM), and grown in the shaking incubator (150 rpm) at 24°C for four days. Each treatment was done in triplicate and the experiment was done three times. Statistical analysis was done using the t test with n = 3 cultures/strain/experiment where $P<0.01$ was deemed significant.

2.3.5 Germination

Spores were harvested as described in section 2.3.3 and 100 spores from WT and KO strains were spotted in each of 5 locations on CM agar in 60x 15 mm plates. To aid visualization of spotted areas, a template containing five spots was printed onto transparency sheets and taped to the bottom of each plate prior to inoculation. Since two plates (10 spots) were counted at each time interval, a total of 12 plates were set up for each strain and incubated at 24°C. Immediately before viewing, spots were stained with lactophenol blue, and the numbers of germinated and ungerminated spores were counted every two hours between four and 14 hours post inoculation (hpi). Plates were discarded after counting. This experiment was done twice.

2.3.6 Glycogen Accumulation

CM agar cultures were initiated with WT and KO spores from silica gel stocks, and grown at 24°C for two weeks before 0.5 cm plugs were taken from the growing margins and plated onto CM. Glycogen accumulation was determined by inverting 7 and 14 dpi cultures for 15 min over a Petri dish containing one g iodine crystals; sublimated iodine strains glycogen purple (Sigma-Alderich, St. Louis MO). Cultures were photographed immediately afterwards.

2.3.7 Microscopy to assess *VdATG8* expression and localization

VdATG8 expression and VdATG8 localization were visualized with depression well slide cultures: 10 µL of $5x10^5$ or $1x10^4$ spores/mL of VDAT 74, 75 or 77 were spread onto 200 µL BM agar, and incubated at 24˚C or 28˚C. Cultures grown from suspensions of $5x10^5$ spores/mL were used to examine MCS formation, while suspensions of $1x10^4$ spores/mL enabled examination of conidiophore development. Over a five day period, the depression well cultures were examined daily with a Leica TCS SP2 confocal scanning microscope with HCPL Fluotar, 10x, 4 mm objective. Images were captured in cyan, yellow and transmitted light channels using integrated Leica software (Leica Microsystems, Wetzler, Germany).

Slide cultures were used for staining with monodansylcadaverine (MDC) (Sigma-Aldrich), which selectively stains autophagosomes (Biederbick, 1995). Agar plugs (1.0 cm^2) from BM, BM-N, CM, CM+10 ng rapamycin/mL and CM+1 mM 3-methyladenine were inoculated on all four sides with 1 µL $1x10^7$ spores from VDAT 77, wild-type and mutant strains. Sterile coverslips were placed over the agar plugs, and the slides were

incubated in a moist, sterile chamber at 24˚C for four days. Four hours prior to staining with MDC, 10 µL 2 mM serine protease inhibitor phenylmethylsulfonyl fluoride (PMSF), was added directly to the slide to delay autophagosome degradation. Cultures were stained for 10 min with 50 µM MDC solution, de-stained with water, and visualized with the Leica TCS SP2 confocal scanning microscope and UV laser.

2.4 *In planta* Analyses

2.4.1 Pathogenicity assays with *V. dahliae* and *V. albo-atrum*

CM agar was inoculated with silica stocks, and cultures were grown at 24°C for two weeks before 0.5 cm plugs from the growing margins were used to inoculate 200 mL flasks containing 35 mL liquid CM. Spores were harvested as described in section 2.3.3. Spores were re-suspended in sterile distilled water, counted with a haemocytometer and diluted to 5 x 10^7 spores/mL in 10 mL 0.5% gelatin. Sand-grown Bonny Best tomato seedlings (14 day-old) were gently extracted from the sand, and their roots were rinsed with distilled water before a two minute root dip inoculation into either the spore suspension (pathogen treatment), or 0.5% gelatin (mock-inoculated treatment). Ten plants were inoculated for each treatment. All seedlings were planted into 4-inch pots of pre-moistened PROMIX (Premier Horticulture, Inc., Red Hill, PA). Fertilization with 1X 20-20-20 (Plant-Prod®, Brampton, Ontario) was done once per week. Plants were grown at 24˚C with 16 hours of light per day. Disease symptoms were visually scored once a week over four weeks using a previously defined rating system (Klimes & Dobinson 2006). At four weeks, the plants were cut 1 cm above the soil line so that the whole plant

could be weighed. All experiments were done twice. The t test was done where $P<0.01$ was deemed significant with n = 10 plants/strain/experiment.

2.4.2 Stem section analysis to assess *in planta* colonization

To qualitatively determine fungal presence relative to symptom development, and potential differences in the rate of plant colonization by wild-type and *vdatg8*-KO strains, 0.5 cm sections of root, stem and leaf sections were cut from three week old Bonny Best tomatoes that had been root dip inoculated with *V. dahliae* spores as described in section 2.4.1. Prior to sectioning, the entire plant was surface sterilized by immersion into 1.5% hypochlorite solution for 30 s, rinsed three times with sterile water and air dried on sterile paper towels. The sections were placed on a semi-selective agar medium (Soil Pectate Tergitol) (SPT) (Hawke & Lazarovits 1994) agar and incubated at 24°C. Every four hours post-inoculation three plants from each treatment were sectioned, from zero hours to 60 hours. Statistical analysis was done using the t test with n = 3 plants/strain/experiment where $P<0.01$ was deemed significant.

2.4.3 Quantitative PCR analysis of *V. dahliae* DNA in plant tissue

Three week old Bonny Best tomato seedlings were root dip inoculated with spores from wild-type and mutant strains as described above. Plants were surface sterilized as described in section 2.4.2, and DNA was extracted from single 1.5 cm stem sections that were cut from the apex of the plant. Every two days over a 14 day period post-inoculation, stem sections from two plants per treatment were collected, and frozen in liquid nitrogen.

To extract DNA from the stem, two sections from each time point (i.e. two plants) were pooled and ground to a fine powder in liquid nitrogen with a mortar and pestle. The DNA extraction protocol was modified from that described by Murray & Thompson (1980). The ground plant tissue (0.05 g) was homogenized by vortexing 30 s in 1.8 mL extraction buffer (0.7 M NaCl, 50 mM TRIS, 10 mM EDTA, 2% CTAB, 1% β-Mercaptoethanol), and then incubated for 30 min at 70°C. Once samples had cooled to room temperature, DNA was extracted by mixing with $CHCl_3$: isoamyl alcohol (24:1) and centrifuged at 12 000 *g* for 15 min. The aqueous (upper) phase was precipitated with 0.7 volume of 2-isopropanol and spun at 12 000 *g* for 45 min to pellet the nucleic acids. The resulting pellet was washed with 70% ETOH, air dried and re-suspended in 1xTE (10 mM TRIS, 1 mM EDTA pH8) with RNaseA (1 µg/mL). DNA concentration was determined with the Nanodrop 1000 3.6.0 Spectophotometer (Thermo Scientific, Wilmington, DE, USA).

The amount of *V. dahliae* DNA in infected plant tissue was quantified using a competitive PCR assay (Hu et al 1993). For these assays, the pVDint2 plasmid containing the *V. dahliae* ribosomal RNA internal transcribed spacer (ITS) sequence (supplied by Dr. Jane Robb, University of Guelph) was used as the internal control (IC) template. A 230 bp product is amplified from this plasmid using the ribosomal RNA internal transcribed spacer (ITS) sequence primers, VD1 and VD2, while the same primer set amplifies a 300 bp product from DNA isolated from infected plant tissue. Twenty-five µL PCR amplification reactions contained 0.05 mM of each deoxynucleotide triphosphate, 5 pmol of each oligonucleotide primer, 1 pg internal control template, 0.5

unit of Platinum TAQ polymerase, and 1 uL of DNA extracted from plant tissue. PCR amplification included an initial two minute denaturation step at 94°C, followed by 29 cycles of denaturation at 94°C for 30 s, annealing at 65°C for 30 s, and elongation at 72°C for one min, and a final 5 min elongation step at 72°C. Amplicons were visualized on 0.8% agarose gels and quantified using Molecular Analyst Software (Quantity One 4.4.1 BioRad, Hercules, CA).

Fungal biomass was quantified against a standard curve. Since previous studies established that 1pg of internal control allowed amplification of both the internal control, and the lowest concentration of fungal DNA extracted from plant tissue, a standard curve was generated from purified Dvd-T5 genomic DNA ranging from 0.001 ng to 10 ng, in the presence of 1 pg internal control (Hu et al. 1993). The ratio between purified DNA and 1pg internal control template yielded a standard curve via non linear regression. To determine the concentration of extracted fungal DNA, the ratio of fungal amplicon to internal control template were fitted to the equation of the standard curve.

2.5 Gene Expression Assays

2.5.1 RNA extraction

For agar-grown cultures, plates of BM and CM agar were overlaid with cellulose membranes (Research Products International, Mount Prospect, IL), and inoculated by spreading $1x10^6$ spores from wild-type and mutant strains over the cellophane surface. After two days growth, the membranes were moved to BM, BM-N, BM-C, CM, CM+ 10ng rapamycin/ml or CM+1mM 3-methyladenine media, and grown for another 2 days. To assess the influence of time and temperature on relative expression levels of *VdATG8*,

the fungal strains were inoculated onto CM agar overlaid with cellophane, and grown for two, four and seven days at 24˚C and 28˚C. Mycelia was then scraped off the cellophane into liquid nitrogen and ground with mortar and pestle. Liquid grown cultures were inoculated with 0.5 cm mycelial plugs, and grown for four days in 200 mL flasks containing 35 mL liquid CM, and grown in a shaking incubator (150 rpm). Mycelia and spores were separated via filtration through sterile Miracloth. Mycelia was frozen immediately, while the spores were pelleted by centrifugation at 1500 *g* for 10 min before freezing and grinding. RNA was then extracted from 100 mg of each sample with an RNeasy® Plant Mini Kit (Qiagen, Maryland USA) following the manufacturer's directions. The amount of RNA was determined with the Nanodrop (Thermo Scientific) and quality was assessed using the 2100 Bioanalyzer (Agilent, Waldbronn, Germany).

2.5.2 Quantitative RT-PCR of *VdATG8*

For reverse transcription (RT)-PCR, 1 µg RNA was treated with DNase I, and reverse-transcribed with SuperScript™ II reverse transcriptase and oligo $(dT)_{12-18}$ primer (Invitrogen Canada Inc.), according to the manufacturer's instructions. *VdATG8* and *V. dahliae* actin gene sequences were amplified from cDNA and genomic DNA using autophagy primers, autoF5 and autoR2, and actin primers, HO2-1 and HO2-2, respectively.

For quantitative RT-PCR (qRT-PCR), intron flanking primers were used to amplify actin, β-tubulin and *VdATG8* genes. Each amplification reaction contained 5 µl SsoFast™ EvaGreen® super mix (BioRad, Hercules, CA), 300 µM of each primer, 2.5 µL cDNA template and sterile distilled water to a final volume of 10 µL. PCRs were

done in 96 well WHT-CLR hard shell microtitre plates sealed with Microseal® 'B' Film (BioRad, Hercules, CA).

Standard curves for the qRT-PCR assays were generated for *ATG8*, actin, and β-tubulin genes using svt-q-atg8-F4/svt-q-atg-R6, AK1F-actin/AK1R-actin and AK2F-Btub/AK2R-Btub primers, respectively (Appendix I), and 10-fold dilutions of template cDNA from 4 day-old cultures grown on CM. PCR amplification was done in a BioRad CFX96 real time cycler with an initial 3 min denaturation followed by 34 cycles of 10 s denaturation at 95˚C and 30 s annealing at 58˚C. The melting curve started at 65˚C, and increased by 0.05˚C increments to 95˚C. Relative transcript abundance was calculated using the Delta-Delta CT method with BioRad CFX manager software version 1.6.

To study the effect of autophagy–inducing and –inhibiting conditions on *VdATG8* gene expression, cDNA was prepared from cultures grown on CM, CM+rapamycin, CM+3-methyladenine, BM, BM-C, or BM-N. Triplicate reactions containing 2.5 µl of the 1/5 dilutions of cDNA from each culture were set up with actin, autophagy and β-tubulin primers. Thus, a total of 9 wells with each type of cDNA were set up, with 3 wells allotted for each primer pair. To control for genomic contamination in the cDNA, negative controls (lacking reverse transcriptase) in duplicate for each cDNA. To control for contamination in reagents, no template controls were set up in triplicate for each primer pair. For each qRT-PCR experiment, three wells in the plate were reserved for a calibrator sample of cDNA from a CM-grown culture.

The setup described above was used to study the effect of growth temperature on relative expression of *VdATG8*. cDNA was extracted from cultures grown on CM at

24°C or 28°C for two, four, or seven days and diluted 1/5. For each cDNA sample triplicate reactions were set up with each of the aforementioned primer sets, and the same no reverse transcriptase, and no template controls were used.

2.5.3 RT-PCR for Gene Expression Studies

RT-PCR analysis was done for two experiments: 1) to determine whether *ATG8* was expressed in hydrophobin (*vdh1*) and map kinase (*vmk1*) mutants, and conversely, if *VDH1* and *VMK1* were expressed in *vdatg8* and *vaatg8* strains, and 2) to determine whether expression of other putative autophagy genes was altered in *vdatg8* or *vaatg8* mutant strains.

RNA was extracted as described in section 2.5.1 from wild-type and *atg8, vdhl,* and *vmk1* knockout strains of *V. dahliae* and *V. albo-atrum* grown for 2 and 4 days on BM or CM agar. RT-PCR was done as described in section 2.5.2. Briefly, 1 μg of RNA was treated with DNase I, and reverse-transcribed with SuperScript™ II reverse transcriptase and oligo $(dT)_{12-18}$ primer (Invitrogen Canada Inc.) according to the manufacturer's instructions. cDNA quality was assessed by amplification of the actin gene (HO2-1 and HO2-2 primers) using the standard PCR protocol: initial denaturation at 94°C for 2 min, then 30 amplification cycles of the following: 94°C for 45 s, 65°C for 45 s, 72°C for 60 s, with a final extension at 72°C for 5 min.

The standard PCR protocol described above was used to amplify all three genes, with an annealing temperature of 65°C for *VMK1* and *VdATG8*, and 60°C for *VDH1*. *VMK1* was amplified from *vdatg8* and *vaatg8* cDNA with VMK 1F and VMK 2R primers, while the *ATG8* gene homolog was amplified from *vdh1* and *vmk1* cDNA with

autoF2 and autoR2 primers, and *VDH1* was amplified from *atg8* cDNA with C24-1A and C24-2A primers.

To identify in *V. dahliae* and V. *albo-atrum* homologs of other autophagy genes (ATG1, 3, 12, and 16) a feature search was done of the Saccharomyces Genome database (SGD http://www.yeastgenome.org/cgi-bin/seqTools). Protein sequences from the SGD were then compared to sequences in the Broad Institute Verticillium Group Database (BIVGB) using the National Centre for Biotechnology Information (NCBI) Basic Local Alignment Search Tool (BLAST) program. The resulting hits were then compared (by BlastP analysis) to the sequences of the NCBI protein databases. Finally, an alignment using CLUSTALW (Higgins et al. 1996) was done to compare the protein sequences from SGD with those identified in BIVGB, and other fungal autophagy genes identified by the BLAST analyses.

Intron-flanking primers were designed from the BIVGB sequences. ATG 3, 12 and 16 gene homologs were amplified with atg3F2/R6, atg12F5/R3 and atg16F1/R1 primer sets respectively, using touchdown PCR: initial 2 min denaturation at 95°C, 15 amplification cycles of the following: 95°C for 45 s, 70°C for 45 s, 72°C for 90 s, then 20 amplification cycles of 95°C for 45 s, 60°C for 45 s, 72°C for 90 s, with a final extension of 72°C for 5 min. The *ATG1* sequence was amplified with the atg1F2/R1 primer set using the standard protocol, and an annealing temperature of 60°C.

CHAPTER 3: RESULTS

3.1.1 Colony morphology

Morphological comparative analysis was done of *V. dahliae* and *V. albo-atrum* wild-type and *ATG8* knockout strains (*vdatg8* and *vaatg8*, respectively). With our standard growth medium and conditions (complete media (CM) at 24˚C), the mycelium of *V. dahliae* WT colonies appeared white, while *vdatg8* colonies had distinctive cream coloured centres surrounded by a 0.5 cm white, outer margin of the growing colony (Figure 3.1A). Examination of the underside of colonies showed that WT colonies were producing microsclerotia (MCS), but that *vdatg8* were not (Figure 3.1B). However, when grown at 28˚C, WT colonies produced more MCS than they did at 24˚C, and *vdatg8* colonies also produced MCS (Figure 3.1B). Thus, under these standard growth conditions, *vdatg8* mutants were found to have a defect in MCS formation.

V. albo-atrum WT and knockout (*vaatg8)* cultures produced dark resting mycelia (DRM) at 24˚C on CM (Figure 3.2A) and both and KO cultures produced more DRM at 28˚C than at 24˚C (Figure 3.2A).

A.

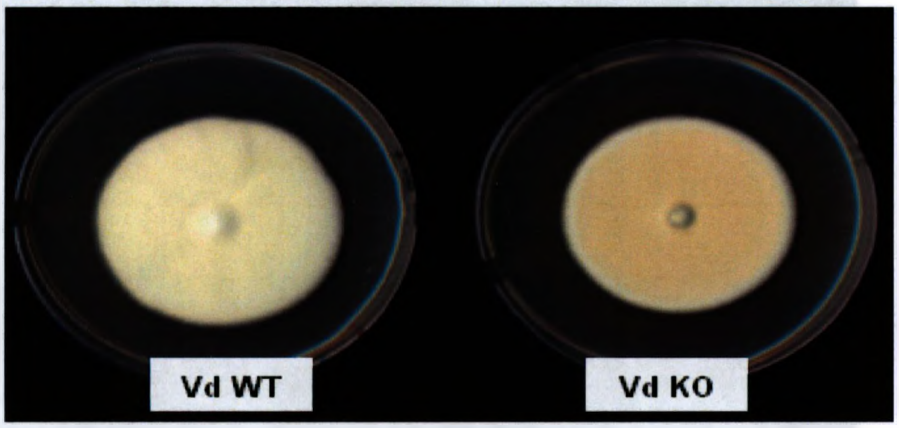

B.

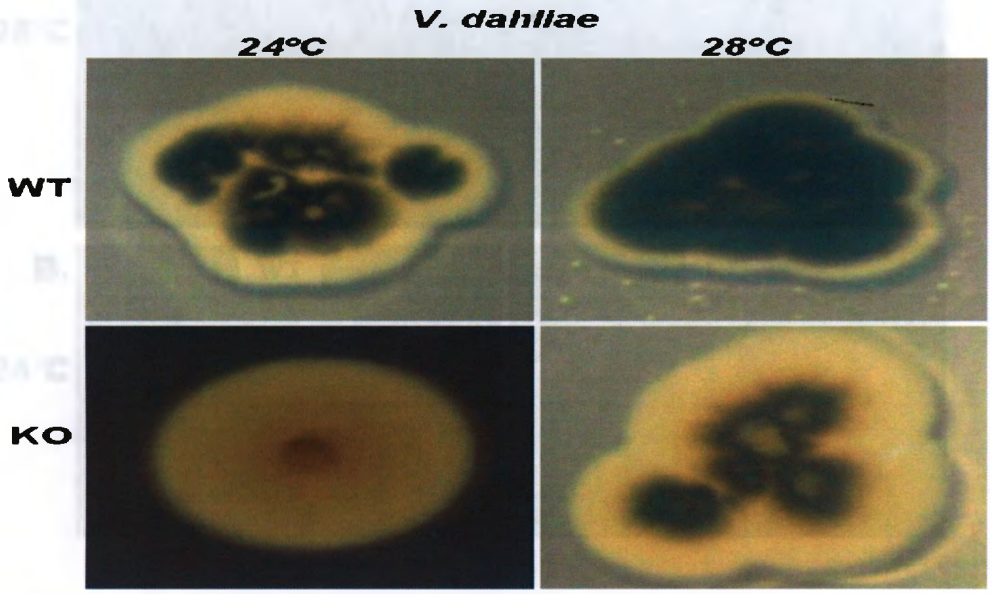

Figure 3.1 Effect of temperature on MCS formation by *V. dahliae* WT and *vdatg8* KO cultures. A. Colony morphologies of WT (Dvd-T5; left panel) and KO (VDAT38-5; right panel) cultures grown for 14 days on CM at 24˚C. **B.** Cultures were grown on CM for seven days. WT and KO cultures in the left panels were grown at 24˚C, while cultures on the right panels were grown at 28˚C. Top panels: WT cultures produce some MCS at 24˚C, and even more at 28˚C. Lower panels: *vdatg8* does not produce MCS at 24˚C, but does at 28˚C.

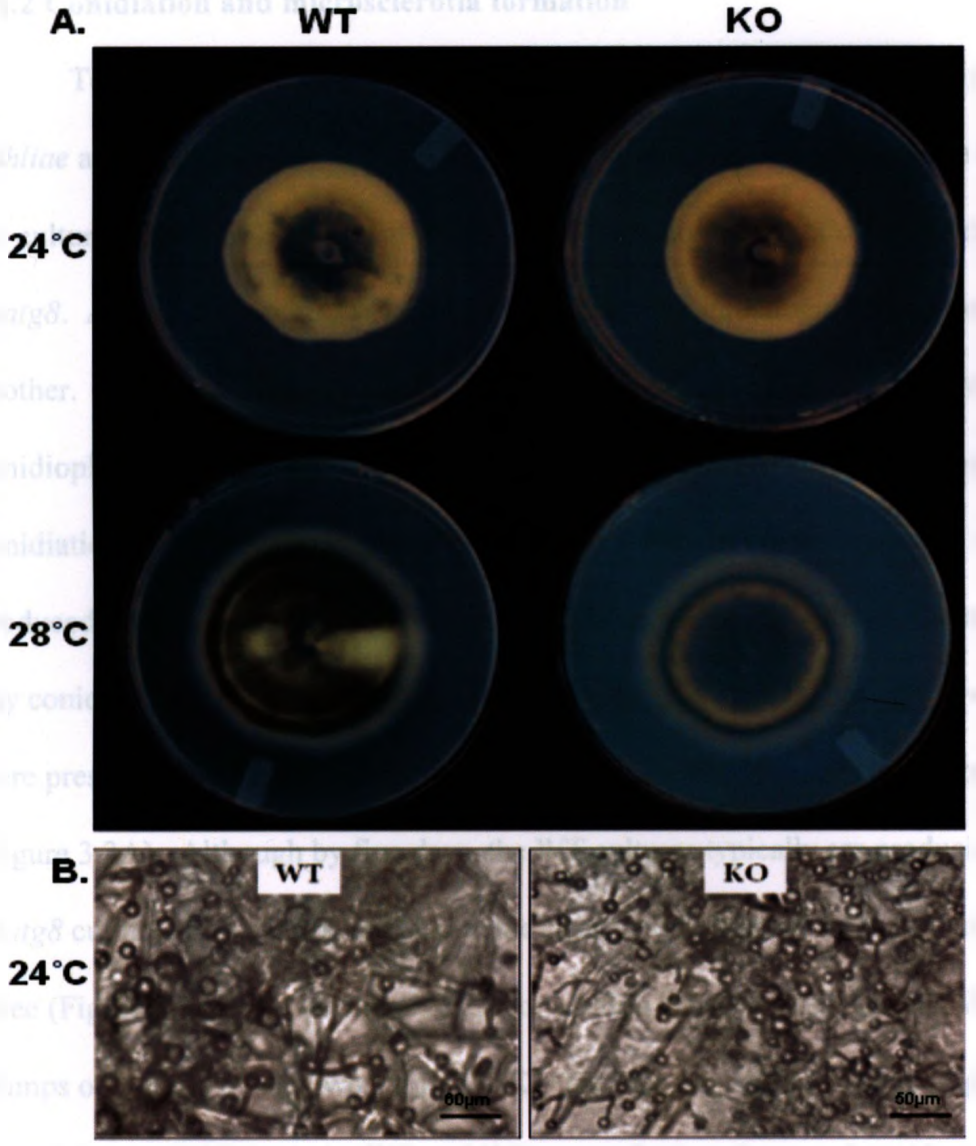

Figure 3.2 Effect of temperature on DRM formation and conidiation in *V. albo-atrum* WT and KO cultures. A. All cultures were grown on CM for seven days. WT (383-2) and KO (VAAT10-12) cultures produce DRM at 24˚C (upper panel). DRM production is greater for both WT (383-2) and KO (VAAT10-12) cultures at 28˚C (lower panel). **B.** WT (383-2) and KO (VAAT10-12) cultures were grown on depression well slides for three days on BM at 24˚C and examined microscopically. Scale bar for the WT is 60µm and 50µm for the KO.

3.1.2 Conidiation and microsclerotia formation

To examine conidiation and resting structure production more closely in *V. dahliae* and *V. albo-atrum* WT and KO strains, microscopy was done over a time course for cultures grown at 24˚C and at 28˚C. There were no defects or delays in conidiation in *vaatg8*. At each time point, WT and KO cultures were indistinguishable from one another. As seen in Figure 3.2B, by day three both WT and KO cultures were producing conidiophores and conidia. As anticipated from the observed colony morphologies, conidiation in *vdatg8* was defective at 24˚C. As shown in Figure 3.3A, WT cultures produced conidia at two days post inoculation (dpi), while KO cultures did not produce any conidia. At three dpi, KO hyphae were swollen and septate, but very few conidia were present compared to WT cultures, which had produced many clusters of conidia (Figure 3.3A). Although by five days, the WT cultures typically are producing MCS, *vdatg8* cultures appeared be arrested at the same developmental stage as that seen at day three (Figure 3.3A). However, at 28˚C, conidiation is accelerated, and the WT produces clumps of conidia by day two, while the KO has swollen septate hyphae (Figure 3.3B). By day five at 28˚C, both the WT and KO are producing clumps of conidia, and MCS initials (Figure 3.3B). Thus, increased temperature accelerates MCS formation in the WT and restores MCS formation in the KO. The appearance of melanized MCS in *vdatg8* indicates that temperature can restore the wild-type phenotype in *vdatg8*.

Figure 3.3 Effect of growth temperature on conidiation and MCS formation in *V. dahliae* WT and *vdatg8* KO cultures. Cultures were grown on BM agar in depression well slides for five days at 24°C (A) and 28°C (B). **A**. Top panels: KO (VDAT38-5) shown at two, three and five days post inoculation. Scale bars represent (left (L) to right (R)) approximately 110, 100, and 120μm respectively. Arrows indicate swollen hyphae (KO day three), clumps of conidia (WT day three),and MCS (WT day five). Lower panels: WT (Dvd-T5) shown at two, three and five days post inoculation. Scale bars represent (left to right) approximately 100, 85, and 80 μm respectively. **B.** Top panels: KO (VDAT38-5) shown at 2, 3 and 5 days post inoculation. Scale bars represent (L to R): approximately 100, 100 and 80 μm respectively. Lower panels: WT (Dvd-T5) shown at two, three and five days post inoculation. Scale bars: (L to R) approximately 100, 80 and 100 μm.

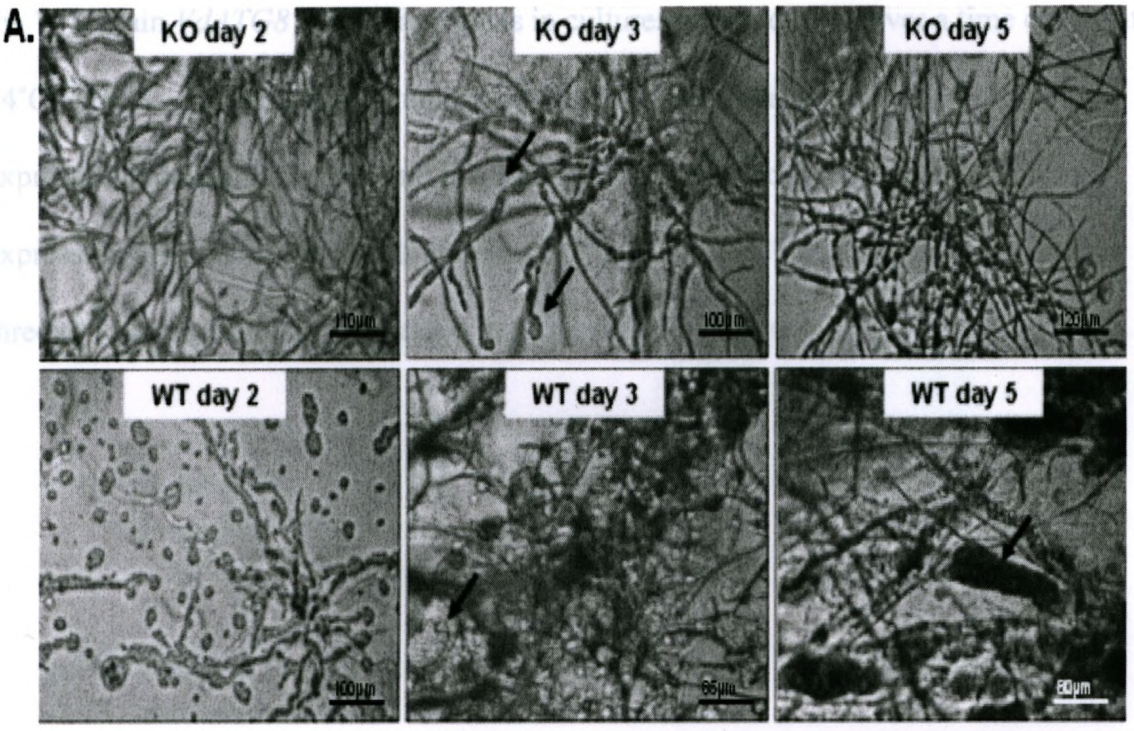
A.
KO day 2
KO day 3
KO day 5
WT day 2
WT day 3
WT day 5
B.
KO day 2
KO day 3
KO day 5
WT day 2
WT day 3
WT day 5

3.1.3 Influence of temperature on *VdATG8* expression

Quantitative reverse transcriptase PCR (qRT-PCR) was done to assess changes in the WT strain *VdATG8* expression levels in cultures grown on BM over a time course at 24˚C or 28˚C. As shown in Figure 3.4, at 24˚C, it takes four days before *VdATG8* is expressed at detectible levels, and this expression is elevated by day seven. This expression coincides with development, since at 24˚C conidiation occurs between days three to four, and microsclerotia develop from day five onwards (Figure 3.3A).

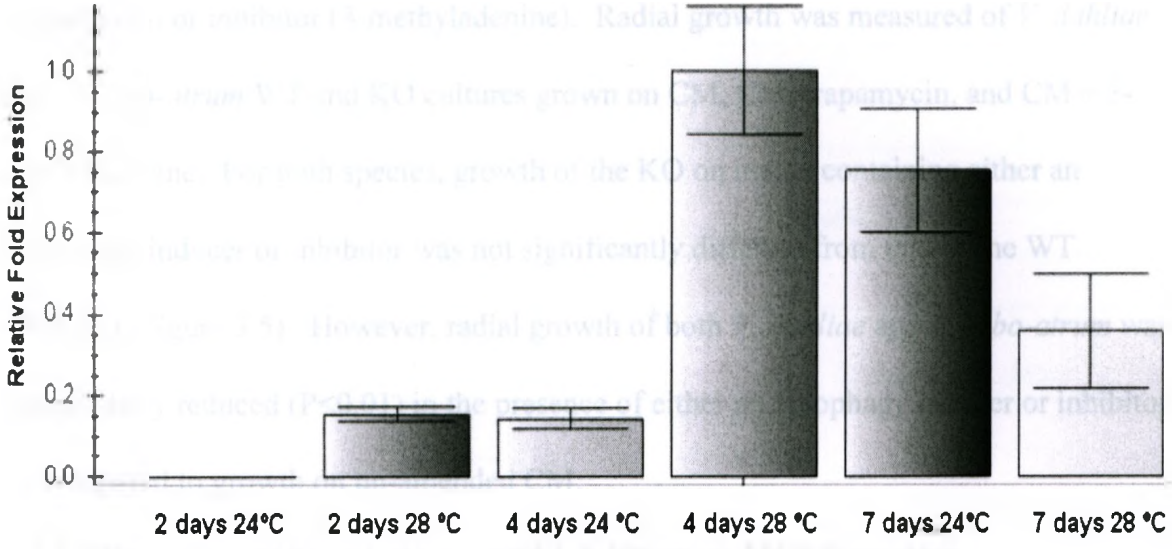

Figure 3.4 Effect of temperature on *VdATG8* expression levels over time.

Quantitative reverse transcriptase (qRT)-PCR of *VdATG8* transcript levels in Dvd-T5 cultures grown for two, four or seven days at 24˚C or at 28˚C on BM. *VdATG8* transcript levels were measured relative to those of β-tubulin.

3.1.4 Effect of autophagy inducers and inhibitors on radial growth

To understand the effect of autophagy on radial growth of both wild-type and *atg8* disrupted strains, strains were grown on media amended with an autophagy inducer (rapamycin) or inhibitor (3-methyladenine). Radial growth was measured of *V. dahliae* and *V. albo-atrum* WT and KO cultures grown on CM, CM +rapamycin, and CM + 3-methyladenine. For both species, growth of the KO on media containing either an autophagy inducer or inhibitor was not significantly different from that of the WT ($P>0.01$) (Figure 3.5). However, radial growth of both *V. dahliae* and *V. albo-atrum* was significantly reduced ($P<0.01$) in the presence of either an autophagy inducer or inhibitor as compared to growth on un-amended CM.

3.1.5 Effect of autophagy inducers and inhibitors on MCS formation

In addition to measuring radial growth of cultures grown on media amended with autophagy inhibitors or inducers, colony morphology and resting structure formation was also examined macroscopically and microscopically. In order to visualize developing MCS cultures were sectioned, and stained with lactophenol acid fuchsin prior to microscopic examination. *V. dahliae* WT cultures treated with rapamycin (autophagy inducer) produced melanized MCS initials, and intriguingly, chains of swollen, hyaline cells that could be precursors to MCS, while the KO produced only a few melanized MCS, and no chains of hyaline, swollen cells (Figure 3.6). Conversely, when treated with the autophagy inhibitor 3-methyladenine, neither WT nor KO cultures produced MCS (Figure 3.6). Hyphae in both cultures remained undifferentiated, and did not exhibit the swelling or septation that typically precedes MCS development.

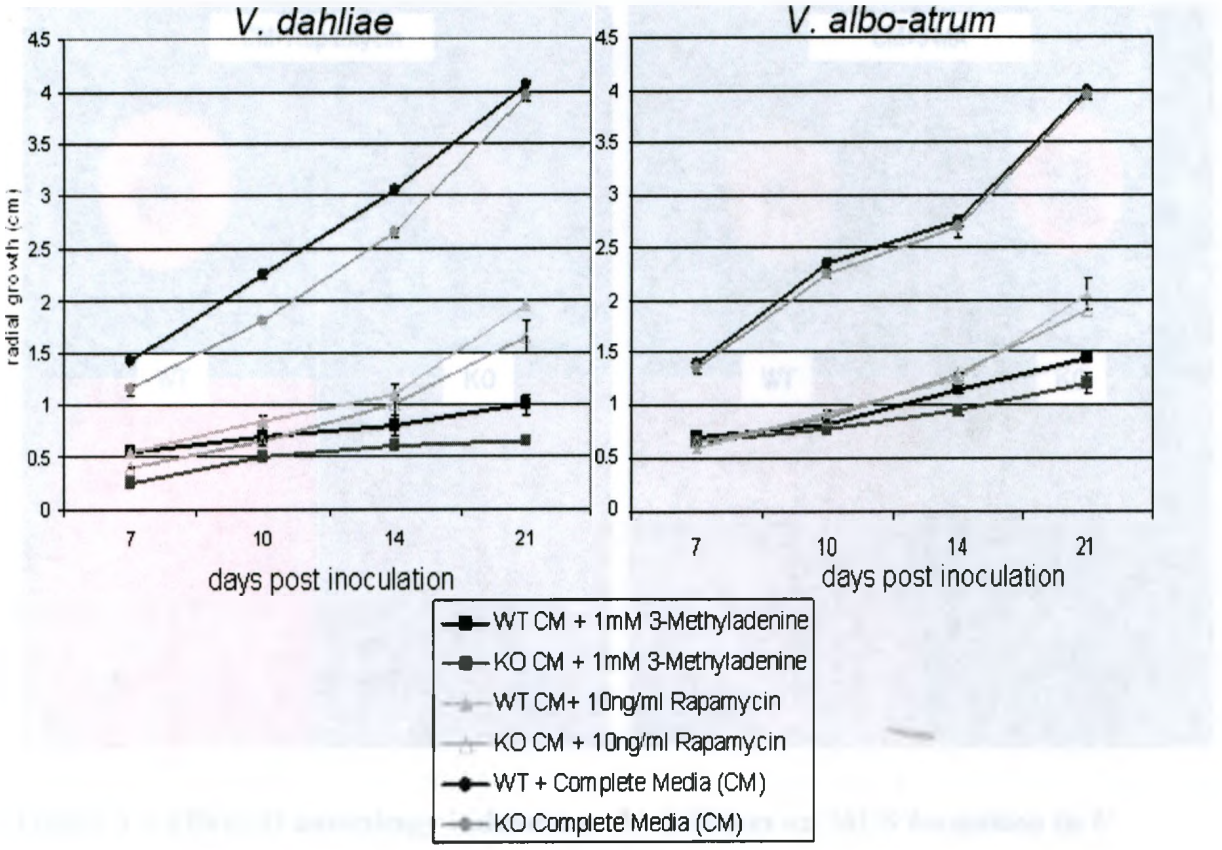

Figure 3.5 Effect of autophagy inducers and inhibitors on radial growth of *V. dahliae* and *V. albo-atrum* WT and *atg8* KO cultures. Radial growth (cm) is shown of *V. dahliae* (left panel) and *V. albo-atrum* cultures (right panel) grown at 24˚C on CM, CM + 10ng/μLrapamycin or CM + 1mM 3-methyladenine.

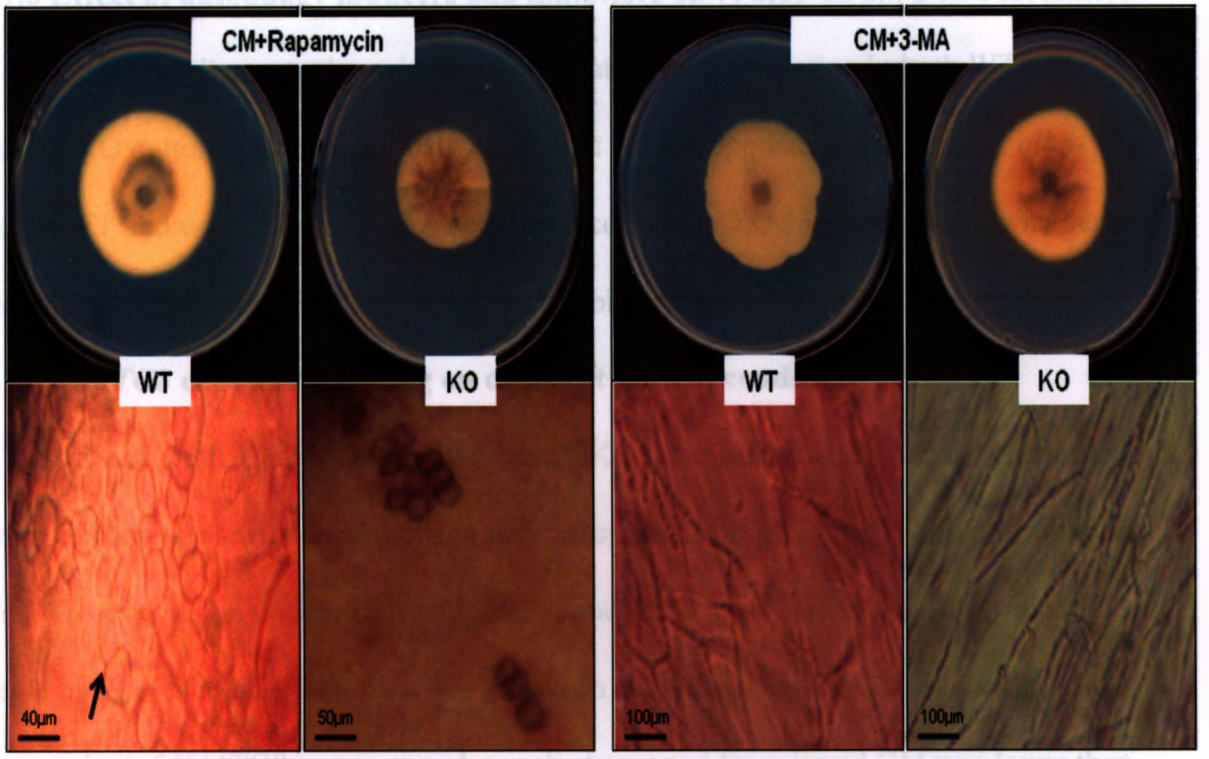

Figure 3.6 Effect of autophagy inducers and inhibitors on MCS formation in *V. dahliae* Underside of 14 day old cultures grown at 24°C. Top left panel: colonies of WT (Dvd-T5) and KO (VDAT38-5) on CM amended with rapamycin (autophagy inducer). Lower left panel: microscopic view of sectioned colonies stained with lactophenol acid fuchsin. Scale bar for WT is approximately 40 µm and 50 µm for KO. Top right panel: colonies of WT and KO on CM amended with 3-methyladenine (3-MA; autophagy inhibitor). Lower right panel: microscopic view of colonies treated with lactophenol acid fuchsin. Scale bars for WT and KO are approximately 100 µm.

3.1.6 Effect of autophagy inducers and inhibitors on *V. albo-atrum* DRM formation

In *V. dahliae* autophagy inducers promoted MCS formation in both WT and *vdatg8* KO cultures, while autophagy inhibitors did the opposite. However, *V. albo-atrum* WT and *vaatg8* KO cultures both produced some DRM irrespective of whether the medium was treated with an inducer or an inhibitor (Figure 3.7).

3.1.7 *VdATG8* expression during on different growth conditions

Since, both *V. dahliae* WT and *vdatg8* KO strains exhibited different phenotypes on media amended with an autophagy inducer or inhibitor, qRT-PCR was done to assess *VdATG8* expression under different growth conditions. *VdATG8* expression varied depending on whether *V. dahliae* was grown on solid medium or in liquid media. Expression of *VdATG8* in spores and mycelia harvested from liquid CM was lower than expression during growth on CM agar (Figure 3.8). Expression on autophagy-inducing media was slightly higher than on autophagy-inhibiting media, however amendment with either agent greatly reduced *VdATG8* expression compared to that in unamended CM (Figure 3.8).

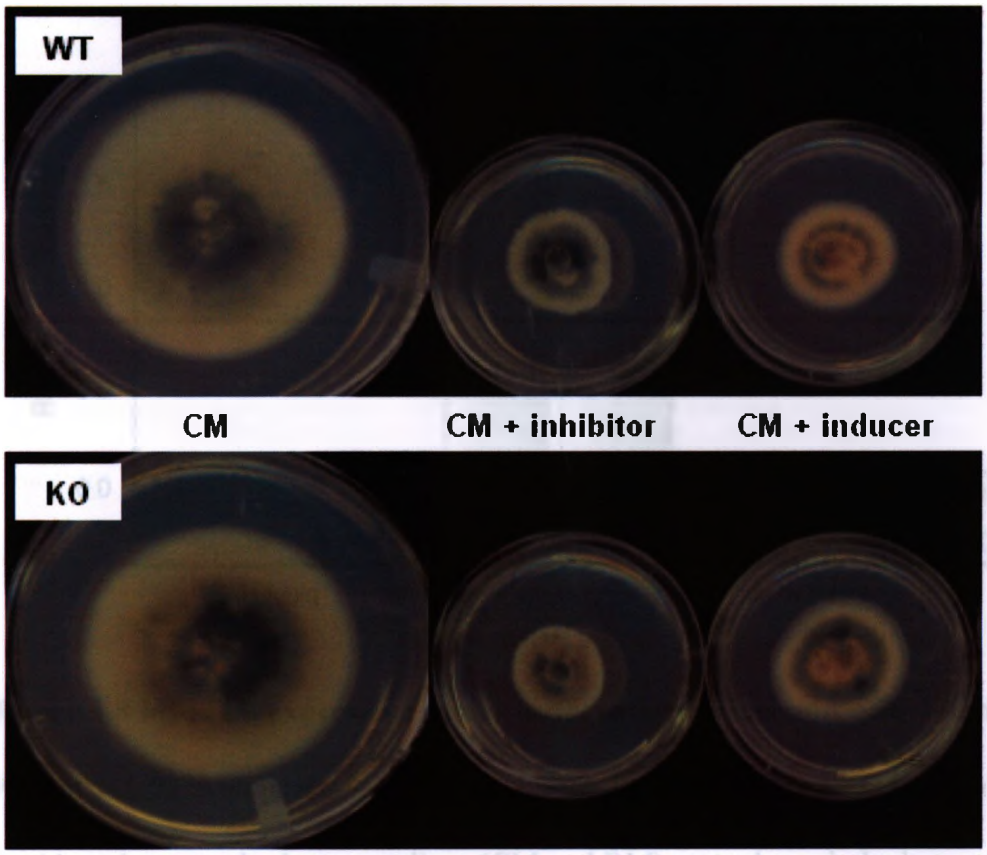

Figure 3.7 Effect of autophagy inducer and inhibitor on DRM formation in *V. albo-atrum* Underside of 14 day old *V. albo-atrum* cultures grown at 24˚C. Cultures (left to right) were grown on CM, CM + 3-methyladenine (inhibitor), and CM + rapamycin (inducer). WT cultures are shown on the top panel, and *vaatg8* KO cultures are shown on the lower panel.

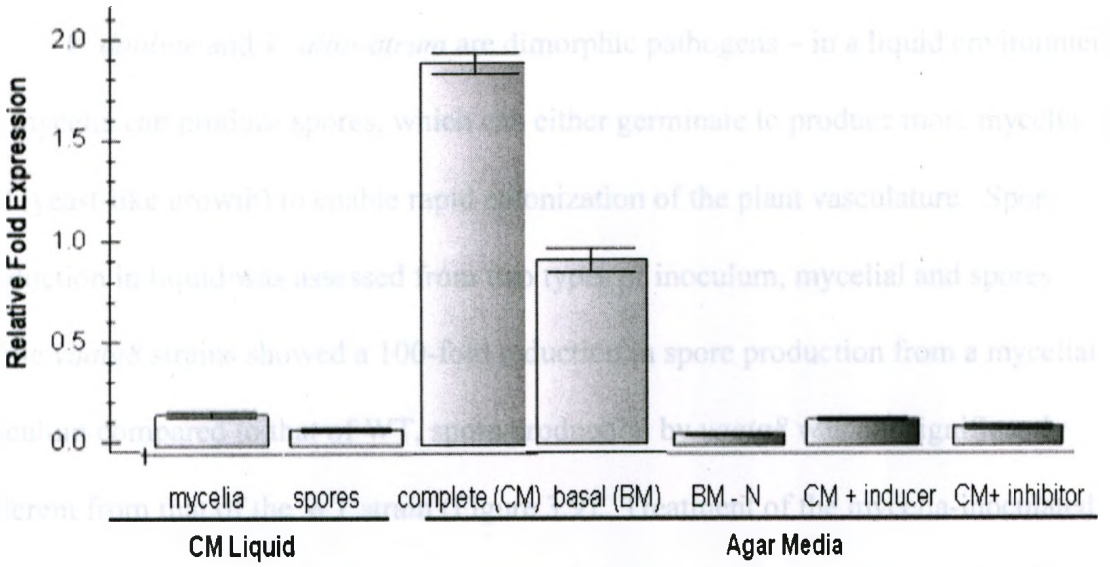

Figure 3.8 *VdATG8* expression under different growth conditions. Quantitative RT-PCR of *VdATG8* transcript levels in Dvd-T5 cultures grown at 24˚C for four days in CM liquid, and on standard agar medium (CM and BM), autophagy-inducing media (CM+rapamycin and BM lacking nitrate) and autophagy-inhibiting medium (CM+3-methyladenine). *VdATG8* transcript levels were measured relative to those of β-tubulin.

3.1.8 Dimorphic growth

V. dahliae and *V. albo-atrum* are dimorphic pathogens – in a liquid environment, the mycelia can produce spores, which can either germinate to produce more mycelia, or bud (yeast-like growth) to enable rapid colonization of the plant vasculature. Spore production in liquid was assessed from two types of inoculum, mycelial and spores. While *vdatg8* strains showed a 100-fold reduction in spore production from a mycelial inoculum compared to that of WT, spore production by *vaatg8* was not significantly different from that of the WT strain (Figure 3.9). Treatment of the mycelia-inoculated cultures with the autophagy inhibitor 3-methyladenine eliminated spore production in *vdatg8*, and significantly reduced spore production in *V. dahliae* WT (Figure 3.9). However, spore production by both *V. albo atrum* WT and KO was not significantly affected by 3-methyladenine (Figure 3.9).

Spore production was unaffected in spore-inoculated cultures of *vdatg8* and *vaatg8* strains; both *V. dahliae* and *V. albo-atrum* WT and KO strains produced between $1.5x10^6 – 1.5x10^7$ spores/mL (Figure 3.10). Thus, spore production in liquid was only defective in *vdatg8* if cultures were initiated from mycelia, and not from spores.

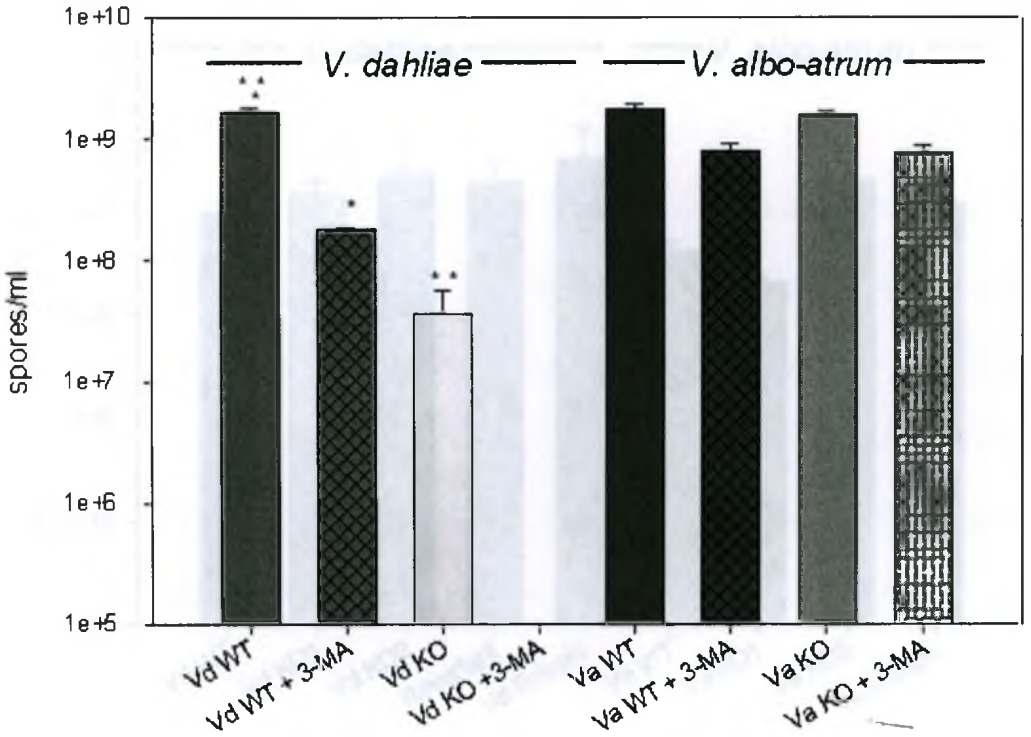

Figure 3.9 Spore production in liquid CM from *V. dahliae* and *V. albo-atrum* inoculated with mycelia of WT and KO strains

Spores were grown at 24˚C for four days, harvested and counted as described in materials and methods. Results from three separate experiments were pooled. Double stars indicate significant differences ($P<0.01$) in spore production between *V. dahliae* WT and KO (VDAT38-5) strains, while single stars indicate significant differences in spore production between Dvd-T5 cultures grown in CM and in CM amended with 3-methyladenine ($P<0.01$).

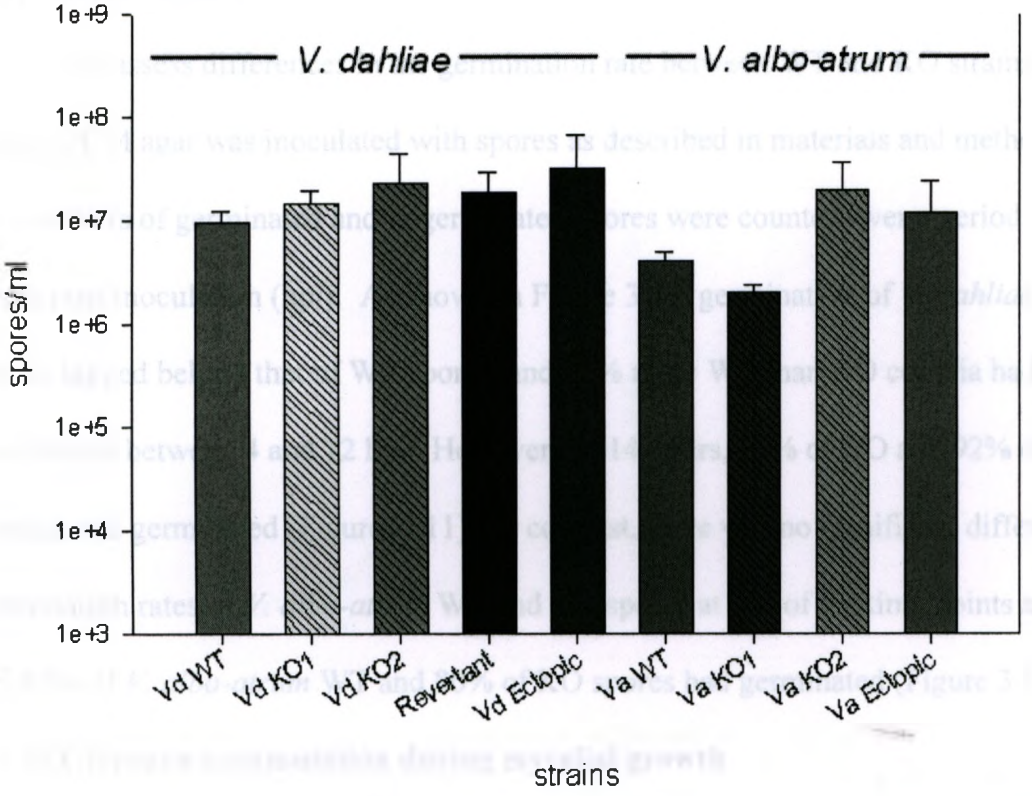

Figure 3.10 Spore production in liquid simulated xylem fluid medium (SXM) from spore inoculated cultures of *V. dahliae* and *V. albo-atrum* WT and mutant strains. Cultures were inoculated with $1x10^5$spores/ml from the following strains: *V. dahliae* WT (Dvd-T5), KO (KO1 is VDAT38-5, KO2 is VDAT38-3), revertant (VDAT44-7) and ectopic transformant (VDAT38-6) strains, and *V. albo-atrum* WT, KO (KO1 is VAAT10-9, KO2 is VAAT10-12), and ectopic transformant (VAAT10-10). Spore inoculum was generated from liquid CM cultures which had been inoculated with mycelial plugs of the respective strains grown for four days at 24°C, and harvested as described in materials and methods. The spore inoculated cultures were then grown in simulated xylem fluid medium

3.1.9 Germination

To assess differences in the germination rate between WT and KO strains of both species, CM agar was inoculated with spores as described in materials and methods, and the numbers of germinated and ungerminated spores were counted over a period of 14 hours post inoculation (hpi). As shown in Figure 3.11, germination of *V. dahliae* KO spores lagged behind that of WT spores, and 20% more WT than KO conidia had germinated between 4 and 12 hpi. However, by 14 hours, 80% of KO and 92% of WT conidia had germinated (Figure 3. 11). In contrast, there was no significant difference in germination rates of *V. albo-atrum* WT and KO spores at any of the time points and by 14 hpi 83% of *V. albo-atrum* WT and 80% of KO spores had germinated (Figure 3.11).

3.1.10 Glycogen accumulation during mycelial growth

Since autophagy enables cellular survival during nutrient limiting conditions, this process is also involved in the regulation of long-term energy storage molecules like glycogen (Deng et al. 2009). To assess the effect of *ATG8* KO on glycogen accumulation, seven and fourteen days-old mycelial cultures were inverted over iodine crystal vapour which stains glycogen dark purple. As shown in Figure 3.12, both *V. dahliae* WT and KO strains accumulated similar amounts of glycogen in the growing margin of the mycelia. However, *V. albo-atrum* WT accumulated much more glycogen than did *V. dahliae* WT, and glycogen accumulation was reduced in *vaatg8* (Figure 3.12).

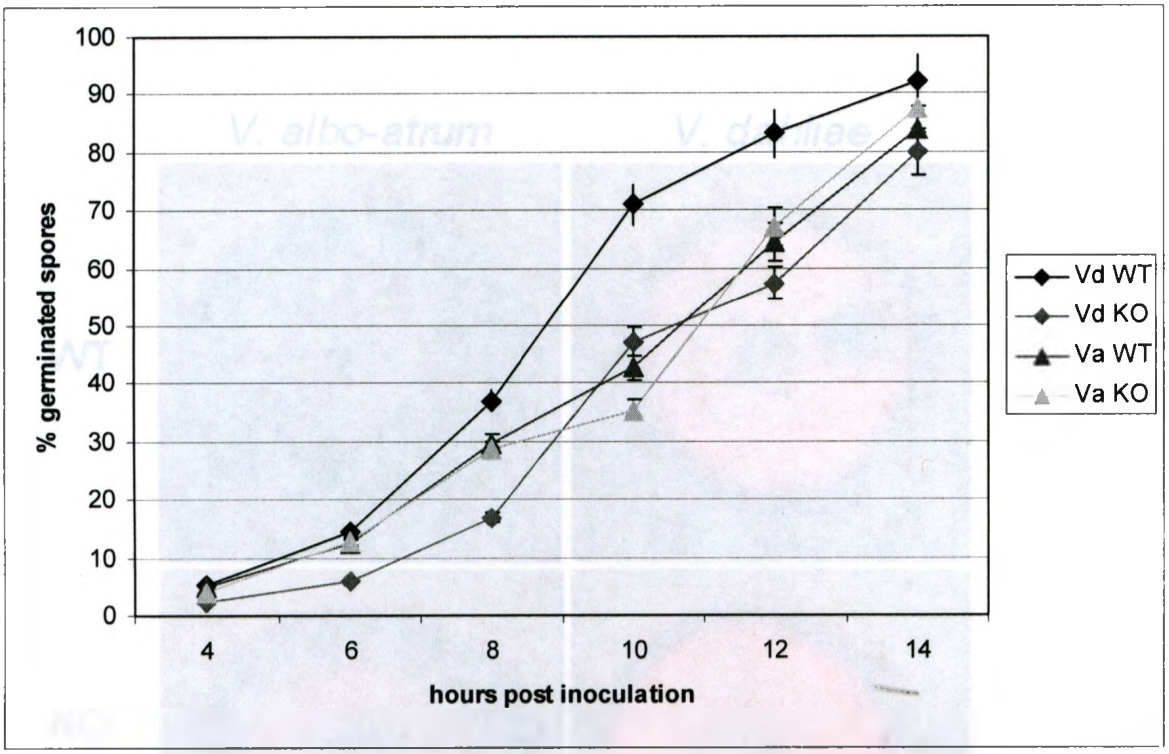

Figure 3.11 Germination of *V. dahliae* and *V. albo-atrum* WT and KO conidia. CM plates were inoculated with spores from Dvd-T5, VDAT38-5, Va383-2 and VAAT10-12 cultures and incubated at 24°C for 14 hours. Germinating spores were first counted at four hours post inoculation. The experiment was done twice, and 500 spores of each strain were counted at each time point.

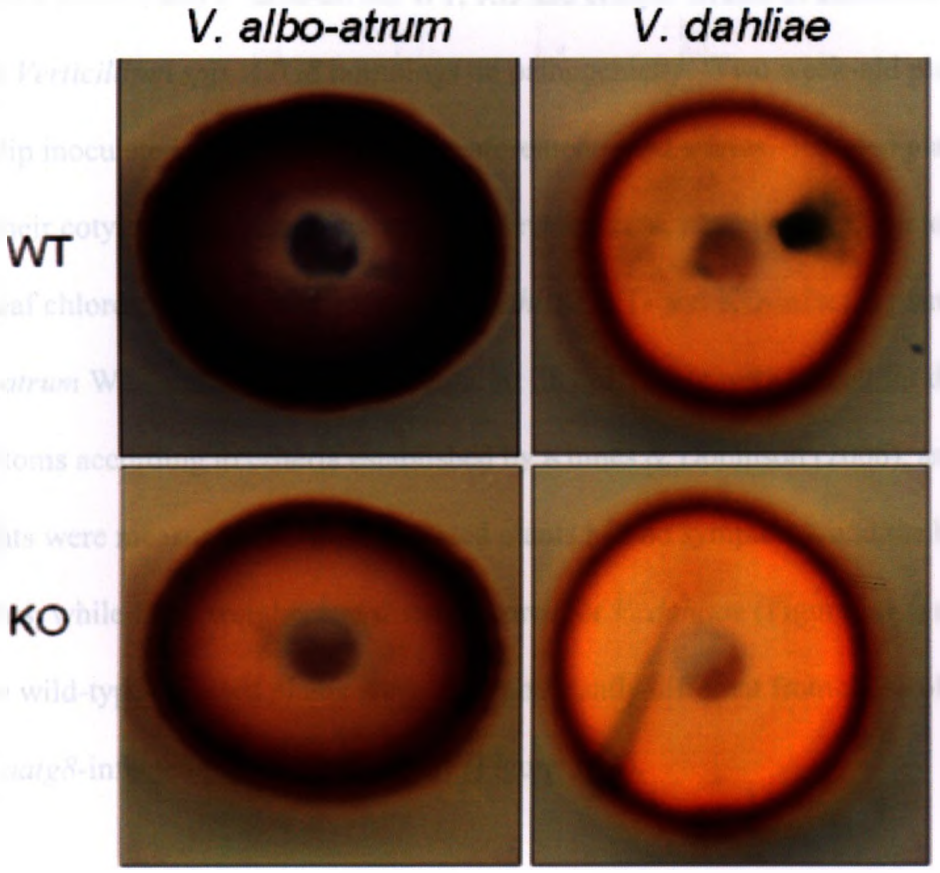

Figure 3.12 Glycogen accumulation in *V. dahliae* and *V. albo-atrum* WT and KO cultures. Top view of two-week old cultures grown on CM at 24˚C. Glycogen is stained purple by iodine vapour. Top panel: *V. albo-atrum* (383-2) (left) and *V. dahliae* (Dvd-T5) (right) WT strains. Lower panel: KO strains: *vaatg8* (VAAT10-12) and *vdatg8* (VDAT38-5).

3.2.1 Pathogenicity Assays

Bonny Best tomatoes were infected with *V. dahliae* WT, KO, ectopic and revertant strains, and *V. albo-atrum* WT, KO and ectopic strains to assess the importance of the *Verticillium spp. ATG8* homologs on pathogenicity. Two week-old plants were root dip inoculated with spores from the aforementioned strains. Infected plants started to lose their cotyledons by 14 dpi. Symptom development, namely cotyledon loss, wilting, and leaf chlorosis was similar between *V. dahliae* WT- and KO-infected plants, and *V. albo-atrum* WT- and KO-infected plants. At 28 dpi, plants were scored for disease symptoms according to criteria established by Klimes & Dobinson (2006), and fresh weights were measured. Mock-inoculated plants had no symptoms, and the highest fresh weights, while fresh weights and disease scores for *V. dahliae* (Figure 3.13) and *V. albo-atrum* wild-type-infected plants were not significantly different from those of the *vdatg8*, and *vaatg8*-infected plants, respectively (Figure 3.14).

Figure 3.13 Symptoms, fresh weights, and disease scores in tomato plants 28 days after mock inoculation, or inoculation with *V. dahliae* wild-type (WT; Dvd-T5), *vdatg8* knockout (KO; VDAT38-5), or the revertant strain (R1; VDAT44-7).

A. Mock-inoculated plants show no symptoms, while plants infected with WT, KO and revertant strains show similar disease symptoms, namely stunting, clorosis and necrosis of leaves.

B. Fresh weights of infected and mock-inoculated plants at 28 dpi. Data were pooled from three experiments (n = 10 plants/treatment/experiment). Differences between mock-inoculated plants, and infected plants were all significant ($P<0.01$). Differences in fresh weights between plants infected with the wild-type and knockout strains, and between plants infected with wild-type and revertant strains were not significantly different ($P>0.01$).

C. Disease scores of plants infected with *V. dahliae* WT, KO, R1, or mock-inoculated. Disease symptoms were scored visually at 28 dpi. Scores were assigned based on the criteria established by Klimes 2006, with scores ranging from 0 – 5, (0 = neglible chlorosis or wilting, 1= chlorosis, wilting and/or curling in individual leaves, 2 = necrosis in leaves, 3 = at least one dead branch, 4 = wilt and/or chlorosis upper leaves, and/or two or more branches dead and 5 = dead plant, or most leaves dying/necrotic). Diseased plants also exhibited stunting. Disease scores of wild-type and *vdatg8* knockout-infected plants were not significantly different ($P>0.01$).

Figure 3.13

A.

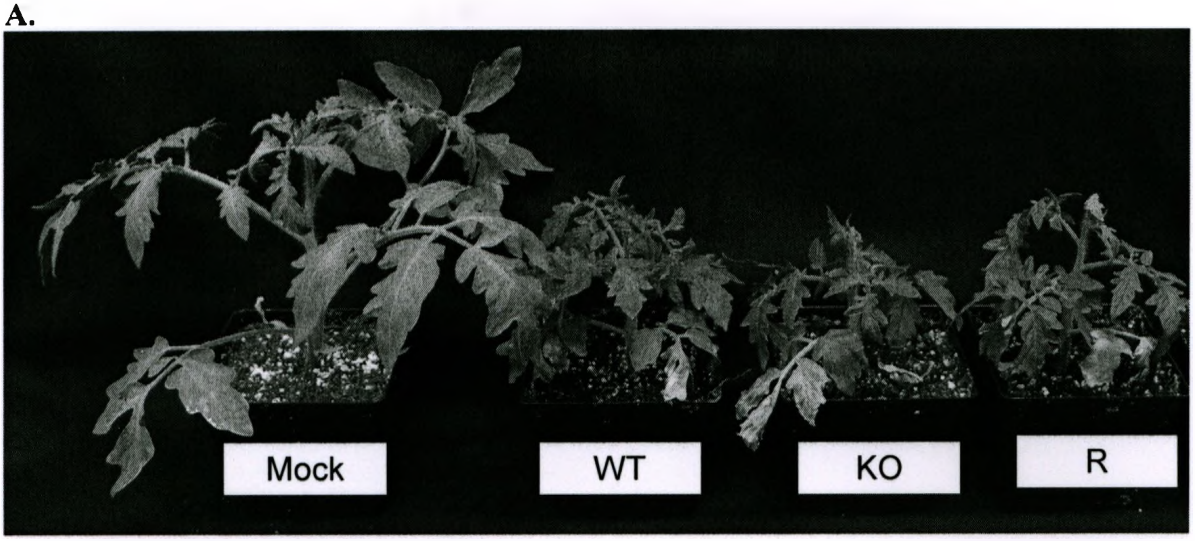

B.

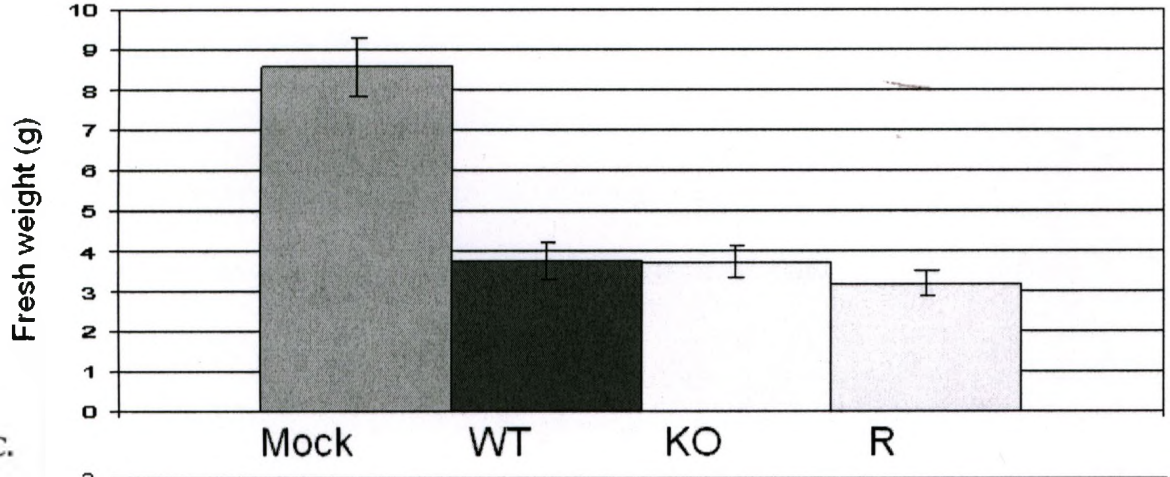

C.

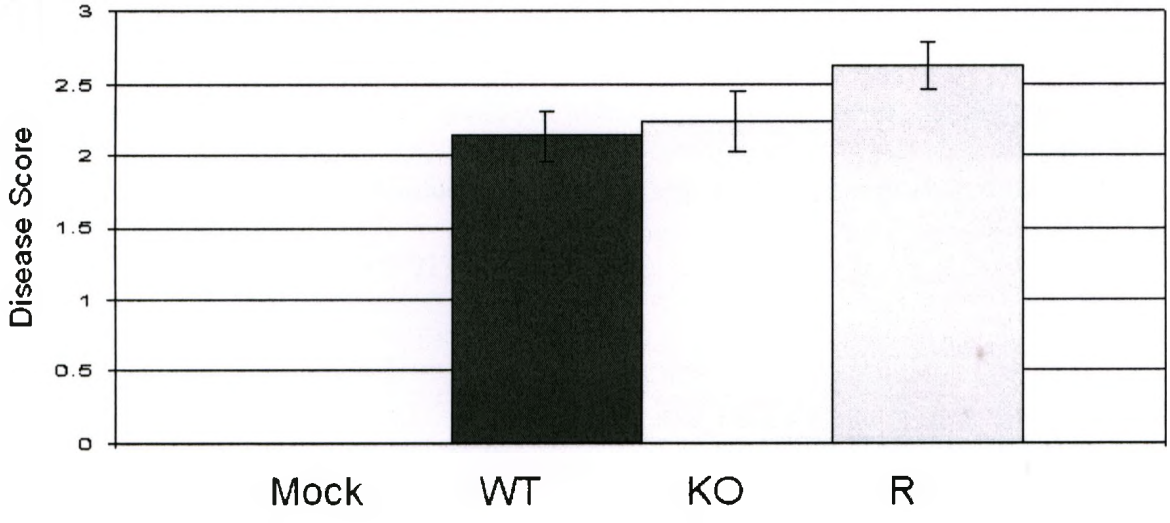

Figure 3.14 Symptoms, fresh weights, and disease scores in tomato plants 28 days after mock inoculation, or inoculation with *V. albo-atrum* wild-type (WT; 383-2), *vaatg8* knockouts (KO 1 to 3 correspond to VAAT 10-9, 10-11 and 10-12, respectively), or ectopic transformant (VAAT 10-10)

A. Mock-inoculated plants show no symptoms, while plants infected with WT, KO, or ectopic transformant strains show similar disease symptoms, namely stunting, with chlorotic and necrotic leaves.

B. Fresh weights of infected and mock-inoculated plants were measured at 28 days post inoculation. Data were pooled from 2 experiments (n = 10 plants/treatment/experiment). Differences between mock-inoculated plants and all fungus-infected plants were significant ($P<0.01$), while there were no significant differences in fresh weights of plants infected with the wild-type or knockout strains ($P>0.01$).

C. Disease scores of plants infected with *V. albo-atrum* WT, KO or ectopic strains. Mock plants had no symptoms. Disease scores were not significantly different ($P>0.01$) between wild-type infected plants and all knockout infected plants. However, the average disease score for ectopic transformant-infected plants was significantly higher than those of the WT- or KO-infected plants ($P<0.01$).

Figure 3.14

A.

B.

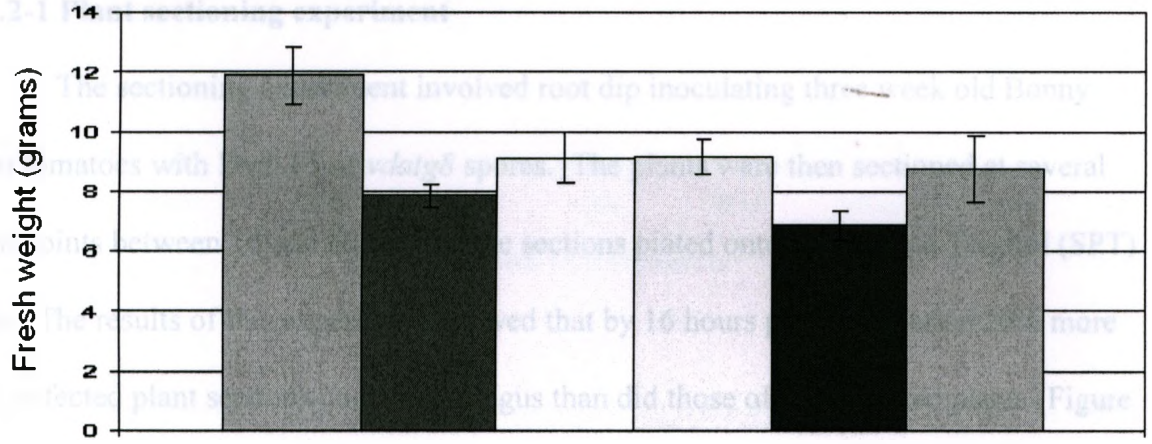

C.

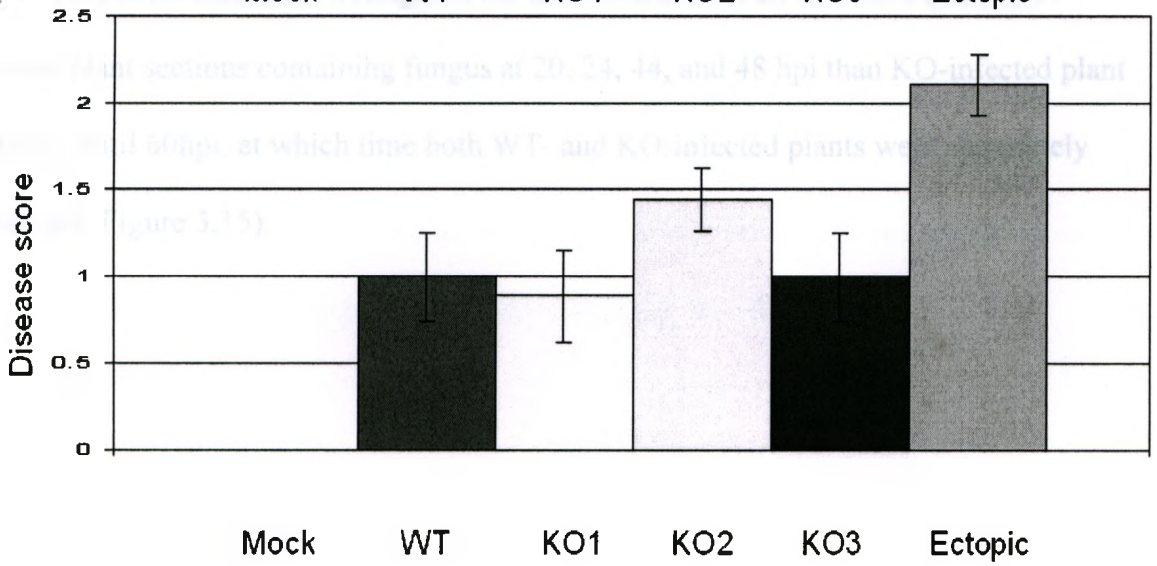

3.2.2 *In planta* colonization

The pathogenicity assays showed that *vdatg8* and *vaatg8* strains retained pathogenicity, and did not generate significantly different disease scores or fresh weights from those of the wild-type strains (Figures 3.13 and 3.14). However, one phenotype – the transition from mycelial growth to spore production in a liquid environment – was shown to be defective in *vdatg8* mutants (Figure 3.9). Two types of experiments, stem sectioning and a competitive PCR assay, were therefore done to determine whether this defect would influence plant colonization.

3.2.2-1 Plant sectioning experiment

The sectioning experiment involved root dip inoculating three week old Bonny Best tomatoes with Dvd-T5 or *vdatg8* spores. The plants were then sectioned at several time points between 16 and 60hpi, and the sections plated onto soil pectate Tergitol (SPT) agar. The results of this experiment showed that by 16 hours post inoculation 20% more WT-infected plant sections contained fungus than did those of KO-infected plants (Figure 3.15). This trend continued throughout the time course with 20% to 30% more WT-infected plant sections containing fungus at 20, 24, 44, and 48 hpi than KO-infected plant sections, until 60hpi, at which time both WT- and KO-infected plants were completely colonized (Figure 3.15).

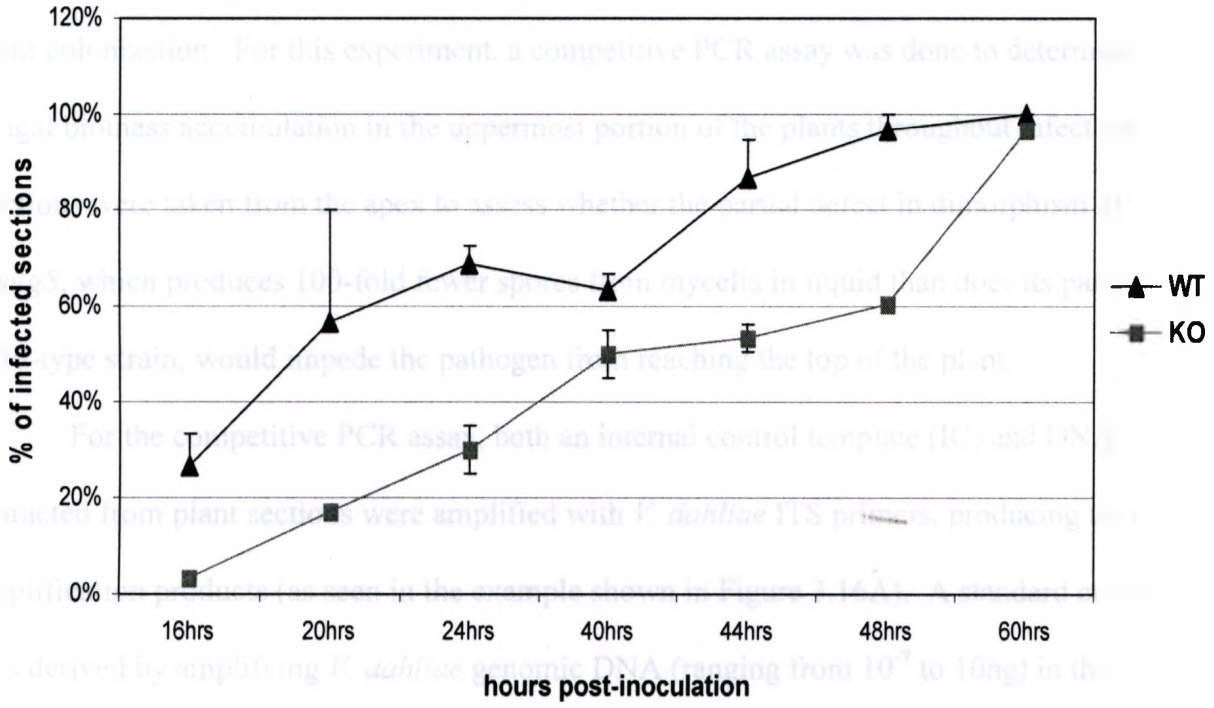

Figure 3.15 Percentage of plant sections colonized by wild-type *V. dahliae* (Dvd-T5) and *vdatg8* (VDAT38-5) over a 60 hour time course. Plants were root-dip inoculated with wild-type or *vdatg8* spores, and sectioned at different time points as described in materials and methods. The difference in percentage colonization of wild-type and *vdatg8* infected plant sections was significant ($P < 0.01$) at all time points except 40 and 60 hours. Data from three experiments were compiled, (n = three plants/strain/experiment).

3.2.2-2 Competitive PCR assay

Since the sectioning experiment showed that *vdatg8* initially colonized plants more slowly than did the wild-type, another independent experiment was done to evaluate plant colonization. For this experiment, a competitive PCR assay was done to determine fungal biomass accumulation in the uppermost portion of the plants throughout infection. Sections were taken from the apex to assess whether the partial defect in dimorphism of *vdatg8*, which produces 100-fold fewer spores from mycelia in liquid than does its parent wild-type strain, would impede the pathogen from reaching the top of the plant.

For the competitive PCR assay, both an internal control template (IC) and DNA extracted from plant sections were amplified with *V. dahliae* ITS primers, producing two amplification products (as seen in the example shown in Figure 3.16A). A standard curve was derived by amplifying *V. dahliae* genomic DNA (ranging from 10^{-7} to 10ng) in the presence of 1pg of internal control template. The quantity of fungal biomass in the plant DNA samples was determined by fitting the gDNA:IC amplicon ratio to the equation of the standard curve (shown in Figure 3.16B).

By two dpi fungal DNA was detectable at the apex of both wild-type- and *vdatg8*-inoculated plants, and the concentration for both was 0.69-0.70 ng/g plant tissue (Figure 3.17). Biomass increased sharply over the first two days following inoculation, and from two to sixteen days post inoculation levels of fungal biomass remained relatively constant with fluctuations between 0.65-0.83 ng/g of plant tissue (Figure 3.17).

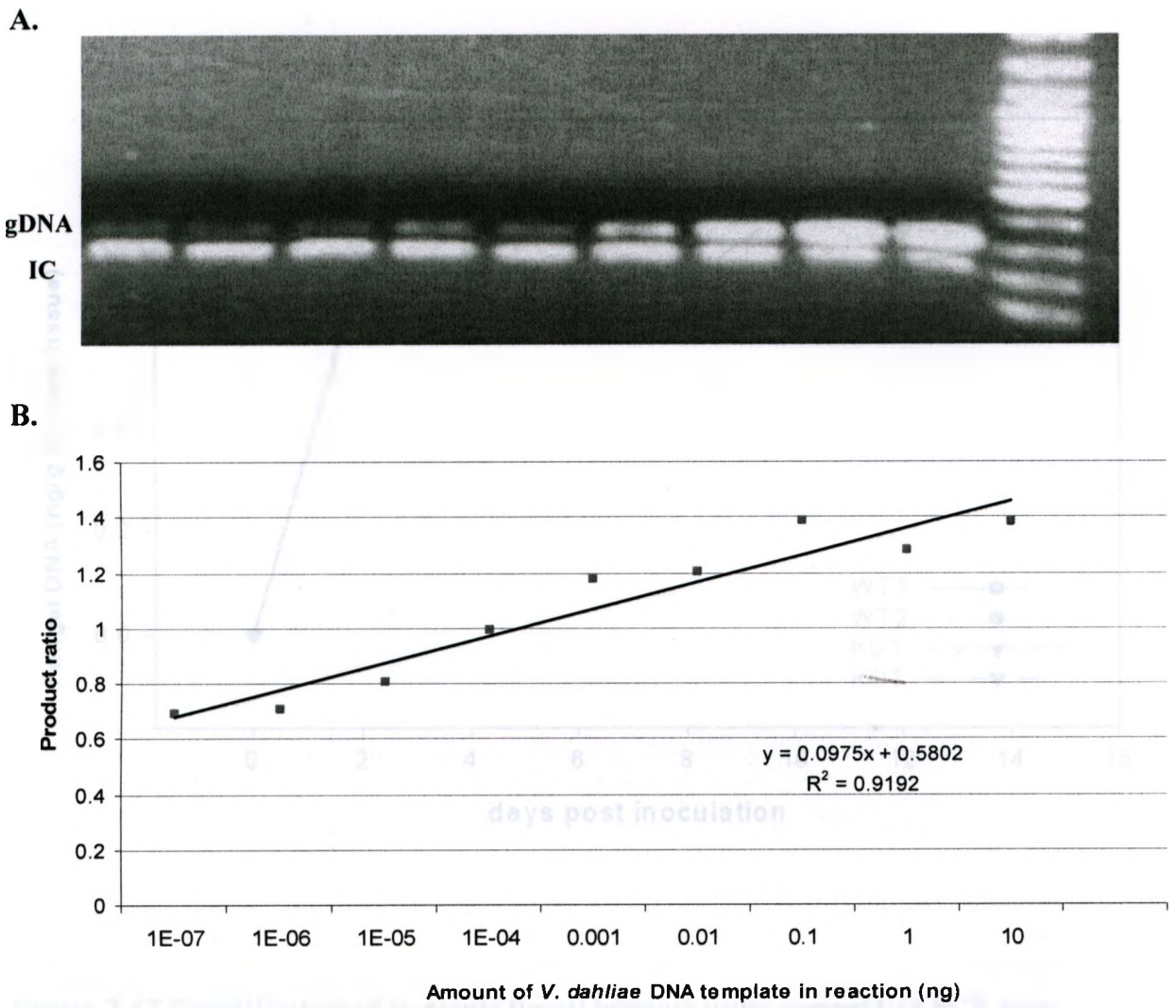

Figure 3.16: Standard curve generated by amplification of internal control template and different concentrations of *V. dahliae* gDNA. A. The competitive PCR results in two amplification products, the internal control (IC; lower band at 231bp) and an amplicon synthesized from the *V. dahliae* genomic DNA (upper band at approximately 300bp). From left to right: 100bp DNA ladder, and amplicons synthesized from 1pg of internal control template and 10, 1, 0.1, 0.01, 0.001, 10^{-4}, 10^{-5}, 10^{-6}, and 10^{-7} ng *V.dahliae* DNA. **B.** Standard curve of the IC: *V. dahliae* gDNA amplicon ratios that were used to measure fungal biomass *in planta.*

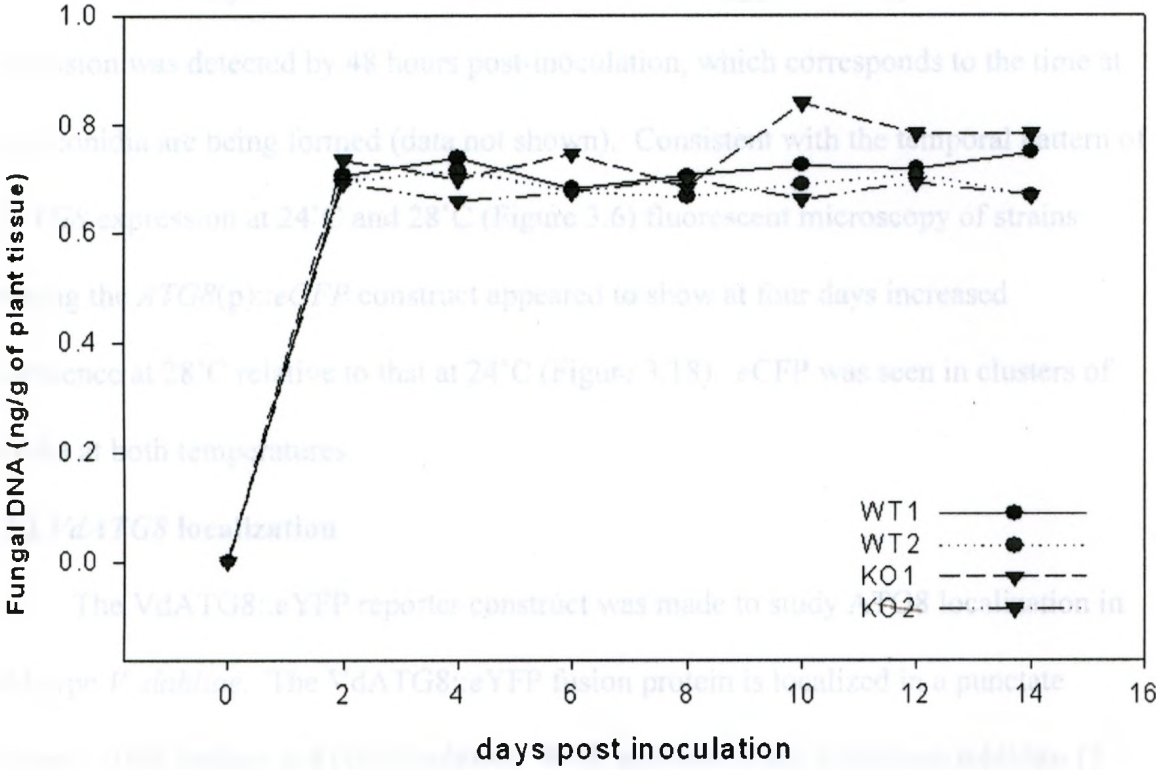

Figure 3.17 Quantification of *in planta* fungal biomass using competitive PCR assay. Samples were analyzed from three week old tomatoes inoculated with WT and KO *V. dahliae* strains

3.3.1 *VdATG8* expression

VdATG8 expression was visualized with an *ATG8*(p)::*eCFP* reporter construct. Expression was detected by 48 hours post-inoculation, which corresponds to the time at when conidia are being formed (data not shown). Consistent with the temporal pattern of *VdATG8* expression at 24˚C and 28˚C (Figure 3.6) fluorescent microscopy of strains carrying the *ATG8*(p)::*eCFP* construct appeared to show at four days increased florescence at 28˚C relative to that at 24˚C (Figure 3.18). *e*CFP was seen in clusters of conidia at both temperatures.

3.3.2 *VdATG8* localization

The VdATG8::*e*YFP reporter construct was made to study ATG8 localization in wild-type *V. dahliae*. The VdATG8::*e*YFP fusion protein is localized in a punctate manner within hyphae and conidiophores. With addition of the autophagy inhibitor (3-methyladenine) to the growth medium, the number of fluorescent spots was markedly decreased, while during growth in the presence of autophagy inducer rapamycin or on CM, the number of fluorescent spots increased (Figure 3.19). In wild-type *V. dahliae* grown under autophagy-inducing conditions (rapamycin shown in Figures 3.19 and 3.20, or BM lacking nitrate shown in Figure 3.20), the punctate localization of the eYFP-tagged VdATG8 corresponds to potential autophagosomes, which can be stained with monodansylcadaverine (MDC) (Figure 3.20). However, MDC staining is diffuse in the *vdatg8* strains under all growth conditions, and in the WT strain under autophagy-inhibiting conditions (Figure 3.20).

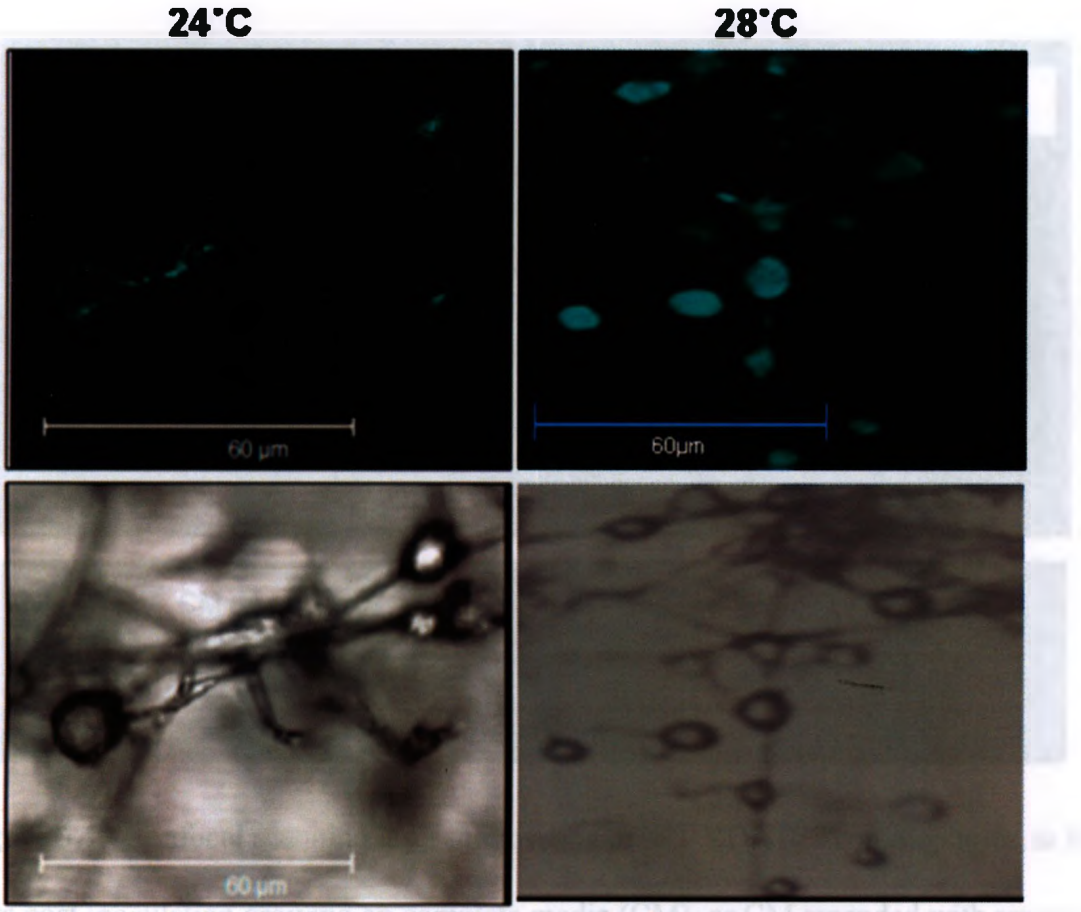

Figure 3.18 Confocal scanning laser microscopy of *V. dahliae* conidiophores, at four days post inoculation, growing on basal medium agar in depression well slides. Top panel: Expression of *VdATG8*(p)::*e*CFP in WT VDAT75-5 at 24˚C (left panel) and 28 ˚C (right panel) visualized in the cyan channel. Lower panel: Corresponding transmission light images. Scale bar is 60µm for all images.

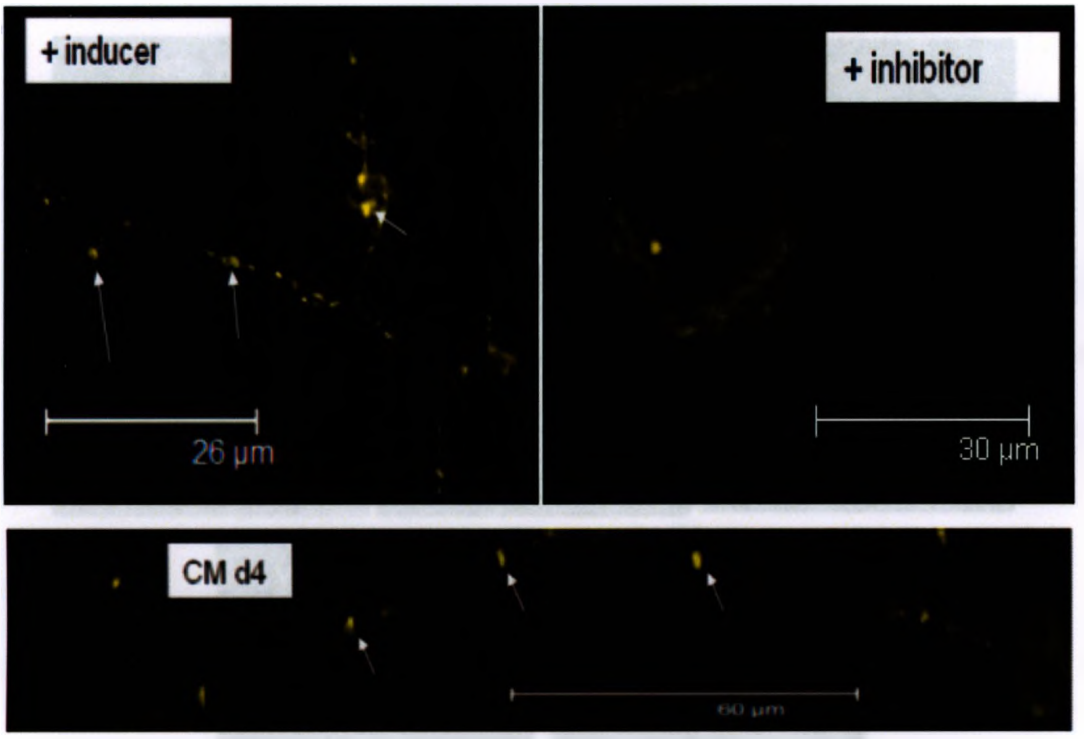

Figure 3.19 Confocal scanning laser microscopy of WT VDAT77 conidiophores, at four days post inoculation growing on complete media (CM), or CM amended with rapamycin (+ inducer) or 3-methyladenine (3-MA) (+inhibitor). When grown on media amended with 3-MA, the cultures formed small spherical cell clusters.

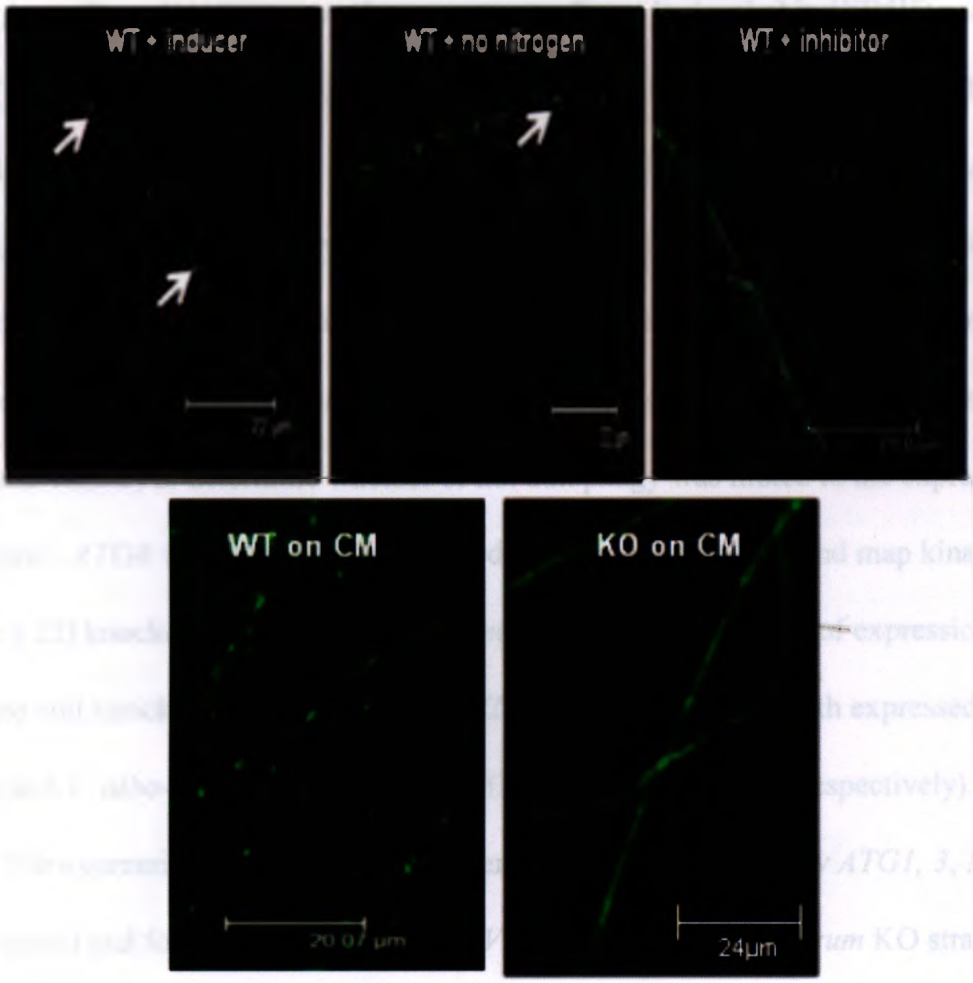

Figure 3.20 Confocal scanning laser microscopy of *V. dahliae* WT and *vdatg8* hyphae stained with monodansylcadaverine to detect autophagosomes. WT cultures were grown under autophagy-inducing (CM+rapamycin; BM lacking nitrogen), or -inhibiting conditions (CM+3-methyladenine) for four days at 24°C. Lower panel: *V. dahliae* WT and KO cultures grown on CM for four days. Hyphae were stained with monodansylcadaverine prior to visualization.

3.3.3 *ATG8* expression in other mutants

Apart from *VdATG8* two other genes, encoding a hydrophobin (*VDH1*) and a map kinase (*VMK1*), have been found to have a role in *V. dahliae* MCS formation. While *VDH1* is involved in both MCS and DRM formation (Klimes & Dobinson 2006; Amyotte 2010), deletion of *VMK1* activity affected resting structure production only in *V. dahliae* (Amyotte 2010). *ATG8* expression was therefore assessed in both hydrophobin and map kinase knockout strains of *V. dahliae* (*vdh1* and *vmk1*, respectively), and *V. albo-atrum* (*vah1*, and *vamk1*) to determine whether or not autophagy was linked to the expression of either gene. *ATG8* was expressed in both hydrophobin (Figure 3.21 and map kinase (Figure 3.22) knockout strains with no noticeable difference in levels of expression in the wild-type and knockout strains. Similarly, *VDH1* and *VMK1* were both expressed in *V. dahliae* and *V. albo-atrum ATG8* knockouts (Figures 3.23 and 3.24, respectively).

The expression of other autophagy gene homologs, specifically *ATG1, 3, 12*, and *16* was tested and found to be unaffected in *V. dahliae* and *V. albo-atrum* KO strains (Figure 3.25).

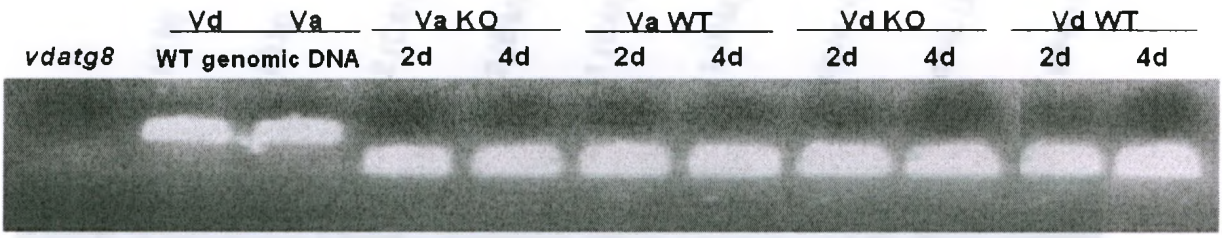

Figure 3.21 RT (reverse transcriptase) PCR showing expression of the *ATG8* gene homologs in *vdh1* and *vah1* grown on BM for two or four days at 24°C. Va KO is VAAT6-8, and the genomic DNA is from *V. albo-atrum* 383 DNA, while Vd KO is VDAT2-17, and WT is Dvd-T5 genomic DNA. Amplification of cDNA from the *vdatg8* strain was included as a negative control.

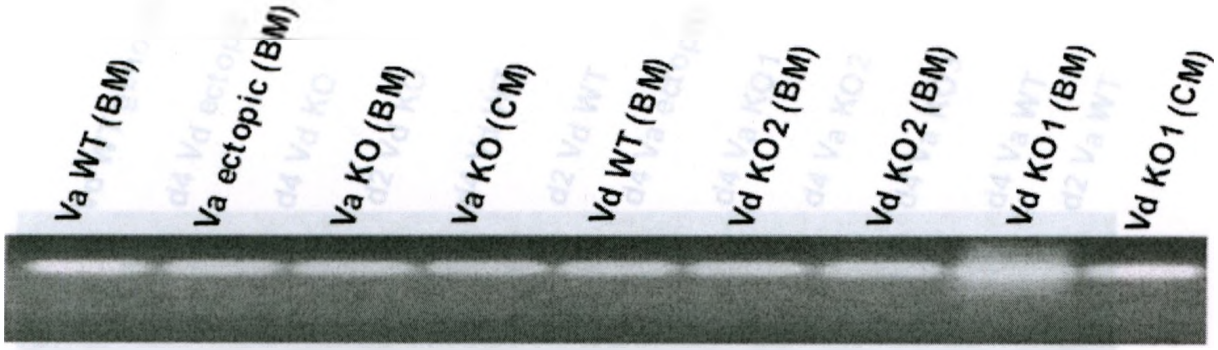

Figure 3.22 RT-PCR showing expression of the *V. dahliae* and *V. albo-atrum ATG8* gene homologs in map kinase knockouts of *V. dahliae* and *V. albo-atrum* (*vmk1* and *vamk1*, respectively) grown on BM or CM for four dpi at 24°C. VaWT, VaKO, and Va ectopic correspond to *V. albo-atrum* wild-type strain 383-2, and transformants VAAT8-9 and VAAT8-6, respectively. VdWT, VdKO1 and VdKO2 are *V. dahliae* Dvd-T5, and transformants VDAT38-5 and VDAT38-3, respectively.

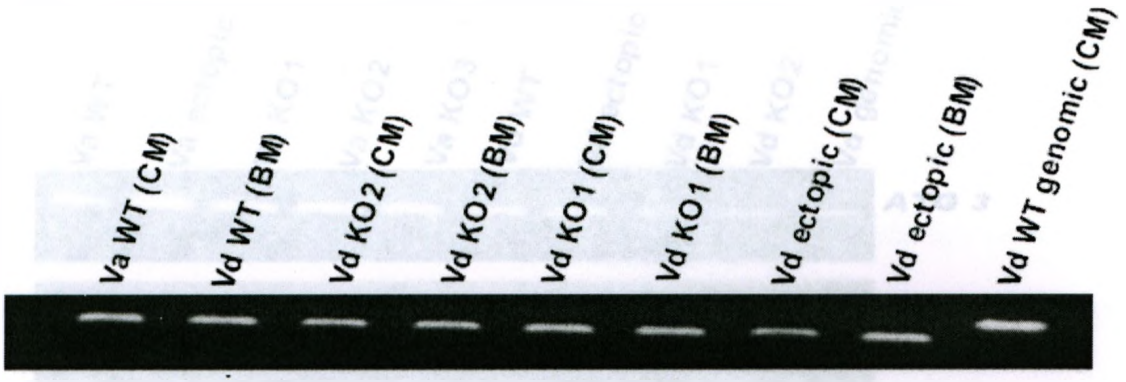

Figure 3.23 RT-PCR showing expression of hydrophobin gene *VDH1* in *vdatg8* knockouts of *V. dahliae*. All strains were grown for four days on either CM or BM at 24°C. VdWT, VdKO1, VdKO2 and Vd ectopic correspond to Dvd-T5, and transformants VDAT38-5, VDAT 38-3, and VDAT38-6, respectively. Vd WT genomic is Dvd-T5 DNA.

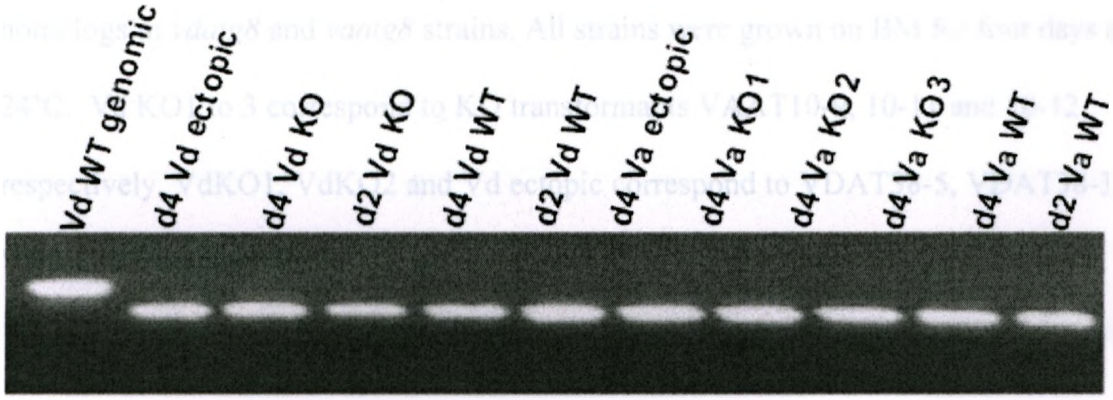

Figure 3.24 RT-PCR showing expression of map kinase (*VMK1*) gene in *V. dahliae* (*vdatg8*) and *V. albo-atrum (vaatg8*) strains grown on BM for two days or four days. VaKO1-3 are KO transformants VAAT-9, 10-11, and 10-12, respectively. Vd WT genomic is Dvd-T5 DNA.

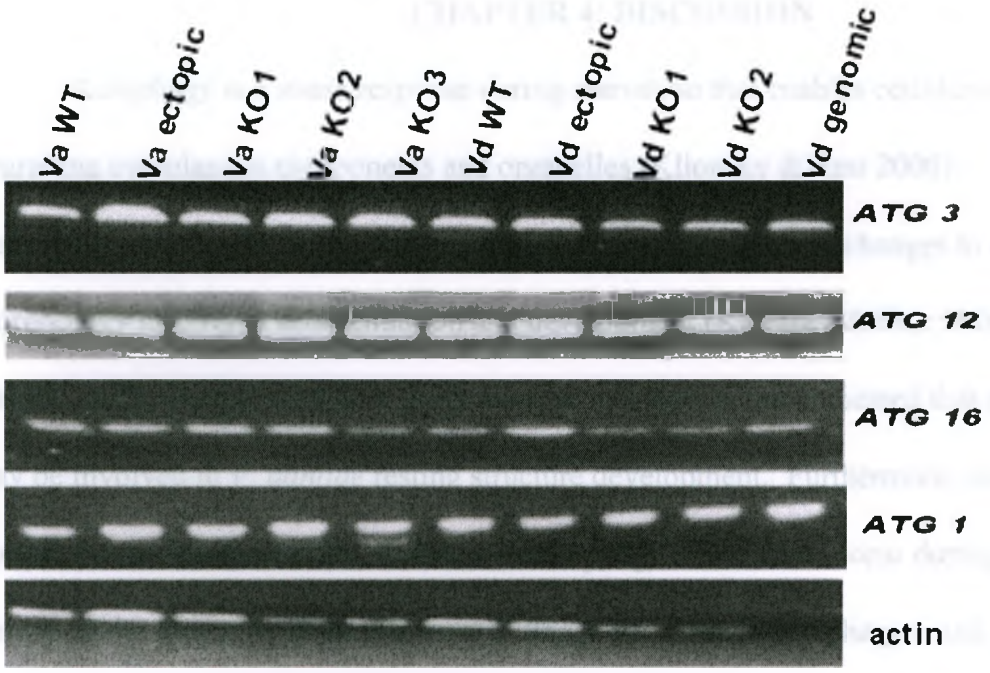

Figure 3.25 RT-PCR showing expression of actin and putative *ATG 3, 12, 16, 1* gene homologs in *vdatg8* and *vaatg8* strains. All strains were grown on BM for four days at 24°C. Va KO1 to 3 correspond to KO transformants VAAT10-9, 10-11 and 10-12 respectively. VdKO1, VdKO2 and Vd ectopic correspond to VDAT38-5, VDAT38-3, and VDAT38-6 respectively.

CHAPTER 4: DISCUSSION

Autophagy is a stress response during starvation that enables cellular survival by degrading cytoplasmic components and organelles (Klionsky & Emr 2000). Reconstitution of cellular components during autophagy results in changes to cellular morphology leading to differentiation and development (Klionsky & Emr 2000). Our interest in *ATG8* originates from early microscopic studies that indicated that autophagy may be involved in *V. dahliae* resting structure development. Furthermore, autolysis, another process that could be attributed to autophagy is known to occur during parasitic growth of the fungus *in planta* (Vessey & Pegg 1973) Since autophagy could play a role in both resting structure formation, and dimorphic growth during the parasitic phase, we decided that the *ATG8* gene homologs in *V. dahliae (VdATG8)* and *V. albo-atrum* (*VaATG8*) could be used to study autophagy and its potential roles in resting structure development, and pathogenicity.

Comparative analysis of WT and *atg8* KO strains in *V. dahliae* and *V. albo-atrum*

The roles of autophagy appear to be species specific since *vdatg8* KO strains exhibited developmental defects, while *vaatg8* KO strains were indistinguishable from the wild-type strain. Specifically, *vdatg8* strains showed delayed conidial germination, defective MCS production, reduced conidiation, and reduced sporulation initiated from mycelia during growth in liquid medium. In addition, under standard growth conditions at 24°C, *vdatg8* colonies had a distinctive cream coloured centre, and did not produce MCS. These data are consistent with the developmental defects, such as reduced numbers of aerial hyphae, disrupted conidiation, and delayed spore germination that have

been observed in *ATG8* KO strains in other fungal species such as *Magnaporthe grisea* (Liu et al. 2007) *Podospora anserina* (Pinan-Lucarré et al. 2005; Pinan-Lucarré et al. 2003), *Aspergillus oryzae* (Kikuma et al. 2006), and *Aspergillus fumigatus* (Richie et al. 2007).

In contrast to the observable mutant phenotypes seen in *V. dahliae vdatg8* strains, *V. albo-atrum vaatg8* strains did not have observable phenotypic defects. Conidial germination, dark resting mycelia formation, conidiation, and sporulation initiated from mycelia during growth in liquid were unaffected in *vaatg8* strains relative to wild-type *V. albo-atrum*. Similar to the lack of mutant phenotype in *V. albo-atrum*, disruption of autophagy by knocking out another autophagy gene *ATG9*, had no effect on hyphal differentiation or chlamydospore formation in the filamentous yeast *Candida albicans* (Palmer et al. 2007). Thus the role of autophagy in fungi appears to also be species specific.

Effect of temperature on resting structure formation

The surprising observation that *vdatg8* cultures could produce MCS at 28°C, but not 24°C led to further investigation of the effects of temperature on resting structure development in wild-type and *atg8* disrupted strains of *V. dahliae* and *V. albo-atrum*. *V. dahliae* has been found to produce MCS within 2 weeks at 15, 19.5, 24 and 29.5˚C, but took four weeks to produce MCS at 10˚C, while *V. albo-atrum* has been shown to produce DRM at 24˚C within two weeks and at 19.5˚C and 29.5˚C within three weeks (Soesantol & Termorshuizen 2001). Similarly, Wilhelm (1948) found that MCS formed at temperatures between 25-31˚C, and studies on MCS development in abscised cotton

leaves infected with *V. dahliae* showed production of MCS between 18-30˚C (Brinkerhoff 1969). Thus, the resting structure production that we observed in both species in response to temperatures between 24-29.5˚C is consistent with the results of previous studies, and suggests that these responses may not be specific to isolate Dvd-T5 (the parental strain of *vdatg8*). Furthermore, although the quantity of resting structures was not noted in any of the previous studies, Bell et al. (1976) showed that numbers of MCS produced are directly proportional to the number of hyphal fusions. Consistent with these data, at 28˚C conidiation was accelerated in cultures of wild-type *V. dahliae*, while *vdatg8* produced conidiophores, which can fuse to form MCS (Figure 3.3). Since *vdatg8* can produce MCS at 28°C, autophagy appears to be, at least partially, functionally redundant in *V. dahliae* as well as in *V. albo-atrum.*

The fact that *vdatg8* does not produce MCS at 24°C, and that increased *VdATG8* expression is concomitant with conidiation and MCS formation, suggests that autophagy does play a role in MCS formation. Previous studies in our laboratory have shown that VDH1, a class II hydrophobin, is required for MCS formation (Klimes & Dobinson 2006). While *vdh1* mutants do not produce MCS at 24˚C (Klimes & Dobinson 2006), my studies have shown that at 28˚C *vdh1* mutants do produce some MCS like the *vdatg8* strains. Given that increased temperature induces MCS formation in these two amicrosclerotial mutants there appears to be considerable functional redundancy in the pathways leading to MCS formation, with increased temperature triggering other pathways besides autophagy to produce resting structures.

In the context of the *V. dahliae* lifecycle, it is possible that increased temperatures at the end of the growing season may induce MCS formation in senescing plant tissue. In a study on MCS accumulation in plants grown at different temperatures, for example, the most rapidly senescing plants had been grown at the highest temperature and contained the most MCS per unit of plant material (Soesanto & Termorshuizen 2001). These and our data suggest a clear linkage between temperature, plant senescence, and MCS formation.

Effect of starvation on *atg8* mutant phenotypes

Although *atg8* mutants of other fungi showed similar phenotypes to *vdatg8* in terms of defective conidiation and germination, their defects in conidiation and spore germination could be restored by nutrient supplementation, while those of *vdatg8* could not. In *A. fumigatus*, for example, conidiation by an *atg1* knockout was restored by supplementing carbon- or nitrogen- deficient media with metal ions (Richie et al. 2007). Similarly, conidial germination of *A. oryzae atg8* deletion mutants was delayed (up to 16 hours) in nitrogen-deficient media, but not in nutrient-rich media (Kikuma et al. 2006). In contrast, conidial germination of *vdatg8* was tested on nutrient-rich complete medium (CM), and found, like that of *A. oryzae* grown in nitrogen-deficient medium, to be delayed by 20-30% at each time point relative to wild-type *V. dahliae* until 16hpi (Figure 3.11). Thus, although conidial viability was not affected in *V. dahliae* by the defect in autophagy, and since conidial germination of *vdatg8* strains was delayed even under nutrient-rich growth conditions, autophagy may not be as critical for nutrient cycling in *V. dahliae* as it is in other fungi. However, the initial delay in *vdatg8* conidial germination

suggests that autophagy may play some other morphological role in the early stages of germination.

Unlike other species such as *A. fumigatus*, in which *atg1* knockouts did not grow at all on minimal media (Richie et al. 2007), there is no difference in radial growth or colony morphology of *V. dahliae* WT and KO strains grown on nutritionally-deficient media such as water agar, or BM lacking nitrogen or carbon. In addition, q-RT PCR showed that *ATG8* expression levels were lower on BM lacking nitrate than on BM with nitrate. The response of *V. dahliae* to nutrient limitation is in fact opposite to that of *S. cerevisae* and *U. maydis* which accumulate *ATG8* transcripts under nutrient limiting conditions (Nadal & Gold 2010).

Consistent with the data which indicate that autophagy plays different roles in growth and development of *V. dahliae* and *V. albo-atrum*, glycogen accumulation was found to be defective in *vaatg8,* but not *vdatg8* strains. In *M. oryzae*, autophagy has been shown to facilitate glycogen homeostasis to ensure proper asexual differentiation (Deng et al. 2009). In *moatg8* mutants, for example, conidiation was restored by exogenous glucose or sucrose (Deng et al. 2009). Conidiation of *moatg8* mutants was also restored by addition of glucose-6-phosphate (G6P), or loss of glycogen phosphorylase (*Gph1*), which catalyses glycogen breakdown. Overproduction of *Gph1* enhanced glycogen breakdown, and reduced conidiation in wild-type *M. oryzae* (Deng et al. 2009). Another study found that vacuolar glucoamylase *SGA,* which hydrolyses glycogen to provide nutrients for asexual development in *M. grisea* was essential for conidia formation, but dispensable for pathogenicity (Deng & Naqvi 2010).

Finally, *SNF1*, a protein kinase required for glucose repression and glycogen metabolism may regulate autophagy via *ATG1* and/or *ATG13* in yeast (Wang et al. 2001). *SNF1* has been studied in plant pathogens since many cell wall degrading enzymes are regulated by glucose repression (Nadal 2009). While disruption of *SNF1* homologs in *Fusarium oxysporum* (Ospina-Giraldo et al. 2003), *Cochliobolus carbonum*(Tonukari et al. 2000), and recently *V. dahliae* (Tzima et al. 2011) reduced the expression of cell wall degrading enzymes, and consequently decreased pathogen virulence, disruption of *SNF1* did not affect virulence in *U. maydis* (Nadal 2009). Thus, the fact that defects in autophagy affect *V. albo-atrum* glycogen accumulation but not that of *V. dahliae* suggests that glycogen metabolism may be regulated differently in different pathogens, which could subsequently affect expression of cell wall degrading enzymes.

Regulation of resting structure formation

Previous studies in our laboratory have shown that VDH1, a class II hydrophobin is required for MCS formation, and VDH1 was proposed to induce MCS formation by facilitating fusion and adhesion of aerial structures. Another gene involved in resting structure development is the map kinase gene *VMK1*. Like *ATG8*, both *VDH1* and *VMK1* homologs are highly conserved between *V. dahliae* and *V. albo-atrum*, but the corresponding gene knockout strains show different phenotypes in the two species. While *vdh1* mutants do not produce MCS, DRM formation is unaffected in *vah1* mutants (Amyotte 2010). On the other hand, *V. albo-atrum vamk1* mutants did not produce DRM (Amyotte 2010), while the *V. dahliae vmk1* mutants did produce some MCS (Rauyaree et al. 2005). *VDH1* was expressed in *vmk1* mutants that produced some MCS, but not in the

amicrosclerotial *vmk1* mutant, while *VAH1* expression was unaffected in the *vamk1* mutant (Amyotte 2010). In my study *ATG8* was expressed in both hydrophobin, and map kinase mutants of both *V. dahliae* and *V. albo-atrum*. Similarly, *VDH1, VAH1,* and *VMK1* were expressed in *atg8* mutants of both species. Thus autophagy seems to operate either independently or in parallel with the *VAH1* and *VMK1* genes.

In the overall scheme of resting structure formation autophagy does play a role in MCS formation, and the results of my studies have shown that temperature, but not nutrient stress induces other pathways involved in MCS development. Autophagy has been implicated in facilitating hyphal autolysis for resting structure development by providing a nutrient source for developing MCS (Griffiths 1970). However, the fact that MCS and DRM can be formed in autophagy-defective mutants suggests that that autolysis may not be autophagic in origin, or that autolysis may occur independently of autophagy. The hyphal fusions, adhesion and collapse of condiophores that facilitate resting structure formation may also help release nutrients without employing autophagy.

Effect of autophagy inhibitors and inducers on growth

Autophagy inhibitors and inducers were used to verify that autophagy was responsible for the observed *atg8* mutant phenotypes. Rapamycin, an autophagy inducer that blocks activation of TOR kinase, induced formation of both chains of hyaline cells, and melanized MCS in wild-type *V. dahliae*, and the production of a few melanized MCS in the *vdatg8* strains. Conversely, 3-methyladenine, an autophagy inhibitor that blocks autophagosome formation via inhibition of type III phosphatidylinositol 3-kinases,

inhibited MCS formation in both *vdatg8* and *V. dahliae* wild-type cultures, significantly decreased spore production in *V. dahliae* WT, and eliminated spore production in *vdatg8*.

Finally staining cultures with monodansyl cadaverine (MDC) a dye known to selectively stain autophagosomes (Beiderbeck 1995), showed up as fluorescent spots in the hyphae and conidiophores, but not knockout *V. dahliae* strains under autophagy-inducing conditions, and those distinctive structures were lacking in KO cultures, and in WT cultures grown on media supplemented with the autophagy inhibitor. Disruption of *VdATG8* does therefore, as in other fungi, result in an autophagy-defective growth that decreases the accumulation of autophagosomes.

Under autophagy-inducing conditions the VdATG8::*e*YFP fusion protein was localized in a punctate manner like that in cells stained with MDC. The punctate localization of VdATG8::*e*YFP fusion protein is consistent with data from the studies of *P. anserina* (Pinan-Lucarre et al. 2005), *A. oryzae* (Kikuma et al. 2006), and *A. fumigatus* (Kikuma et al. 2006), which showed that ATG8 localized in a punctuate manner within vacuoles during nutrient stress.

Since the autophagy inhibitor affected spore production and resting formation in *V. dahliae*, but not *V. albo-atrum*, autophagy appears to be dispensable for conidiation and resting structure in *V. albo-atrum*, but not *V. dahliae*. Although the C terminal glycine that is needed for autophagosome formation is conserved in both species, differential regulation of *VdATG8* and *VaATG8* is possible, since the genes are not identical, but show variation in the size and placement of the 5' region intron, and to the size, and sequence of the corresponding proteins.

Effect of *ATG8* on Pathogenicity

Autophagy has been shown to be required for pathogenicity in several fungal plant pathogens. In *Collectotrichum lindemuthianum*, for example, *atg1* deletion mutants are defective in leaf penetration (Dufresne et al. 1998), and in the rice blast fungus *Magnaporthe grisea* disruption of *MgATG8* or *MgATG1* renders the fungus non-pathogenic (Veneault-Fourrey 2006; Liu et al. 2007). In both of these pathogens, penetration of the plant relies upon the pressure generated by infection structures (appressoria), and the abovementioned deletion mutants were shown to produce fewer appressoria, and have lower turgor pressure in appressoria (Liu et al. 2007; Veneault-Fourrey et al. 2006). Finally, *atg1* and *atg8* mutants in the corn smut pathogen *Ustilago maydis* exhibited decreased teliospore production, and subsequent decreases in gall formation and virulence while defects in double *atg1/atg8* mutants were enhanced, thus eliminating gall formation entirely (Nadal & Gold 2010). Like other species that require autophagy for pathogencity, wild-type *U. maydis* produces an infective hypha which produces a poorly differentiated appressorium at the pathogen entry site (Snetselaar & Mims 1994). Since *Verticillium* does not require specialized structures to facilitate entry into the plant, and relies upon mycelial invasion through wounds or root hairs (Fradin & Thomma 2006) autophagy would not be expected to be necessary for pathogen penetration.

The results of my study showed that there was no difference in symptom severity or onset between that of the *vdatg8* and *vaatg8*, and corresponding wild-type parental strains. Efficient spread through the vascular system by *Verticillium* spp. relies upon the

production of mycelia, which can germinate from spores, and also on spore production by either mycelia, or spore budding (yeast-like growth). Since *vdatg8* strains showed initial delays in conidial germination, and a 100-fold reduction in the number of spores produced from mycelia in liquid environments, I hypothesized that this reduction would slow the plant colonization rate by these strains. However, although the stem section analysis showed that plant colonization by *vdatg8* was delayed relative to that by the wild-type strain during the first 40 hpi, by 60hpi both *vdatg8* and wild-type strains had infected the entire plant.

Previous studies have shown that amounts of fungal biomass *in planta* were inversely proportional to levels of plant defence gene phenylalanine ammonia lyase gene (PAL) (Heinz et al. 1998), and the observed cyclical pattern of proliferation and elimination of fungal biomass in the plant vasculature was attributed to such plant defences (Heinz et al. 1998). Given that hyphal autolysis occurs during growth i*n planta* (Vessey & Pegg 1973), that autophagy has been shown to precede autolysis (Cebollero & Gonzalez 2006), and that *VdATG8* sequences were found in the parasitic cDNA library, I wondered whether autophagy might play a significant role in the reduction of fungal biomass during parasitic growth. However, the fact that colonization is unimpeded after being initially delayed suggests that a threshold of fungal biomass must accumulate before infection can proceed.

Because *Verticillium* spp. produce numerous pectinases, and other plant cell wall degrading enzymes (Cooper & Wood 1975) that could release sufficient nutrients from the plant to support fungal growth, the endogenous nutrient cycling provided by

autophagy may not be required by *V. dahliae in planta*. In addition, high levels of amino acids in xylem fluid have been observed during *Verticillium* infections of tomato (Dixon & Pegg 1972). Thus, *V. dahliae* may be capable of utilizing amino acids found in the xylem. Finally, in terms of colonization it is important to note that in *vdatg8* strains the dimorphic growth defect is in only the production of spores from mycelial cells, and not in subsequent budding. Thus, this partial defect in dimorphism has only a minor effect on fungal colonization, and suggests that autophagy may be uninvolved in or subsidiary to *V. dahliae* pathogenicity.

Conclusions and future directions

Disruption of the *V. dahliae* autophagy gene homolog *VdATG8* resulted in a defect in dimorphic growth and amicrosclerotial morphology at a growth temperature of 24°C, with temperature stress, but not nutrient limitation as reported in other fungi, restoring conidiation and MCS formation. However, *vaatg8* strains had no detectable mutant phenotype other than a defect in glycogen accumulation, and as with other, recent comparative studies of *V. dahliae* and *V. albo-atrum*, my analysis of the *ATG8* homologs in the two species demonstrated that despite the sequence similarity of the gene homologs, the roles of the genes are different for each species.

An important finding of this study was that increased growth temperature restored MCS formation and conidiation in the *vdatg8* strains, and those data, together with the observation that temperature stress also triggered MCS production in the (amicrosclerotial) *vdh1* strain, suggest that there is considerable functional redundancy in linked pathways (genes) responsible for MCS formation.

This unexpected finding that temperature stress induces resting structure formation opens up many avenues to further investigate resting structure development. It would be useful to set up a microarray study of both *V. dahliae* and *V. albo-atrum* grown at 24˚C, and at 28˚C to further examine the possibility that temperature acts as a stress response to induce other genes involved in resting structure formation. I propose the microarray approach because it has already proven useful for identification of *V. dahliae* genes involved in parasitic growth and microsclerotia formation (Klimes & Dobinson 2006). In addition, information already exists for *V. dahliae* grown at 24˚C, and provides a baseline from which to compare data from 28˚C. Genes that are differentially expressed between the two species or at different temperatures could determine which genes are involved in DRM versus MCS formation.

Another possibility for future studies would be to test whether or not any of the other hydrophobins that have been identified in the *V. dahliae* genome are upregulated in *vdh1* in response to temperature. RT-PCR of all the hydrophobin genes would need to be done for *vdh1* mutants grown at 24˚C, and at 28˚C.

To further study induction of autophagy, and potential redundancies in the autophagic pathway in *V. dahliae*, I have made *vdatg1* and *atg1/atg8* (double) knockouts in *V. dahliae*. Characterization of these strains may yield further insight into regulation of autophagy. Creation of *atg1/atg8* double knockouts in *V. albo-atrum* would be useful since my studies have shown that autophagy affects glycogen accumulation in *V. albo-atrum*, but not *V. dahliae*, and since *ATG1* is speculated to have a role in regulation of glycogen metabolism (Wang et al. 2001). The *atg1/atg8* double mutant would help

determine whether the *vaatg8* defect in glycogen accumulation is due to defects in glycogen synthesis, or defective glycogen storage.

Since *SNF1* has been implicated in glucose repression, and found to decrease production of cell wall degrading enzymes, and pathogenicity in *V. dahliae* (Tzima et al. 2011), it would be very interesting to study the function of *SNF1* in *V. albo-atrum* given that glycogen accumulation differs between the two species. Studying *SNF1* function with respect to autophagy and expression of cell wall degrading enzymes may yield greater understanding of glucose metabolism and factors affecting pathogencity in both species.

Lastly, although *VMK1* is expressed in *vdatg8* mutants, it would be useful to create double *vdatg8/vmk1* mutants. Conidiophore formation and MCS formation at 24˚C is abolished in both *vdatg8* and *vmk1* mutants. However, temperature stress at 28˚C restores conidiation and MCS formation in *vdatg8*, but not *vmk1*, and dimorphism is only defective in *vdatg8*. The *vdatg8/vmk1* mutant would help determine if the two genes are involved in separate, independent pathways, and whether or not MCS formation can be abolished entirely by mutations of both pathways.

REFERENCES

Abeliovich, H. & Klionsky, D.J., 2001. Autophagy in yeast: mechanistic insights and physiological function. *Microbiology and Molecular Biology Reviews*, 65(3), 463.

Amyotte, S.G. 2010., Comparative analysis of *Verticillium dahliae* and *Verticillium albo-atrum*; from genetic diversity to developmental processes. PhD Thesis. University of Western Ontario.

Bell, A.A., Puhalla, J.E., Tolmsoff, W.J. & Stipanovic, R.D., 1976. Use of mutants to establish (+)-scytalone as an intermediate in melanin biosynthesis by *Verticillium dahliae. Canadian Journal of Microbiology*, 22, 787-799.

Biederbick, A. Kem. H.F. & Elsasser, H.P., 1995. Mondansylcadaverine (MDC) is a specific in vivo marker for autophagic vacuoles. *European Journal of Cell Biology*, 66(1), 3-14.

Brinkerhoff, L.A., 1969. The influence of temperature, aeration, and soil microflora on microsclerotia development in abscised cotton leaves. *Phytopathology*, 59, 805-808.

Cebollero, E. & Gonzalez, R., 2007. Autophagy: From basic research to its application in food biotechnology. *Biotechnology Advances*, 25(4), 396-409.

Chen, P., Lee, B. & Robb, J., 2004. Tolerance to a non-host isolate of *Verticillium dahliae* in tomato. *Physiological and Molecular Plant Pathology*, 64(6), 283-291.

Codogno, P. & Meijer, A.J., 2000. Autophagy and signaling: their role in cell survival and cell death. *Cell Death and Differentiation*, 12, 1509-1518.

Cooper, R. & Wood, R., 1975. Regulation of synthesis of cell wall degrading enzymes by *Verticillium albo-atrum* and *Fusarium oxysporum f. sp. lycopersici. Physiological Plant Pathology*, 5(2), 135-156.

Deng, Y. & Naqvi, N.I., 2010. A vacuolar glucoamylase, Sga1, participates in glycogen autophagy for proper asexual differentiation in *Magnaporthe oryzae. Autophagy*, 6(4). Available at: http://pubget.com/paper/20383057 [Accessed December 14, 2010].

Deng Y.Z., Ramos-Pamplona, M. & Naqvi, N.I., 2009. Autophagy-assisted glycogen catabolism regulates asexual differentiation in *Magnaporthe oryzae. Autophagy*, 5:33 Available at: http://pubget.com/paper/19115483 [Accessed December 14, 2010].

Dixon, G.R. & Pegg, G.F., 1972. Changes in the amino acid content of tomato xylem sap following infection with strains of *Verticillium albo-atrum*. *Annals of Botany*, 36, 147–154.

Dobinson, K.F., Grant, S.J. & Kang, S., 2004. Cloning and targeted disruption, via *Agrobacterium tumefaciens*-mediated transformation, of a trypsin protease gene from the vascular wilt fungus *Verticillium dahliae*. *Current Genetics*, 45, 104-110.

Dobinson, K.F., Harris, R.E. & Hamer, J.E. 1993. Grasshopper, a long terminal repeat (LTR) retroelement in the phytopathogenic fungus *Magnaporthe grisea*. *Molecular Plant-Microbe Interactions*, 6, 114-126.

Dobinson, K.F., Tenuta, G.K. & Lazarovits, G., 1996. Occurrence of race 2 of *Verticillium dahliae* in processing tomato fields in southwestern Ontario. *Canadian Journal of Plant Pathology*, 18, 55-58.

Dufresne, M., Bailey, J.A., Dron, M. & Langin, T., 1998. clk1, a serine/threonine protein kinase-encoding gene, is involved in pathogenicity of *Colletotrichum lindemuthianum* on common bean. *Molecular Plant-Microbe Interactions*, 11(2), 99-108.

Fradin, E.F. & Thomma, B.P.H.J., 2006. Physiology and molecular aspects of Verticillium wilt diseases caused by *V. dahliae* and *V. albo-atrum*. *Molecular Plant Pathology*, 7(2), 71-86.

Gold, J. & Robb, J., 1995. The role of the coating response in Craigella tomatoes infected with *Verticillium dahliae*, races 1 and 2. *Physiological and Molecular Plant Pathology*, 47(3), 141-157.

Gordee, R.S. & Porter, C.L., 1961. Structure, germination, and physiology of microsclerotia of *Verticillium albo-atrum*. *Mycologia*, 53, 171-182.

Griffiths, D.A., 1970. The fine structure of developing microsclerotia of *Verticillium dahliae* Kleb. *Archives of Microbiology*, 74(3), 207–212.

Griffiths, D.A. & Campbell, W.P., 1971. The fine structure of resting mycelium of *Verticillium albo-atrum* R. & B. *Canadian Journal of Microbiology,* 17, 1533.

Grogan, R.G., Ioannou, R.W., Schneider, M.A. & Sall, K.A. 1979. Verticillium wilt on resistant tomato cultivars in California: virulence of isolates from plants and soil and relationship of inoculum density to disease. *Phytopathology,* 69, 1176-1180.

Hawke, M.A., Lazarovits, G., 1994. Production and manipulation of individual microsclerotia of *Verticillium dahliae* for use in studies of survival. *Phytopathology*, 84, 883-890.

Heinz, R. Lee, S.W., Saparno, A., Nazar, R.N. & Robb, J., 1998. Cyclical systemic colonization in Verticillium-infected tomato. *Physiological and Molecular Plant Pathology*, 52(6), 385-396.

Higgins, D.G., Thompson, J.D. & Gibson, T.J. 1996. Using CLUSTAL for multiple sequence alignments. *Methods in Enzymology*, 266, 383-402.

Hu, X., Nazar, R.N. & Robb, J., 1993. Quantification of *Verticillium* biomass in wilt disease development. *Physiological and Molecular Plant Pathology*, 42(1), 23-36.

Ichimura, Y., Imamura, Y., Emoto, K. & Umeda, M., 2004. In vivo and in vitro Reconstitution of Atg8 conjugation essential for autophagy. *Journal of Biological Chemistry*, 279(39), 40584-40592.

Isaac, I., 1967. Speciation in *Verticillium*. *Annual Review of Phytopathology*, 5, 201-222.

Jimenez-Diaz, R. & Millar, R., 1988. Sporulation on infected tissues, and presence of airborne *Verticillium albo-atrum* in alfalfa fields in New York. *Plant Pathology*, 37(1), 64-70.

Karapapa, V.K., Bainbridge B.W. & Heale J. B., 1997. Morphological and molecular characterization of *Verticillium longisporum* comb. nov., pathogenic to oilseed rape. *Mycological Research*, 101(11),1281-1294.

Kikuma, T. Ohneda, M., Arioka, M. & Kitamoto, K., 2006. Functional analysis of the ATG8 homolog Aoatg8 and role of autophagy in differentiation and germination in *Aspergillus oryzae*. *Eukaryotic Cell*, 5(8), 1328-1336.

Klimes, A. & Dobinson, K.F., 2006. A hydrophobin gene, VDH1, is involved in microsclerotial development and spore viability in the plant pathogen *Verticillium dahliae*. *Fungal Genetics and Biology*, 43(4), 283-294.

Klimes, A. Amyotte, S.G., Grant, S., Kang, S. & Dobinson, K.F., 2008. Microsclerotia development in *Verticillium dahliae*: regulation and differential expression of the hydrophobin gene *VDH1, Fungal Genetics and Biology*, 45(12), 1525-1532.

Klionsky, D.J. & Emr, S.D., 2000. Autophagy as a regulated pathway of cellular degradation. *Science*, 290(5497), 717-21.

Klosterman, S.J., Atallah, Z.K., Vallad, G.E., & Subbarao, K.V., 2009. Diversity, pathogenicity and management of *Verticillium* species. *Annual Review of Phytopathology,* 47, 39–62.

Levine, B. & Klionsky, D.J., 2004. Development by self-digestion: molecular mechanisms and biological functions of autophagy. *Developmental Cell*, 6(4), 463–477.

Liu, X., Lu, P., Zhang, L., Dong, B., Min, H. & Lin F., 2007. Involvement of a *Magnaporthe grisea* serine/threonine kinase gene, MgATG1, in appressorium turgor and pathogenesis. *Eukaryotic Cell*, 6(6), 997-1005.

Mizushima, N. & Levine, B., 2010. Autophagy in mammalian development and differentiation. *Nature Cell Biology.* 12(9), 323-830.

Mullins, E.D., Chen, X., Romaine, P., Raina, R., Geiser, D.M. & Kang, S., 2001. *Agrobacterium*-mediated transformation of *Fusarium oxysporum*: an efficient tool for insertional mutagenesis and gene transfer. *Phytopathology,* 91(2), 173–180.

Murray, M.G. & Thompson, W.F. 1980. Rapid isolation of high molecular weight plant DNA. *Nucleic Acids Research*, 8(19), 4231-4325.

Nadal, M., 2009. Exploring the role of autophagy and cell wall degrading enzymes in the lifecycle and pathogen development of basidiomycete fungal plant pathogen *Ustilago maydis*. PhD thesis. University of Georgia.

Nadal, M. & Gold, S.E., 2010. The autophagy genes atg8 and atg1 affect morphogenesis and pathogenicity in *Ustilago maydis*. *Molecular Plant Pathology*, 11(4), 463-478.

Nair, U. & Klionsky, D.J., 2005. Molecular mechanisms and regulation of specific and nonspecific autophagy pathways in yeast. *Journal of Biological Chemistry*, 280(51), 41785 -41788.

Neumann, M.J. & Dobinson, K.F., 2003. Sequence tag analysis of gene expression during pathogenic growth and microsclerotia development in the vascular wilt pathogen *Verticillium dahliae*. *Fungal Genetics and Biology*, 38(1), 54-62.

Nicot, P.C. & Rouse, D.I., 1987. Relationship between soil inoculum density of *Verticillium dahliae* and systematic colonization of potato stems in commercial fields over time. *Phytopathology,* 77, 1346-1355.

Ospina-Giraldo, M., Mullins, E. & Kang, S., 2003. Loss of function of the *Fusarium oxysporum* SNF1 gene reduces virulence on cabbage and arabidopsis. *Current Genetics*, 44(1), 49-57.

Palmer, G.E., Kelly, M.N. & Sturtevan, J.E., 2007. Autophagy in the pathogen *Candida albicans. Microbiology* 153, 51-58.

Pegg, G.F., & Brady, B.L., 2002. *Verticillium* wilts. CABI Publishing, New York, NY

Pinan-Lucarré, B., Balguerie, A. & Clavé C., 2005. Accelerated cell death in *Podospora* autophagy mtuants. *American Society for Microbiology*, 4(11), 1765-1774.

Pinan-Lucarré, B., Paoletti, M., Dementhon, K., Coulary-Salin, B. & Clavé C., 2003. Autophagy is induced during cell death by incompatibility and is essential for differentiation in the filamentous fungus *Podospora anserina. Molecular Microbiology*, 47(2), 321–333.

Pollack, J.K., Harris, S.D. & Marten, M.R., 2009. Autophagy in filamentous fungi. *Fungal Genetics and Biology*, 46(1), 1–8.

Rauyaree, P., Ospina-Giraldo, D.M., Kang, S., Bhat R.G. & Subbarao, K.V. Grant, S.J. & Dobinson, K.F., 2005. Mutations in *VMK1*, a mitogen-activated protein kinase gene, affect microsclerotia formation and pathogenicity in *Verticillium dahliae*. *Current Genetics*, 48 (2), 109-116.

Richie, D.L. Fuller, K.K., Fortwendel, J., Miley, M.D., McCarthy, J.W., Feldmesser, M., Rhodes, J.C., & Askew, D.A., 2007. Unexpected link between metal ion deficiency and autophagy in *Aspergillus fumigatus*. *Eukaryotic Cell*, 6(12), 2437-2447.

Schnathorst, W.C. 1963. Theoretical relationsips between inoculum potential and disease severity based on a study of the variation in virulence among isolates of *V. albo-atrum. Phytopathology*, 53, 888.

Schnathorst, W.C., 1981. Life cycle and epidemiology of Verticillium. In *Fungal Wilt Diseases of Plants*. Toronto: Academic Press, 81-111.

Snetselaar, K.M. & Mims, C.W., 1994. Light and electron microscopy of *Ustilago maydis* hyphae in maize. *Mycological Research*, 98(3), 347-355.

Sewell, G.W.F. & Wilson, J.F., 1964. The occurrence and dispersal of *Verticillium* conidia in xylem sap of the hop (*Humulus lupulus L.*), *Nature (London)*, 204, 901.

Soesanto L. & Termorshuizen, A., 2001. Effect of temperature on the formation of microsclerotia in *Verticillium dahliae*. *Journal of Phytopathology.* 149(11), 685-691.

Stark, C., 1961. Das auftreten der Verticillium-tracheomykosen in hamburger gartenbaukulturen. *Gartenbauwissenschaft*, 26, 493-528.

Subbarao K.V., Chassot, A., Hubbard, T.R., Mullin, J.C., Okamoto, P., Davis, R.M. & Koike, S.T., 1995. Genetic relationships and cross pathogenicities of *Verticillium dahliae* isolates from cauliflower and other crops. *Phytopathology,* 85 (10), 1105-1112.

Tzima, A.K., Paplomatas, E.J., Rauyaree, P., Ospina-Giraldo, M.D. & Kang, S., 2011. *VdSNF1*, the sucrose nonfermenting protein kinase gene of *Verticillium dahliae*, is required for virulence and expression of genes involved in cell-wall degradation. *Molecular Plant-Microbe Interactions*, 24(1), 129-142.

Veneault-Fourrey, C., Barooah, M., Egan, M., Wakley, G. & Talbot, N.J., 2006. Autophagic fungal cell death is necessary for infection by the rice blast fungus. *Science*, 312(5773), 580-583.

Vessey, J.C. & Pegg, G.F., 1973. Autolysis and chitinase production in cultures of *Verticillium albo-atrum*. *Transactions of the British Mycological Society.* 60 (1), 133-143.

Wang, Z. Wilson, W.A., Fujino, M.A. & Roach, P.J., 2001. Antagonistic controls of autophagy and glycogen accumulation by Snf1p, the yeast homolog of AMP-activated protein kinase, and the cyclin-dependent kinase Pho85p. *Molecular and Cellular Biology*, 21(17), 5742-5752.

Wheeler, M.H., Tolmsoff, W.J., Bell, A.A. & Mollenhauer, H.H. 1978. Ultrastructural and chemical distinction of melanins formed by *Verticillium dahliae* from (+)-scytalone, 1,8-dihydroxynaphthalene, catechol, and L-3,4-dihydroxyphenylalanine. Canadian Journal of Microbiology, 3, 289-297.

Wilhelm, S., 1948. The effect of temperature on the taxonomic characters of *Verticillium albo-atrum* Rke et Bert. *Phytopathology*, 38, 919.

Wilhelm, S., 1955. Longevity of the *Verticillium* wilt fungus in the laboratory and field. *Phytopathology*, 45, 180-181.

Yang, Y., Liang, Z., Gu, Z. & Qin, Z., 2005. Molecular mechanism and regulation of autophagy. *Acta Pharmacologica Sinica*, 26(12), 1421-1434.

Appendix I: Primers used in this study

Primer name	Primer sequence	Purpose in this study
atg8EcoF1	5'-GTGCGACTTGAATTCGATCAGCCAG	*VdATG8*(p)::eCFP construct
atg8promoterBam R1	5'-GATCCTGTCGGTTGTGGTTG	
M13R	5'-AGCGGATAACAATTTCACACAGG	Sequencing for constructs containing a pDHt vector
M13F	5'-CCCAGTCACGACGTTGTAAAACG	
Sp6	5'-TATTTAGGTGACACTATAGAAT	Sequencing for constructs containing a pDHt vector
T7	5'-ACGACTCACTATAGGGCGAATTGG	
atg8EcoF1	5'-GTGCGACTTGAATTCGATCAGCCAG	$VdATG8_N$::eYFP construct creation
atg8promoterBam R1	5'-GATCCTGTCGGTTGTGGTTG	
yfpBamF2	5'-CCAGGATCCAAAATGGTGAGCAAGGGCG	
yfpPstR4	5'-TGTACTGCGGTCCATGCCGAAGAGTG	
atgPstF2	5'-CACACTGCAGAGTATGCGATCCAAGTTACCGG	
atg8PstR2	5'-CGCTCTGCAGTTTGAGTTGGGGTCTGTC	
pMODF	5'-ATTCAGGCTGCGCAACTGT	Sequencing of Tn for *ATG8* KO construct
pMODR	5'-GTCAGTGAGCGAGGAAGCGGAAG	
autoF1	5'-GGTGCTGGTGCTGGTGAC	Sequencing of *VdATG8*(p)::eCFP
autoR5	5'-CAAGTTCAAGGACGAGCACC	
autoF7	5'-AACCAACCCAACTCTACCTCTC	
autoF10	5'-TAATTAGTCACCTGCCAGCC	
auto-R2	5'-GCAGTAGGCCTTCGCATAGTT-	DIG-labelled probes and *ATG8* amplification
auto-F5	5'-CAAGTTCAAGGACGAGCACC	
Vd1	5'-GCCGGTCCATCAGTCTCTCTG	rDNA ITS primers used for *in planta* competitive PCR analysis
Vd2	5'-GGACTCCGATGCGAGCTGTAAC	
HO2-1	5'-GTAGAAACCAACACCCGAACTT	*V. dahliae* actin gene primers
HO2-2	5'-CAACACTGTCTACTCCAACAAGG	
svt-q-atg8-F4	5'-TACGAGGAGCACAAGGACGAGGAC	Quantitative RT-PCR
svt-q-atg8-R6	5'-GGTGTTCTCGCCAGAGTAGGTAATG	
F-actin AK-1	5'-AGCAATGGCGTCTACA	
R-actin AK-1	5'-GCAAGAGTACCCATACCG	
F- β tubulin AK-2	5'-CCAACATCAAGATGCGT	
R- β tubulin AK-2	5'-CTCAGTGTAGTGACCCTTT	

C24-1A	5'-CTATTGCGATTGCTCTG	RT PCR of *VDH1*
C24-2A	5'-GAGCTCAAGGTTTTCGTG	
VMK 1F	5'-CGCAGCAACGCCCCTAATC	RT-PCR of *VMK1*
VMK 2R	5'-CTTTCAGGTCGCAGTTGG	
ATG3-F2	5'-CGTTGCTGCGGGCGACTATC	RT-PCR of autophagy genes
ATG3-R6	5'-CCACCCTAATCGCAACCTCCTG	
ATG12 F5	5'-TTCTCCGGCGCAGCAGTCC	
ATG12 R3	5'-GCTGGTGTCATGGAGTAAGAGATAACG	
ATG16 F1	5'-TTACGCAACAAGGCCAAGACAG	
ATG16 R1	5'-TCCTGGGCCATTCTCTTCATCC	
ATG1 F2	5'-ATCTCGAGGGTTGCGTAATCTC	
ATG1 R1	5'-CGTACCTGCTGCTGGCTCTGC	

Appendix II: Previously generated *VdATG* gene knock-out (KO), and revertant strains

The *VdATG8* knockout (KO) vector was made by J. Cucullo using methods described by Dobinson et al. (2004), and used to create both the *vdatg8* and *vaatg8* mutant strains. To make this vector, the *VdATG8* PCR amplicon was ligated into the pGEM-T Easy vector to generate pGEM(*VdATG8*). The pGEM(*VdATG8*) vector was electroporated into Amp^R Blue MRF' *E. coli* and the plasmid was purified from two colonies, and sequenced to confirm presence and correctness of the *VdATG8* sequence. The pGEM(*VdATG8*) plasmid and pDHt binary vector (which contains a kanamycin resistance gene) (Mullins et al. 2001) were then digested with *Eco*RI restriction endonuclease. pDHt was dephosphorylated using shrimp alkaline phosphatase, and the *VdATG* gene fragment was ligated into the *Eco*RI site. The ligation mixture was electroporated into *E. coli.*

After identification of clones containing a plasmid with the *VdATG8* gene fragment, the resulting plasmid (designated pJCATG) was purified from one of the transformants, digested with *Eco*R1, and used for transposon (Tn) mutagenesis with the EZ::TN system (Epicentre Technologies, Madison, Wis.). The Tn cassette randomly inserts into the plasmid DNA and carries both a chloramphenicol ($chlor^R$) under control of a bacterial promoter, and a hygromycin B resistance (Hyg^R) under the control of a constitutive fungal promoter. The mutagenesis reaction products were electroporated into *E. coli* and PCR amplification from Kan^R/$Chlor^R$ colonies was done with pMODF and pMODR primers to determine Tn location, and autoF2/R2. Of these, two transformants

(designated pJCATG(Tn)4 and pJCATG(Tn)5) had a Tn located within the *VdATG8* gene fragment. Both the pJCATG(Tn)4 and pJCATG(Tn)5 gene KO vectors were electroporated into *A. tumefaciens* cells, and Kan^R and $Chlor^R$ transformants were identified. Hyg^R transformants containing a Tn in the mutant allele construct from pJCATG(Tn)4 and pJCATG(Tn)5 were designated VDAT 38-5 and VDAT 38-3 respectively.

S. Grant constructed two types of revertants by transforming into *vdatg8* cells an intact *VdATG8* gene containing a downstream geneticin resistance marker gene into *vdatg8* cells. The revertant cells are hygromycin sensitive and geneticin resistant. On the other hand, ectopic revertants have the same intact *VdATG8* gene located ectopically, and are resistant to both hygromycin and geneticin.

Appendix III: Compositions of growth media, and solutions

Complete medium (CM) contains 1 x nitrate salts ($NaNO_3$ (6 g/L), KCl (0.52 g/L), $MgSO_4$.7H2O (0.52 g/L), KH_2PO_4 (1.52 g/L), 1 x trace elements ($ZnSO_4.7H_2O$ (0.022 g/L), H_3BO_3 (.011 g/L), $MnCl_2.4H_2O$ (0.005 g/L), $FeSO_4.7H_2O$ (0.005 g/L), $CoCl_2$ $6H_2O$ (.0017 g/L), $CuSO_4.5H_2O$ (0.0016 g/L), Na_2MoO_4 $2H_2O$ (.0015 g/L), Na_4EDTA (0.05 g/L), glucose (10 g/L), peptone (2 g/L), yeast extract (1 g/L), casamino acids (1 g/L) and 1 x vitamin solution (biotin, pyridoxine, thiamine, riboflavin, *p*-aminobenzoic acid, nicotinic acid, all at 0.01% (w/v)). Adapted from Bennett and Lasure (1991).

Basal medium (BM) contains glucose (10 g/L), sodium nitrate (0.2 g/L), 1x potassium salts (KCl 0.52 g /L, $MgSO_4$ $7H_2O$ 0.52 g /L, and KH_2PO_4 1.52g /L), 3 µM thiamine HCl, and 0.1 µM biotin. Adapted from Bennett and Lasure (1991).

Minimal medium (used for *Agrobacterium tumefaciens*-mediated transformation (ATMT)) (Hooykas et al., 1979; Mullins et al., 2001) contains K_2HPO_4 (2 g/L), KH_2PO_4 (1.45 g/L), $MgSO_4.7H_2O$ (0.6 g/L), NaCl (0.3 g/L), $CaCl_2.2H_2O$ (0.001%weight/volume (w/v)), glucose (0.02% (w/v)), $FeSO_4$ (0.0001% (w/v)), $ZnSO_4.7H_2O$ (100 mg/L), $CuSO_4.5H_2O$ (0.5 mg/L), H3BO3 (0.5 mg/L), $MnSO_4.H_2O$ (0.5 mg/L), $Na_2MoO_4.2H_2O$ (0.5 mg/L), NH_4NO_3 (0.05% (w/v)).

Induction medium (used for ATMT) (Bundock et al., 1995; Mullins et al., 2001) contains K2HPO4 (2g/L), KH_2PO_4 (1.45 g/L), $MgSO_4.7H_2O$ (0.6g/L), NaCl (0.3 g/L), $CaCl_2.2H_2O$ (0.001% weight/volume (w/v)), $FeSO_4$ (0.0001% (w/v)), $ZnSO_4.7H_2O$ (100 mg/L), $CuSO_4.5H_2O$ (0.5 mg/L), H_3BO_3 (0.5 mg/L), $MnSO_4.H_2O$ (0.5 mg/L), $Na_2MoO_4.2H_2O$ (0.5 mg/L), 10 mM glucose, 200 uM acetosyringone.

20 X SSPE contains 3.6 M NaCl, 0.2 M NaH_2PO_4, 22 mM EDTA.

Spore Breakage Buffer (Elder et al. 1983) contains 0.5M NaCl, 0.2M Tris pH 7.5,10 mM EDTA, 1% SDS.

TE buffer contains 10mM Tris-HCl, pH 7.6, 1 mM EDTA.

References for Appendices

Bennet, J.W. & Lasure, L.L., 1991. Appendix B: Growth media. In: More gene manipulations in fungi. Bennet, J.W., Lasure, L.L., (Eds.) Toronto: Academic Press, Inc. pp: 442-456.

Bundock, P., den Dulk-Ras, A., Beijersbergen, A. & Hooykaas, P. J. J., 1995. Trans-kingdom T-DNA transfer from *Agrobacterium tumefaciens* to *Saccharomyces cerevisiae*. *European Molecular Biology Organization*, 14, 3206-3214.

Elder, R.T., Loh, E.L. & Davis, R.W., 1983. RNA from the yeast transposable element Tyl has both ends in direct repeats, a structure similar to retrovirus RNA. *Proceedings of the Natural Academy Sciences of the U.S.A*, 80, 2432-2436.

Hooykaas, P. J. J., Roobol, C. & Schilperoort, R. A., 1979. Regulation of the transfer of Ti-plasmids of *Agrobacterium tumefaciens*. *Journal of General Microbiology,* 110, 99-109.

Mullins, E.D., Chen, X., Romaine, P., Raina, R., Geiser, D.M., Kang, S., 2001 *Agrobacterium*-mediated transformation of *Fusarium oxysporum*: an efficient tool for insertional mutagenesis and gene transfer. *Phytopathology*, 91, 173–180